GOLD(I) PHOSPHINE COMPLEXES AS SELECTIVE ANTI-TUMOUR AGENTS

Chapter One

1.0 Gold compounds as anti-tumour agents

1.1 Early developments

Gold(I) thiolate compounds have been in clinical use for the treatment of rheumatoid arthritis since the 1930's [1, 2]. While there is considerable evidence that gold compounds are amongst the few that actually induce remission of the disease, lack of enthusiasm for gold therapy has arisen as a result of pain associated with the large intramuscular injections required monthly and more importantly, the accumulation of gold in the kidneys following a long course of treatment [3]. Consequently, in the mid 1960's, researchers at Smith, Kline and French began to search for orally-active gold compounds, as they hoped that these would allow blood gold levels to be maintained by a low daily dose, thus preventing the accumulation of gold in tissue, which accompanies large injection doses [3]. A series of lipophilic gold(I) phosphine complexes R_3PAuX (X = Cl or thiosugar), with linear 2-coordinated structures was found to be orally active [4], with Et_3PAuCl being the most active and readily absorbed. However, the latter complex was found to cause severe gastrointestinal irritation and was unsuitable for clinical use. Eventually the thioglucose derivative of triethylphosphine Au(I) (Auranofin, see in *i*) was selected for extensive clinical trials [5] and was approved for clinical use in May 1985 under the trade name Ridaura.

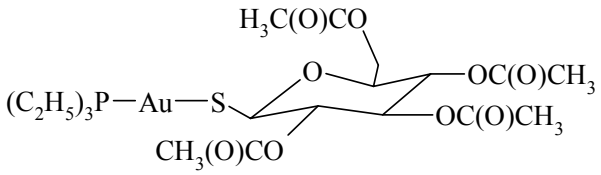

Auranofin, *i*

While this investigation is restricted to Au(I) anti-tumour agents, the application of Au(III) to chemotherapy has received considerable attention owing to it being isoelectronic with platinum(II) which forms similar square-planar complexes. However the biological environment act generally as a reducing agent and therefore compounds

containing gold(III) may be expected to be reduced *in vivo* to gold (I) and metallic gold [6].

1.2 Relationship between structure and anti-cancer activity

The preference for gold to exist in a linear 2-coordinate configuration is reflected in the vast number of bridged di-gold complexes which have undergone biological testing. Smith, Kline and French laboratories have tested some fifty linear 2-coordinated compounds and have concluded that these complexes, [ClAu(P-P)AuCl] (where P-P is a bisphosphine), are more potent than free ligands and exhibit a broad range of anti-cancer activity [7, 8]. The results of a structure-activity study, released in 1987, may indicate that the activity is maximized where the ligands can form strong chelating rings [8]. It has been shown that the bridged di-gold complexes [XAu(dppe)AuX] (X = Cl or β-D-thioglucose) readily undergo rearrangement reactions in the presence of thiols or blood plasma to give the monomeric bis-chelated species, $[Au(dppe)_2]X$ (where dppe is 1,2-bis(diphenylphosphino)ethane) [9]. ^{31}P NMR studies have shown that the addition of 2 mol. equivalents of sodium thioglucose (SGlu) to [ClAu(dppe)AuCl] converted it to [(SGlu)Au(dppe)Au(SGlu)] and with further addition of NaSGlu, the bis-chelated complex, $[Au(dppe)_2]^+$ was formed. Similarly, the addition of glutathione (GSH) at pH 7.0 to [XAu(dppe)AuX], where X is Cl or SGlu, induced the formation of $[Au(dppe)_2]^+$. The observation that dppe bridged di-gold complexes are converted to $[Au(dppe)_2]^+$ in blood plasma, suggested that the tetrahedral species may play an important role in the activity of these bridged complexes [10]. These results have prompted the suggestion that for gold(I) bisphosphine anti-tumour agents, chelation of the metal center is implicated in the mode of action.

This has inspired the synthesis of stable 4-coordinate gold(I) diphosphine complexes [11-13]. The effect of structural variation in chelated bis(diphosphine) gold(I) complexes $[Au(R_2P(CH_2)_nPR_2)]X$ on their cytotoxicity and activity against P388 leukaemia, B16 melanoma and M5076 reticulum cell sarcoma has been studied [23]. These variations included chelate ring size, constituents on phosphorous and counter ions. Changing the

anion, X, had little effect on the anti-tumour activity, as might be expected since these complexes would dissociate in highly polar media to give $[Au(P\text{-}P)_2]^+$ and X^- ions and if the active species were the cation, then the anion would be expected to have little effect on activity. However, it has been suggested that ion pairing, especially with endogenous Cl^-, could be important in the transport of these cations across membranes [14]. Similarly studies on the tetrahedral chelated silver(I) and Cu(I) diphosphine complexes display comparable anti-cancer activities to their Au(I) analogues [3, 15, 16]. The ligands themselves, $Ph_2P(CH_2)_nPPh_2$, also posses high anti-cancer activity where n = 2 or 3; marginal activity where n = 1, 4 and 5, and no activity when n = 0 or 6, or the ethane bridge is replaced by trans –CH=CH-, -C≡C- , and 1,4 phenyl bridged ligands [7, 17]. $[Au(dppe)_2]Cl$ exhibits a comparable level of anti-tumour activity to dppe, but its cytotoxicity in mice is 25-fold greater than the free ligand and it is highly cytotoxic *in vitro*. It has been proposed that the coordination to gold(I) protects the ligand from oxidation prior to delivery to cellular targets [3]. Available data on phosphine oxides show them to be inactive as anti-tumour agents [7]. Replacement of phenyl constituents by ethyl groups reduced both the potency and activity against P388 leukaemia. $[Au(depe)_2]PF_6$, where depe is $Et_2P(CH_2)_2PEt_2$, is inactive against P388 leukaemia and is four times less toxic to B16 melanoma cells *in vitro* than the complex $[Au(dppe)_2]Cl$ [23]. A similar trend has been observed for the free ligand, with depe exhibiting no anti-tumour activity [17]. This has been rationalized by the ease with which depe undergoes oxidation in aqueous media compared to phenyl-substituted diphosphines. Although coordination to Au(I) can protect the phosphine from oxidation, $[Au(depe)_2]^+$ has a lower thermodynamic stability than $[Au(dppe)_2]^+$ and readily decomposes in the presence of Cl^- ions to give the annular complex $[Au_2(depe)_2Cl_2]$ and oxidized depe [12].

1.3 Mode of action

While little is known about the mechanism by which phosphines and their metal complexes kill cells, it has been suggested that the phosphine itself is the cytotoxic agent and the role of the metal may be largely to protect the phosphine and deliver it to cellular targets. The biological profile of the Au(I)diphosphine complexes may results from their high lipophilicity which allows them to penetrate cells and their high kinetic and thermodynamic stability which prevents unwanted side reactions *in vivo* [3]. In addition, the requirement of sufficient lability of the Au-P bond has been proposed, so that the phosphine itself is released at the target site [18]. The Rh(I) complex $[RhCl(PPh_3)dppe]$ and the complexes $[MCl_2(dppe)]$ (M is Pt(II), Pd(II) and Ni(II)) are all inactive against P388 leukaemia [7, 17] which may be attributed to the kinetic stability of the M-P bonds or the non-cationic nature of these complexes. The cytotoxic potency of dppe *in vitro* and its toxicity *in vivo* are significantly increased when it incubated in the presence of non-cytotoxic concentrations of Cu(II) salts, whereas Mg(II), Fe(II), Co(II) and Cd(II) had no effect [20], and has invited the suggestion [3] that a Cu(I)diphosphine may be the ultimate cytotoxic product of the Au(I) and Ag(I) complexes and the ligands themselves. The anti-tumour activity of the uncoordinated ligands is highest for those capable of forming 5- or 6-membered chelating rings, indicating that chelating of metal ions *in vivo* may be important [3].

Although $[Au(dppe)_2]^+$ produced DNA-single strand breaks and DNA-protein cross-links in tumour cells [19] , there is some evidence for an antimitochondrial mode of action [20, 21]. A $[Au(dppe)_2]^+$ resistant subclone of P388 leukemia was found to be highly cross – resistant to Rh123 and other mitochondrial un-couplers, and less capable of sequestering and retaining Rh123 than sensitive cells [20]. The rate of ATP depletion was more rapid in the sensitive than the resistant cells, further suggesting that the cytotoxic mechanism may involve direct interference with mitochondrial function (disruption of ATP synthesis). Furthermore, a related Ag(I) phosphine complex $[Ag(Ph_2P(CH_2)_2PEt_2)_2]^+$, was shown to exhibit selective, primary anti-mitochondrial activity in yeast without major disruption of other cellular functions [22].

Preclinical development of $[Au(dppe)_2]Cl$ was abandoned after the identification of severe hepatotoxicity in dogs [23], attributed to alterations in mitochondrial function [24, 25]. $[Au(dppe)_2]Cl$ is extremely lipophilic (containing eight hydrophobic phenyl substituents) and consequently non-selectively targets mitochondria. This showed very rapid uptake of $[Au(dppe)_2]^+$, changes in O_2 consumption, mitochondrial membrane depolarization, Ca^{2+} efflux, uncoupling of oxidative phosphorylation, ATP depletion and loss of hepatocyte viability within 1 hour of drug exposure [24, 25].

1.4 Recent development

It has recently been suggested that owing to the overall lipophilic cationic nature of $[Au(I)(P\text{-}P)_2]^+$ complexes , that a mode of action involving the mitochondria of targeted cells is implicated [24,25].

1.4.1 Cationic anti-tumour drugs

One of the major roles of mitochondria in the metabolism of eukaryotic cells is the synthesis of ATP by oxidative phosphorylation via the respiratory chain. It was proposed that electrons from the hydrogen on NADH and $FADH_2$ are carried along the respiratory chain at the mitochondrial inner membrane thereby releasing energy that is used to pump protons across the inner membrane from the mitochondrial matrix into the inter-membrane spaces [26]. This process creates a trans-membrane electrochemical gradient, as a consequence of differences in membrane potential (negative inside) and pH differences (acidic outside). The membrane potential of mitochondria *in vitro* is between 180 and 200 mV, which is the maximum a lipid bi-layer can sustain while maintaining its integrity [27]. Although this potential is reduced in living cells and organisms to about 130-150 mV due to metabolic processes such as ATP synthesis and ion transport [28], it is by far the largest within cells. Therefore, positively charged molecules are attracted by mitochondria in response to the highly negative membrane potential. Although most charged molecules cannot enter the mitochondrial matrix because the inner mitochondrial membrane is impermeable to polar molecules, certain amphiphilic compounds are able to

cross both mitochondrial membranes and accumulate in the mitochondrial matrix in response to the negative membrane potential [29].

Among the first described mitochondriotropic cationic amphiphiles were phosphonium salts such as methyltriphenyl phosphonium, which were shown by Liberman *et al*. [30] to be taken up rapidly by mitochondria in living cells. Other examples of mitochondriotropic cations are cynine dyes such as *N,N'*-bis (2-ethyl-1,3-dioxolane) kryptocyanine [31]. It is evident that these mitochondriotropic molecules have two structural features in common. Firstly, they are all amphiphilic in nature, i.e. they combine a hydrophilic charged centre with a hydrophobic core. Secondly, in all structures the π-electron charge density extends to the inter-nuclear region between the hetero-atom and the adjacent carbon atom. This causes a distribution of the positive charge density between two or more atoms, i.e. the positive charge is delocalised.

Mitochondria play a central role in both apoptotic and necrotic cell death [32]. Cells can be considered to die either by a necrotic or an apoptotic pathway: necrotic cell death occurs in response to acute damage and results in rapid, uncontrolled death with subsequent cell-lysis and damaging inflammatory responses. In contrast, during apoptotic cell death an endogenous cell death programme is activated that causes the ordered self-destruction of the cell, ending with its phagocytosis by surrounding cells without leakage of damaging contents and thus no inflammatory responses [33-36]. The distinction between apoptotic and necrotic cell death in response to cell damage is somewhat arbitrary as completion of the apoptotic programme requires ATP, and if the ATP level falls below a critical threshold after initiation of apoptosis the apoptotic programme is aborted and the cell dies by necrosis [37, 38]. Therefore two principally different therapeutic approaches become evident. One approach aims at killing cancer cells by interfering with mitochondrial functions; the other approach is aimed at protecting mitochondria in normal and healthy cell from oxidative damage. The use of lipophilic mitochondriotropic molecules to kill cancer cells is based on the elevated mitochondrial membrane potential many cancer cells have in comparison to normal cells [28, 39, 40]. The higher membrane potential leads to greater accumulation of lipophilic cations in

mitochondria causing cell death by non-specific disruption of mitochondrial functions. Rideout *et al*. have synthesised a whole series of triarylphosphonium salts and shown that these phosphonium salts selectively inhibit growth of carcinoma cells *in vivo*, when compared with normal cells [40].

1.4.2 Lipophilicity, selectivity and anti-tumour activity

The use of aromatic cations (also known as lipophilic cations) as anti-cancer drugs has a long history. Strongly positively charged terephthalanilide derivatives were developed for clinical trials over 30 years ago, but were abandoned because of their toxicity [41]. Studies with other aromatic cations such as rhodamine 123 [42], dequalinium [43] and pyronine Y [44] suggested that a common feature of these compounds is to concentrate in mitochondria. Other investigations led to the identification of active anti-tumour compounds such as ditercalinium [45], AA-1 [46] and MKT-077 [47]. The above mentioned agents appear to have antimitochondrial effects [48, 45].

Studies have shown that there is a parabolic relationship between lipophilicity and anti-tumour properties of aromatic cations [39, 49, 50]. This result was confirmed recently by an independent study [51]. In the same study intermediate lipophilicity showed significant activity with a growth delay of tumour cells [51]. Non specific binding to proteins or other macromolecules might explain the high host toxicity associated with very lipophilic aromatic cations such as SM1 [51]. Another study has shown a relationship between drug lipophilicity and the specificity of binding of aromatic cations to mitochondrial proteins [52]. In contrast, the most hydrophilic compounds may be limited by high rates of excretion as a consequence of low protein binding. Renal clearance has been shown to increase with drug hydrophilicity in another series of compounds [53].

1.4.3 Development of $[Au(P\text{-}P)_2]^+$ type lipophilic cations as anti-tumour agents

The lipophilic cation $[Au(dppe)_2]Cl$ was found to have potent anti-tumour activity *in vitro*, as well as against several tumour models in mice [54]. Moreover, it was active in a cisplatin resistant subline of P388 leukaemia indicating that this class of compounds may have potential for treatment of cisplatin resistant tumours. There was evidence for an antimitochondrial mode of action [21]. However, pre-clinical development of $[Au(dppe)_2]Cl$ was abandoned after the identification of severe hepatoxicity in dogs attributed to alterations in mitochondrial function [23].

The lipophilic cationic properties of $[Au(dppe)_2]Cl$ (contains 8 phenyl groups) promote its non-selective uptake into the mitochondria of all cells (liver and heart are particularly sensitive, being highly aerobic and possessing a high number of mitochondria cell relative to other organs). Initial strategies adopted in previous studies by Berners-Price and co-workers were to develop more hydrophilic analogues that may retain the anti-tumour activity, while being less toxic to mitochondria.

Several classes of lipophilic cations have demonstrated that anti-tumour selectivity is increased as the lipophilic-hydrophilic balance is varied (e.g. bisquaternary ammonium heterocycles [52] and triayalkylphosphonium salts [39]). Bowen and co-workers [55] devised new synthetic routes to 3- and 4-pyridyl substituted phosphines following structural reports of their virtual inaccessibility. They prepared the 3- and 4-pyridyl substituted analogues of $[Au(dppe)_2]Cl$ by replacing some or all of the phenyl substitutents in dppe by hydrophilic pryidyl groups. These variations were designed to encompass a range of water solubilities (as determined by the octanol-water coefficient) and to be representative of symmetric and unsymmetrical bidentate phosphine ligands. In doing so, complexes that have selective anti-tumour activity were identified, and the relationship of activity to the chemistry of the drugs was established.

The 1: 2 adducts of Au(I) and Ag(I) with the ligands d2pype, d3pype and d4pype (where d2pype, d3pype and d4pype are 2-,3- and 4-pyridylphosphine respectively) have octanol/water coefficients between 0.02 and 0.18 and are thus more hydrophilic than the

parent compound $[Au(dppe)_2]^+$ (partition coefficient = 25.4). The compounds were evaluated for anti-tumour activity against a panel of human ovarian carcinoma cell lines *in vitro.* These included examples of cisplatin-sensetive (CH1, 41M) and resistant cell lines which both acquired (CH1cisR, 41McisR) and intrinsic (SKOV3) resistance to cisplatin. The results showed potent and selective activity for the hydrophilic metal complexes with IC_{50} values ranging from 0.18 to 1500 mM [56]. A correlation was established between the degrees of selectivity and octanol-water partition coefficients. For example, the Au(I) 4-pyridyl complex (most hydrophilic) exhibited the greatest selectivity (500- fold range) showing activity against the CH1 and CH1cisR cell lines (IC_{50} of 3.09 and 6.82 μM respectively), but no activity in the 41 M and SKOV3 (IC_{50} > 1000 μM). Increasing the lipophilicity (as in the Ag(I) 3-pyridyl complex) improved the activity in the 41M pair, while retaining activity against the CH1 pair, but SKOV3 was found to be resistant. The Au(I) 2-pyridyl complex was cytotoxic to the CH1 and 41M pairs (IC_{50} > 0.2 – 0.5 μM) as well as the intrinsically cisplatin-resistant SKO3 (IC_{50} = 1.0 μM).

After the development of $[Au(dppe)_2]^+$ was halted by liver toxicity, toxicology studies of the less lipophilic complexes of pyridyl analogues using isolated rat hepatocytes were conducted. The octanol-water coefficients of the pyridyl analogues were used as a means to predict precisely the hepatotoxicity of the complexes [56]. Significantly, cultures of isolated hepatocytes exposed to $[Au(dppe)_2]^+$ leaked lactate dehydrogenase in a concentration and time dependant manner. The Au(I) 4-pyridyl complex in contrast showed no evidence of damage to isolated rat hepatocytes exposed to concentrations of up to 100 μM for up to 24 hours [56].

As noted for some of the asymmetrical bisquaternary ammonium heterocyclic and other phthalanides [51, 58], high tissue concentrations contributed to delayed host toxicity. A similar trend was observed for $[Au(dppe)_2]^+$ during tissue distribution studies which revealed an *in vivo* liver/tumour ratio in mice of 2.26 after 10 days treatement. The hydrophilic cation $[Au(d4pype)_2]^+$ showed higher tumour uptake and a liver/tumour ratio of 0.56. This result was verified with the detection of elevated aminotransferase levels in

$[Au(dppe)_2]^+$ treated mice with advanced Colon 38 adenocarcinoma tumours, whereas none of those treated with $[Au(d4pype)_2]^+$ displayed hepatocellular injury. The tumour growth delay was observed by the most hydrophilic complex, $[Au(d4pype)_2]^+$ (at a dose of 9 μmol/kg/day for 10 days) and this was comparable to those of clinical agents (e.g. cisplatin, carboplatin, etoposide, MKT-077) in this advanced tumour mode [59].

1.4.4 Tin compounds as anti-tumour agents

Organo-tin compounds have shown a wide spectrum of biological effects and have been extensively studied as fungicides, bactericides, acaricides and wood preservatives [60, 61]. They have also shown to have lower toxicity than the corresponding platinum anti-tumour drugs [62]. In 1973 Atushi *et al.* reported the very high affinity of tin compounds for tumours, in fact it was highest among the group 14 elements [62]. Although the first organotin (IV) compound was tested for it's anti-tumour activity in 1929, no systematic study was undertaken until the late 1980's [62].

Barbieri *et al.* [63] prepared some $R_2Sn(IV)$ (R = Me, n-Bu, n-Oct and Ph) complexes of adenine and glycylglycine for their evaluation as potential anti-tumour agents. The hydrolysis of organotin compounds is an important factor for their anti-tumour activities. It was suggested that the action of water on the complex $R_2Sn(IV)(ad)_2$ (see in *ii*) and the adduct $R_2SnX_2 \cdot 2L$ (where R = Me, Et, Pr, n-Bu or Ph; X = F, Cl, Br, I; and 2L = bipyridyl, phenanthroline, 2-aminomethylpyridine) by possible coordination of H_2O to the metal center followed by hydrolysis and dissociation of Sn-N bonds could yield the same tin species. As a consequence, the complex species is transported into the tumour cells which are then attacked by hydrolyzed $R_2Sn(IV)$ moieties.

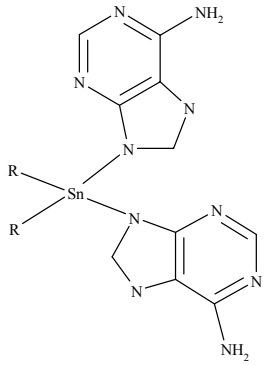

$R_2Sn(ad)_2$, *ii*

Studies by Saxena and Tandon indicated that the presence of highly electronegative groups could greatly enhance the activity of the compounds [64]. Other independent studies indicated that low water solubility of these compounds had a negative impact on their activity [62].

Among the factors responsible for the mode of action of diorganotin compounds R_2SnX_2 is the chain length of the organic group R which also influences the potential activity [65]. Several 1:1 condensation compounds of substituted salicylic acids with diorganotin oxides, having various organic groups R linked to tin, were synthesized and tested for their activity. The results showed all compounds to be less active than the corresponding di-n-butyltin derivatives [65].

A large number of structurally diverse $Bu_2Sn(IV)^{2+}$ carboxylates and other Sn-O bound $Bu_2Sn(IV)^{2+}$ derivatives exhibit consistently high *in vitro* anti-tumour activity and some possess low mammalian toxicity and greater *in vivo* activity than cisplatin. This anti-tumour potency is, in general, structure-dependant, although for some compounds there is evidence of prior hydrolysis to a common $Bu_2Sn(IV)^{2+}$ equivalent species which is responsible for the comparable activity [66, 67].

According to Huber *et al.* the structural effects of all active compounds are characterized by: (i) the availability of coordination sites at Sn, (ii) the occurrence of relatively stable

ligand-Sn bonds and (iii) the possibility of slow hydrolytic decomposition of these bonds [62]. These factors are in agreement with the strong anti-cancer activity of five coordinated Sn (IV) ions as a consequence of the presence of free coordination sites as compared to the lower activity of six coordinated tin(IV) ions [66].

The development of organotin(IV) anti-tumour agents is unfortunately hampered by the paucity of information concerning the cellular targets of these compounds and their mechanism of action, although inhibition of mitochondrial oxidative phosphorylation appears to be an important mode of cytoxicity [68]. $Ph_3Sn(IV)^+$ benzoates exhibit an *in vivo* anti-tumour activity higher than that of cisplatin and comparable with that of mitomycin C [69]. However, recent studies indicated that $Ph_3Sn(IV)$ esters have a greater *in vivo* activity against four human tumour cell lines; this activity is independent of the structure of the moiety and comparable with that of $Ph_3Sn(IV)$ hydroxide, suggesting that hydrolysis affords a common, cytotoxic intermediate [70].

Studies on the hydrolysis of dimethyltin(IV) compounds in aqueous solution indicated that the concentration of various metal species is pH dependant. The most dominant species at particular pH and pK_a values for dimethyltin(IV) species were discussed in relation to their structures [71]. Studies indicate that in acidic media the phosphate groups of DNA can provide suitable sites for dimethyltin ion co-ordination. Above pH 7 the hydrolysis product $R_2Sn(OH)_2$ is the predominant species and the phosphate group of the nucleotide is no longer able to compete with the hydroxide ions [72].

1.4.5 Ruthenium compounds as anti-tumour agents

Many metallic elements play a crucial role in living systems. A characteristic of metals is their ability to easily lose electrons from the familiar elemental or metallic state to form positively charged ions which tend to be soluble in biological fluids. It is in this cationic form that metals play their role in biology. Metal ions are electron deficient, whereas most biological molecules such as proteins and DNA, are electron rich. The attraction of

these opposing charges leads to a general tendency for metal ions to bind to and interact with biological molecules.

The success of cisplatin and related platinum complexes as anti-cancer agents has stimulated a search for other transition metal complexes with anti-tumour activity, and ruthenium in particular has attracted recent attention [73]. The activity of *fac*-$[Ru^{III}Cl_3(NH_3)_3]$ was discovered early [74], but its poor solubility in aqueous media has prevented further use.

Some Ru(III) complexes are known to bind to Fe(III) sites of the proteins lactoferrin and transferrin [75]. The latter is thought to be responsible for the delivery of Ru(III) to cancer cells where it is taken up *via* receptor-mediated endocytosis [76]. Transferrin normally transports Fe(III) in the blood but is only to one third occupied by Fe(III), and so there are vacant sites available for Ru(III) binding.

Another important step in the mechanism of action of Ru(III) complexes is thought to be *in vivo* reduction of the Ru(III) precursor to Ru(II) [77]. The low oxygen content and low pH in tumour cells should favour Ru(II) formation, which generally binds more strongly to bio-molecules than Ru(III), and thus provides for selective cytotoxicity. In 50 mm diameter solid tumours, the relative electrochemical potential was found to be ~100mV lower than in the surrounding normal tissue and this difference is greatest in the centre of the tumour [78]. *In vivo* reduction to Ru(II) can occur by single-electron-transfer proteins, which exist in both the mitochondrial electron-transfer chain and in microsomal electron-transfer systems, with microsomal proteins being more efficient [79].

Owing to the higher metabolism of tumour cells, oxygen is rapidly utilised. In rapidly growing tumours, the growth of new blood vessels often fails to keep pace so that the tissue becomes hypoxic or even anoxic [80]. Glycolysis then becomes the primary energy source, and the production of lactic acid tends to lower the tumour pH [81], which may facilitate the release of ruthenium on histidine or tyrosinate sites on transferrin and also favours the reduction of complexes with a pH-dependant reduction potential [82-84].

1.5 Mixed metals complexes of gold(I)/tin(IV) and gold(I)/ ruthenium(III)

The anti-tumour activity of different metals and ligands was discussed in the previous paragraphs. We were interested to investigate the potential bidentate 2,3-bis(diphenylphosphino) malic acid (dpmaa) as a new class of aromatic lipophilic cations in anti-tumour therapy.

As in the case of dppe, the tetrahedral bis-chelated complex, $[Au(dpmaa)_2]^+$, is available by chelation of the phosphorus atoms of dpmaa to the soft Au(I) center. However, dpmaa provides a site for the formation of stable O-Sn and O-Ru bonds *via* complexation of the bridging carboxyl groups. The resulting mixed Au(I)/Sn and Au(I)/Ru bis-phosphine complexes will not only be unique, but they will offer the advantage of combination chemotherapy in a single drug by virtue of two different modes of action, that is, cytotoxicity by both a mitochondrial mode of action inferred by $[Au(dpmaa)_2]^+$ formation and a cisplatin complementary mode of action inferred by Sn *via* the carboxylate oxygen atoms of the dpmaa ligands.

1.6 Objectives of the project

The thesis is divided into two parts. The objective of part one was the synthesis and characterisation of simple monodentate phosphine halide complexes and their respective 1-azaallyl derivatives. The 1-azaallyl ligand was considered a good candidate for initial studies into Group 11 phosphine complexes due to its well established diversity in bonding modes and the considerable experience with this ligand in our group despite the fact that the stability of the products and therefore their suitability as anti-tumour agents was expected to be rather limited.

The aim of the second part of the project was to develop methods for the synthesis of stable tetra-coordinate Au-, mixed Au/Sn- and Au/Ru-complexes of the bidentate phosphine 2,3-(diphenylphosphino)maleic acid ($dpmaaH_2$). The new complexes were to be fully characterised including X-ray crystallography. Their anti-tumour activity was to

be studied and the influence of the R group on the organotin moiety (R_2Sn) was to be evaluated.

1.7 References

1. P. J. Sadler, *Struct. Bond.,* **1976**, 29, 170.
2. S. J. Berners-Price, P. J. Sadler, (ed. A. V. Xavier), *Frontiers in Bioinorganic Chemistry (VCH Publisher, Weinheim),* **1986**, 376.
3. S. J. Berners-Price, P. J. Sadler, *Struct. Bond.,* **1988**, 70, 27.
4. B. M. Sutton, E. McGusty, D. T. Walz, M. J. DiMartino, *J. Med. Chem.*, **1972**, 15, 1095.
5. R. C. Blodgett, M. A. Heuer, R. G. Pietrusko, *Semin. Arthritis Rheum.,* **1984**, 13, 25.
6. P. Calami, A. Carotti, T. Guerri, L. Messori, E. Mini, P. Orioli, G. P. Speroni, *J. Inorg. Biochem.,* **1997**, 66, 103.
7. R. K. Johnson, C. K. Mirabelli, L. F. Faucette, F. L. McCabe, B. M. Sutton, D. L. Bryan, G. R. Girard, D. T. Hill, *Proc. Amer. Assoc. Cancer Res.,* **1985**, 26, 254.
8. C. K. Mirabelli, L. F. Faucette, F. L. McCabe, B. M. Sutton, D. L. Bryan, G. R. Girard, D. T. Hill, J. O. Bartus, S. T. Crooke, R. K. Johnson, *J. Med. Chem.,* **1987**, 30, 2181.
9. S. J. Berners-Price, P. S. Jarrett, P. J. Sadler, *Inorg. Chem.,* **1987**, 26, 3074.
10. F. Cariati, L. Naldini, G. Simonetta, L. Malatesta, *Inorg. Chim. Acta,* **1967**, 1, 315.
11. S. J. Berners-Price, M. A. Mazid, P. J. Sadler, *J. Chem. Soc., Dalton Trans*., **1984**, 969.
12. S. J. Berners-Price, P. J. Sadler, *Inorg. Chem.,* **1986**, 25, 3822.
13. D. T. Hill, G. R. Girard, *U. S. Patent 4755611 (July)*, **1988**.
14. S. J. Berners-Price, G. R. Girard, D. T. Hill, B. M. Sutton, P. S. Jarrett, L. F. Faucette, R. K. Johnson, C. K. Mirabelli, P. J. Sadler, *J. Med. Chem.,* **1990**, 33, 1386.
15. S. J. Berners-Price, R. K. Johnson, A. J. Giovenella, L. F. Faucette, C. K. Mirabelli, P. J. Sadler, *J. Inorg. Biochem.,* **1988**, 33, 285.
16. S. J. Berners-Price, L. F. Faucette, R. K. Johnson, C. K. Mirabelli, P. J. Sadler, F. L. McCabe, *J. Inorg. Chem.,* **1987**, 26, 3383.
17. S. J. Berners-Price, P. J. Sadler, *Chem. Brit.,* **1987**, 23, 541.

18. S. J. Berners-Price, C. J. Mirabelli, R. K. Johnson, M. R. Mattern, L. F. McCabe, L. Faucette, C. M. Sung, S. -M. Mong, P. J. Sadler, S. T. Crooke, *Cancer Res.*, **1986**, 46, 5486.
19. R. M. Snyder, M. R. Mattern, R. K. Johnson, C. M. Sung, L. F. Faucette, L. F. McCabe, J. P. Zimmerman, M. Whitman, J. C. Hempel, S. T. Crooke, *Cancer Res.*, **1986**, 46, 5054.
20. G. D. Hoke, F. L. McCabe, L. F. Faucette, J. O'L. Bartus, C. –M. Sung, B. D. Jensen, R. Heys, G. F. Rush, D. W. Alberts, R. K. Johnson, C. K. Mirabelli, *Molecular Pharmacol.,* **1991**, 39, 90.
21. Y. Dong, S. J. Berners-Price, D. R. Thorburn, T. Antalis, J. Dickinson, T. Hurst, L. Qui, S. K. Khoo, P. G. Parsons, *Biochem. Pharmacol.,* **1997**, 53, 1673.
22. S. J. Berners-Price, D. C. Collier, M. A. Mazid, P. J. Sadler, R. E. Sue, D. Wilkie, *Metal-Based Drugs,* **1995**, 2, 111.
23. G. F. Rush, D. W. Albers, P. Meunies, K. Leffler, P. F. Smith, *Toxicologist,* **1987**, 7, 59.
24. G. D. Hoke, G. F. Rush, G. E. Bossard, J. V. McArdle, B. D. Jensen, C. K. Mirabelli, *J. Biol. Chem.,* **1988**, 263, 11203.
25. P. F. Smith, G. D. Hoke, D. W. Alberts, P. J. Bugelski, S. Lupo, C. K. Mirabelli, G. F. Rush, *J. Pharmacol. Exp. Therap.,* **1989**, 249, 944.
26. M. P. Mitchell, *Nature*, **1961**, 191**,** 144.
27. M. P. Murphy, *Biochim. Biophys. Acta*, **1989**, 977, 123.
28. M. P. Murphy, R. A. J. Smith; *Adv. Drug Deliv. Rev.*, **2000**, 41, 235.
29. D. G. Nicholls, *Eur. J. Biochem.*, **1974**, 50, 305.
30. E. A. Liberman, V. P. Topaly, L. M. Tsofina, A. A. Jasaitis, V. P. Skulachev, *Nature*, **1969**, 222, 1076.
31. A. R. Oseroff, D. Ohuoha, G. Are, D. McAuliffe, J. Foley, L. Cincotta, *Proc. Natl. Acad. Sci. USA*, **1986**, 83, 9729.
32. G. Schatz, *J. Biol. Chem.*, **1996**, 271, 31763.
33. D. L. Vaux, A. Strasser, *Proc. Natl. Acad. Sci. USA*, **1996**, 93, 2239.
34. J. F. R. Kerr, A. H. Wyllie, A. R. Currie, *Br. J. Cancer*, **1972**, 26, 239.

35. A. J. Hale, C. A. Smith, L. C. Sutherland, V. E. A. Stoneman, V. L. Longthorne, A. C. Culhane, G. T. Williams, *Eur. J. Biochem.*, **1996**, 236, 1.
36. A. H. Wyllie, J. F. R. Kerr, A. R. Currie, *Int. Rev. Cytol.*, **1980**, 68, 251.
37. M. Lesis, P. Nicotera, *Exp. Cell Res.*, **1998**, 239, 183.
38. M. Lesis, P. Nicotera, *Biochem. Biophys. Res. Commun.*, **1997**, 236, 1.
39. D. C. Rideout, T. Calogeropoulous, J. S. Jaworski, R. Dagnino, M. R. McCarthy, *Anti-cancer drug Des*., **1987**, 4, 5444.
40. J. S. Modica-Napolitano, J. R. Aprille, *Adv. Drug Deliv. Rev.*, **2001**, 49, 63.
41. L. L. Bennett, *Prog. Exp. Tumour Res.*, **1965**, 7, 259.
42. L. V. Johnson, M. L. Walsh, L. B. Chen, *Proc. Natl. Acad. Sci. USA*, **1980**, 77, 990.
43. M. J. Weiss, J. R. Wong, C. S. Ha, R. Bleday, R. R. Salem, G. D. Steele, L. B. Chen, *Proc. Natl. Acad. Sci. USA*, **1987**, 84, 5444.
44. Z. Darzynkiewicz, J. Kapuscinsky, S. P. Carter, F. A. Schmid, M. R. Melamed, *Cancer Res.*, **1986**, 46, 5760.
45. B. P. Roques, D. Pelaprat, G. I. Le, G. Porcher, C. Gosse, J. B. Pecq Le, *Biochem. Pharmacol.*, **1979**, 28, 1811.
46. X. Sun, J. R. Wong, K. Song, J. Hu, K. D. Garlid, L. B. Chen, *Cancer Res.*, **1994**, 54, 1465.
47. K. Koya, Y. Li, H. Wang, T. Ukai, N. Tatsuta, M. Kawakami, Shishido, L. B. Chen, *Cancer Res.*, **1996**, 56, 538.
48. J. S. Modica-Napolitano, K. Koya, E. Weisberg, B. T. Brunelli, Y. Li, L. B. Chen, *Cancer Res.*, **1996** , 56, 544.
49. B. F. Cain, G. J. Atwell, R. N. Seelye, *J. Med. Chem.*, **1969**, 12, 199.
50. W. A. Denny, G. J. Atweel, B. C. Baguley, B. F. Cain, *J. Med. Chem.*, **1979**, 22, 134.
51. M. J. McKeage, S. J. Berners-Price, P. Galettis, R. J. Bowen, W. Brouwer, L. Ding, L. Zhuang, B. C. Baguley, *Cancer Chemother. Pharmacol.*, **2000**, 46, 343.
52. K. Schneider, A. Naujok, H. W. Zimmermann, *Histochemistry*, **1994**, 101,
53. J. K. Seydel, K-J. Schaper, *Parmacokinetics and methodology, Pergamon Press, Oxford,* **1986**, pp 311.

54. P. A. Andrews, K. D. Albright, *Cancer Res.*, **1992**, 52, 1895.
55. R. J. Bowen, A. C. Garner, S. J. Bernes-Price, I. D. Jenkis, R. E. Sue, *J. Organomet. Chem.,* **1998**, 554, 81.
56. S. J. Berners-Price, R. J. Bowen, P. Galettis, P. C. Healy, M. McKeage, *J. Coord. Chem. Rev.,* **1999**, 185, 823.
57. J. Plowman, R. H. Adamson, *Pharmacology,* **1978**, 17, 61.
58. C. J. Kensler, P. E. Palm, H. M. Day, S. P. Battista, W. I. Rogers, D. W. Tesair, I. Woinski, *Cancer Res.,* **1965**, 25, 1622.
59. M. J. McKeage, unpublished results
60. C. J. Evans, S. Karpel; *J. Organomet. Chem.*, **1985**, 16, 1.
61. A. K. Saxena, *Appl. Organomet. Chem*., **1987**, 1, 39.
62. A. K. Saxena, F. Huber, *Coord. Chem. Rev*., **1989**, 95, 109.
63. R. Barbieri, L. Pellerito, G. Ruisi, M. T. Lo Giudice, F. Huber, G. Atassi, *Inorg. Chim. Acta*, **1982**, 66, L39.
64. A. Saxena, J. P. Tandon, C*ancer Lett.*, **1983**, 19, 73.
65. M. Gielen, *Coord. Chem. Rev.*, **1996**, 151, 41.
66. M. N. Xanthopoulou, S. K. Hadjikakou, N. Hadjiliadis, M. Scurmann, K. Jurkschat, A. Michaelides, S. Skoulika, T. Bakas, J. Binolis, S. Karkabounas, K. Charalabopoulos, *J. Inorg. Biochem.*, **2003**, 96, 425.
67. A. H. Pennink, M. Bol-Schooenmakers, M. Gellen, W. Sienen, *Main Group Met. Chem.*, **1989**, 12, 1.
68. A. K. Saxena, *Appl. Organomet. Chem.*, **1987**, 1, 39
69. M. Gielen, R. Willem, M. Biesemans, M. Boualam, A. El. Khloufi, D. de Vos, *Appl. Organomet. Chem.*, **1992**, 6, 287.
70. C. J. Traanter, S. J. Berners-Price, J. Cutts, P. G. Parsons, G. Rintoul, D. J. Young, *Main Group Chem.*, **1995**, 1, 165.
71. T. Natsume, S. Aizawa, K. Hatano, S. Funahashi, *J. Chem. Soc., Dalton Trans.*, **1994**, 2749.

72. A. Jancso, L. Nagy, E. Moldrhem, E. Sletten, *J. Chem. Soc., Dalton Trans*., **1999**, 1587.
73. M. J. Clarke, F. Zhu, D. R. Fresaca, *Chem. Rev.*, **1999**, 99, 2511.
74. M. J. Clarke, *Met. Ions Bio. Syst.*, **1980**, 11, 231.
75. C.A. Smith, A. J. Surland Smith, B. K. Keppler, F. Kratz, E. N. Baker, *J. Bio. Inorg. Chem.*, **1996**, 1, 424.
76. D. Frasca, J. Ciampa, J. Emerson, R. S. Umans, M. J. Clarke, *Metal-Based Drugs*, **1996**, 3, 197.
77. M. J. Clarke, *In Metal Complexes in Cancer Chemotherapy,* B. K. Keppler, Ed; VCH: Weinhem, **1993**.
78. D. Miklavcic, G. Sersa, S. Novakovic, *J. Bioelect.*, **1990**, 9, 133.
79. M. J. Clarke, S. Bitler, D. Rennert, M. Buchbinder, A. D. Kelman, *J. Inorg. Biochem.*, **1980**, 12, 79.
80. B. D. Palmer, W. R. Willson, S. M. Pullen, *J. Med. Chem.*, **1990**, 33, 112.
81. J. L. Wike-Hooley, J. Haveman, H. S. Reinhold, *Radiother. Oncol.*, **1984**, 2, 343.
82. O. M. N. Dhubghaill, W. Hagen, B. K. Keppler, K. G. Lipponer, P. J. Sadler, *J. Chem. Soc., Dalton Trans.*, **1994**, 3305.
83. F. Kratz, M. Hartmann, B. Keppler, L. Messori, *J. Biol. Chem.*, **1994,** 269, 2581.
84. P. Vaupel, K. Schlenger, C. Knoop, M. Hockel, *Cancer Res.*, **1991**, 51, 3316.

Chapter Two

2.0 Results and discussion of 1-azaallyl complexes *

2.1 Introduction

We were interested to investigate monodentate isopropyl phosphine complexes of Group 11 metals with halides or 1-azaallyl as counter ions due to our longstanding interest in this type of ligands.

The steric and the electronic properties of the 1-azaallyl ligands give access to complexes with the metal in an unusual oxidation state or coordination number. The 1-azaallyl ligand **A** (see in *iii*) related to the allyl ligand **B**, consists of an N···C···C backbone, shown here in the η^3-mode, i.e. with a delocalized negative charge. A closely similar class of compounds is the alky functionalised pyridyls **C**, related to the benzyl anion **D**. However, they are not 'true' 1-azaallyls in that the nitrogen cannot bear a negative charge unless the pyridine ring loses its aromaticity.

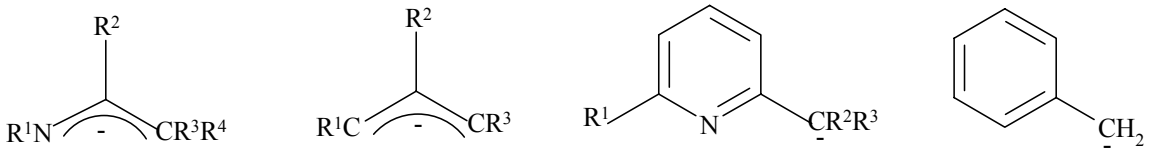

A **B** **C** **D**

Known types of 1-azaallyl ligands, *iii*

The 1-azaallyl ligands have flexibility in adopting different bonding modes as shown in **I - IV** (see in *iv*) depending on the nature of the substituent groups on the ligand, the nature of the metal and the presence or absence of a neutral co-ligand(s) [7]. The enamido configuration **I** is favoured usually in complexes containing bulky 1-azaallyl ligands or where a strong neutral donor such as thf is present, as in $[Li\{\mu\text{-}N(R)C(Ph)C(H)R\}(thf)]_2$ [9]. A bonding mode of **II** is exemplified in this thesis. Configuration **III** is the most common; the presence of sterically hindering groups on the N···C···C backbone serves to

*Published in *Polyhdron*, 2004, 23, 2273.

afford thermally stable compounds of metals in a low-coordination environment. The extent of asymmetrical bonding is dependent upon the natures of the substituent groups. The bridging mode of **IV** has been observed in metal complexes $[M\{\mu\text{-}CR_2(C_5H_4N\text{-}2)\}]_2$ (Li, Cu, Ag or Au) [11, 12] or $[Cu\{\mu\text{-}N(R)C(bu^t)C(H)R\}]_2$ [13] and $[M\{\mu\text{-}N(R)C(Ph)CR_2\}]$ [14] (M = Cu or Au, R = $SiMe_3$) forming eight-membered metallacycles with the trimethylsilyl groups assisting in the stabilization of the two-coordinated metal environments.

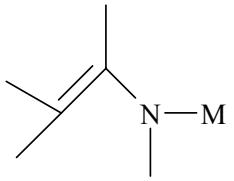

I

η^1-enamido

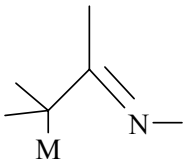

II

η^1-iminoalkyl

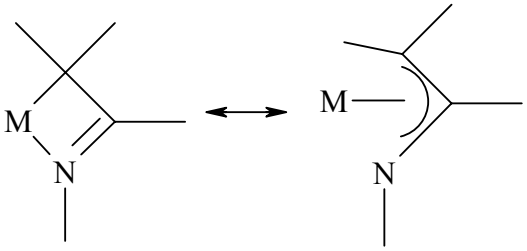

III

η^3-azaallyl

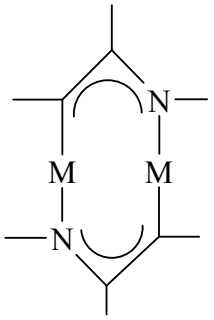

IV

μ^2-bridging

Bonding modes and structural features of 1-azaallyl complexes, *iv*

1-azaallyl complexes of the monomeric phosphine adduct $Ph_3PCu\{\mu\text{-}N(R)C(bu^t)C(H)R\}$ and a lithium cupate $(dme)_3LiCu\{\mu\text{-}N(R)C(bu^t)C(H)R\}_2$ (dme = dimethoxyethane; where R = $SiMe_3$) have been reported [13].

2.1.1 General methods of preparation of 1-azaallyl metal complexes

Two main principal routes exist for preparation of lithium 1-azaallyls. The first involves deprotonation of an aldimine, ketimine or similar unsaturated species, Eq. (1) [8].

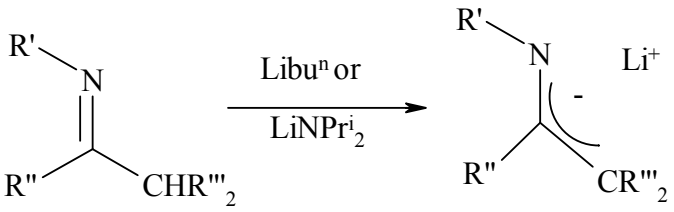

(1)

R', R" or R'"= H, alkyl or aryl

The second route to alkali metal 1-azaallyls is by insertion of an alkali metal bis(trimethysilyl)methyl (≡ $MCHR_2$, R = $SiMe_3$) (or a related compound) in to an α-H-free nitrile R'CN (R' = bu), e.g. Eq. (2) [9, 10].

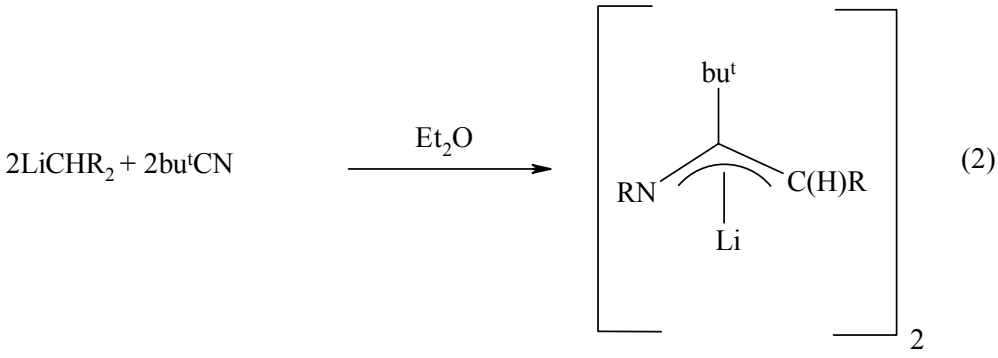

(2)

The latter method (Eq. (2)) was chosen for the synthesis of the Li-azaallyl precursor used in the following section.

2.2 Synthesis

Ph_3PCuLL' [LL' = $CH(SiMe_3)(bu^t)NSiMe_3$] had previously been synthesised by the addition of stoichiometric amounts of triphenylphosphine to the dimeric complex $[CuLL']_2$ [13] [*c.f.* (i) in Scheme 1]. The same synthetic route gave the copper complex bu^i_3PCuLL' 3a in moderate yield [(i) in Scheme 1] but was not applicable for the Ag and Au analogues as the respective parent compounds [MLL'] were not accessible. It was therefore, decided to first synthesise the easily accessible and stable phosphine adducts bu^i_3PM-X 2a-d from the metal halides and free phosphine [(ii) in Scheme 1], which were then reacted with $[LiLL']_2$ [15] to give the 1-azaallyl complexes bu^i_3PMLL' **3a-c** [(iii) in Scheme 1]. [bu^i_3P] was selected as the phosphine of choice as its sterically demanding alkyl groups were expected to convey stability to the metal complexes as well as solubility in non-polar solvents. Preliminary experiments involving the treatment of $(Me_2S)AuCl$ with PPh_3 and subsequent reaction with $[LiLL']_2$ [15] led to the NMR-spectroscopically characterised complex $[Ph_3PAuLL']$ but attempts to purify the product by recrystallisation had been unsuccessful. The bu^i_3P-derivatives 3a-c were in contrast obtained after recrystallisation from hexane as colourless, air- and moisture sensitive crystals in moderate to high yields. While **3c** was indefinitely stable at room temperature in an inert gas atmosphere, the copper (**3a**) and especially the silver analogue (**3b**) were found to be sensitive to light and heat, depositing metal from dissolved and solid samples of the complex even at low temperatures. An attempt to synthesise the aurate complex $[(dme)_3LiAu(LL')_2]$ from **3c** and a second equivalent of $[LiLL']_2$ [15] in the presence of dme was not successful and led to the recovery of the starting materials.

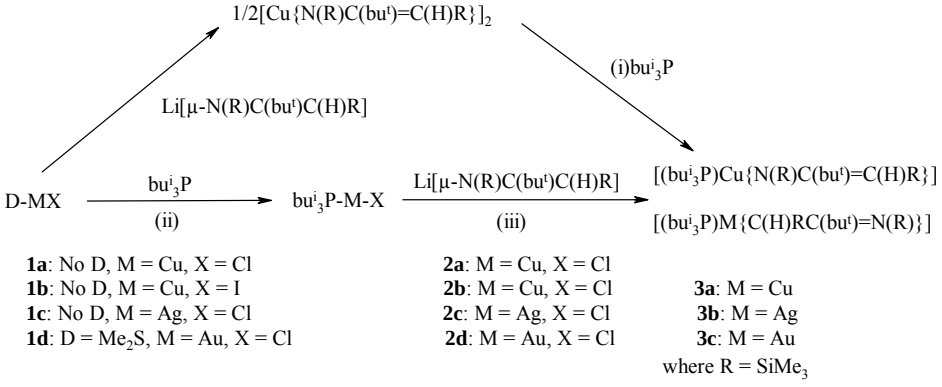

Scheme 1. Synthesis of Group 11 metal 1-azaallyl complexes

2.3 NMR-spectroscopic studies and solution behaviour

Table 1. Selected NMR-spectroscopic data of 1-azaallyl metal complexes in ppm

Compound	CH (^{1}H)	CH (^{13}C)	CN (^{13}C)	^{31}P	Bonding mode*	Ref.
$[(dme)_3LiCuLL'_2]$	5.05	101.9	177.5	-	(I)	13
$[Ph_3PCuLL']$	4.83	101.9	182.3	12.7	(I)	13
$[LiLL']_2$	4.54	93.7	170.8	-	(I,III)	15
$[bu^i_3PCuLL']$ (**3a)**	4.95	103.1	177.8	-19.1	(I)	This work
$[CuLL']_2$	3.11	48.1	220.8	-	(IV)	15
$[bu^i_3PAgLL']$ (**3b)**	3.50	60.1	189.8	-17.4	(II)	This work
$[Ph_3PAuLL']$	3.10 (d)	-	-	42.2	(II)	This work
$[bu^i_3PAuLL']$ (**3c)**	3.01 (d)	50.3 (d)	193.7	21.4	(II)	This work
$[Ph_3PNi(LL')]$	2.50 (d)	56.1 (d)	172.1	31.0	(III)	25

LL' = $CH(SiMe_3)(bu^t)NSiMe_3$

*See bonding modes in *iv*

It had been shown previously that ^{1}H- and ^{13}C-NMR spectroscopy is a powerful tool to distinguish different bonding modes in 1-azaallyl complexes [13, 16]. Table 1 summarises NMR-spectroscopic data of **3a-c** and some related metal complexes featuring the LL' ligand. Previously a signal at low frequency in the ^{1}H- ($\delta \approx 3$) and ^{13}C- ($\delta \approx 50$) NMR spectrum for CH and a signal at high frequency for CN ($\delta \approx 190$) was found to be indicative for an iminoalkyl metal complex (II) while the reverse situation with signals for CH at high frequency [$\delta \approx 5$ (^{1}H), 100 (^{13}C)] and CN at low frequency [$\delta \approx 180$ (^{13}C)] were observed for enamide metal complexes (I). In line with this interpretation the copper phosphine complexes $[Ph_3PCuLL']$ and $[bu^i_3PCuLL']$ **3a** may be classified as enamide complexes (I) with a direct bond between Cu and N and no direct contact to CH while the heavier analogues $[bu^i_3PAgLL']$ **3b**, $[Ph_3PAuLL']$ and $[bu^i_3PAuLL']$ **3c** are better described as iminoalkyl complexes (II).

Further support for this classification comes from the ^{1}H- and ^{13}C-NMR spectra of **3c** that show doublets for the CH group of the 1-azaallyl ligand with coupling constants

$^{3}J(^{31}P,^{1}H)$ and $^{2}J(^{31}P,^{13}C)$ of 10.9 (10.5 for Ph_3PAuLL') and 56.3 Hz, respectively, as a consequence of coupling to P. Coupling constants for $^{3}J(^{31}P,^{1}H)$ in the region of 4 – 16 Hz and $^{2}J(^{31}P,^{13}C)$ around 100 Hz have been reported for other phosphine alkyl complexes [17-21] .

The silver complex **3b** in contrast showed singlets in the ^{13}C-NMR (δ = 24.6) and the ^{1}H NMR spectrum (δ = 3.50). The latter was broad and probably not resolved due to additional $J(^{109/107}Ag,^{13}C)$ coupling and the occurrence of exchange between **3b** and free bu^{i}_3P formed from the decomposition of the silver complex. Similar observations have previously been described for phosphine gold complexes [$RAuPR_3'$] (R = alkyl, R' = alkyl, aryl) where the doublet of the HCAu-fragment either broadens significantly [21] or else collapses to a sharp singlet [20] as a consequence of the addition of small quantities of free phosphine to the metal complexes.

A noteworthy observation is the appearance of two overlapping doublets (attributable to unequal $^{1}J(^{31}P\text{-}^{109}Ag)$ and $^{1}J(^{31}P\text{-}^{107}Ag)$ coupling constants) in the $^{31}P\{^{1}H\}$ NMR spectrum at near ambient temperature (298 K). This is unusual for monodentate phosphine silver complexes, since rapid ligand exchange usually precludes the observation of P-Ag spin-spin coupling. For example, for a series of $[XAg\{ (P(p\text{-tol})_3\}_n]$ complexes (where n = 2-4 and X = a range of counter-anions), the ligands were labile in all the complexes studied so that P-Ag spin-spin coupling was not resolved above –70 °C [22]. Where ligands are too sterically encumbered to participate in the association process believed to be involved in the exchange, most notably, $[Ag(P(trimethyl)_3)_2]$ and $[Ag(P(bu^{t})_3)_2]$, well resolved P-Ag spin-spin coupling is exhibited at ambient temperature [23, 24].

Consistent with the copper complexes being enamide complexes (I) no coupling was observed in their ^{1}H- or ^{13}C-NMR spectrum. The solid state structures of $[Ph_3PCuLL']$ [13], $[(dme)_3LiCuLL'_2]$ [1] and $[bu^{i}_3PAuLL']$ (see Fig. 3) lend the above arguments further support.

The distinction between an η^3-1-azaallyl (III) and an iminoalkyl metal complex (II) on the basis of NMR spectroscopy is however, more ambiguous as may be deduced from the close similarity of the NMR-spectrum (*c.f.* Table 1) of [$Ph_3PNi(I)LL'$] [25] as an example for an η^3-1-azaallyl complex (III) and the discussed iminoalkyl metal complexes (II).

The observed difference in bonding modes between Cu- and Ag/Au-azaallyl complexes, respectively, may be explained on the basis of HSAB theory [26] with the softer, larger metal ion [Ag(I), Au(I)] having a preference for the softer atom (C^-) of the bidentate 1-azaallyl ligand and the harder cation [Cu(I)] binding preferentially to the harder atom (N^-).

2.4 Solid state structures of complexes 2c, 2d and 3c

2.4.1 **Introduction**

Copper- and silver phosphine halides of monodentate phosphines are frequently found to aggregate in the solid state into dimers or higher molecular species by increasing the coordination number of the metal via additional metal halogen bonds [27, 28]. Gold analogues in contrast are known to show linear two coordinate metal atoms that may dimerise via relativistic Au···Au interactions [28, 29]. In order to minimise steric repulsion between the phosphine substituents while at the same time maximising aurophilic interactions the dimers are arranged in a paddle-like fashion with P-Au-Au-P torsion angles close to 90° [28-30]. Mononuclear complexes in contrast are found sterically demanding phosphines with cone angles [31] larger than 130°.

2.4.2 Crystal structure of compound 2c

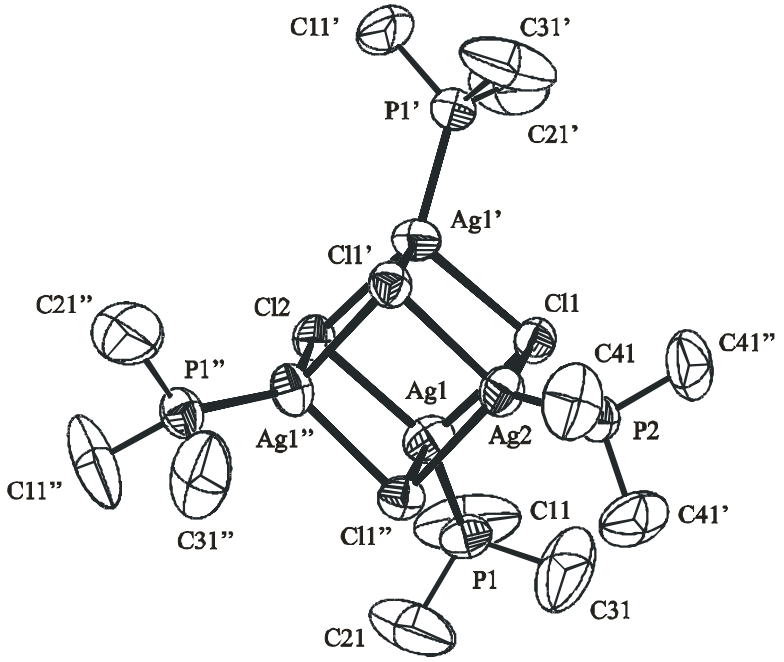

Figure 1. Molecular structure of $[bu^{i}_{3}PAgCl]_4$ **2c**. Thermal ellipsoids are drawn on the 30% probability level. H atoms and isobutyl groups except C atoms directly bound to P have been omitted for clarity.

Table 2. Selected bond distances (Å) and angles (°) for compound **2c**

Ag1-P1	2.371(2)	Ag2-P2	2.383(4)
Ag1-Cl1	2.645(3)	Ag1-Cl2	2.648(2)
Ag1-Cl1*	2.690(2)	Ag2-Cl1	2.676(3)
Cl1-Ag1-Cl2	94.00(6)	Cl1-Ag1-Cl1*	93.04(11)
Cl2-Ag1-Cl1*	92.99(6)	Cl1-Ag2-Cl1**	92.67(8)
Ag1-Cl1-Ag2	87.50(6)	Ag1-Cl1-Ag1**	86.03(8)
Ag2-Cl1-Ag1**	86.60(6)	Ag1'-Cl2-Ag1**	86.81(8)

Symmetry transformations used to generate equivalent atoms:

* –x + y + 1, -x + 2, z ; ** –y + 2, x – y + 1, z

$[bu^{i}_{3}PAgCl]_4$ **2c** crystallises as a tetramer with a cubic AgCl core that has three-fold rotation symmetry (Fig. 1). The Cl-Ag-Cl and Ag-Cl-Ag angles (see Table 2) are close to 90° with the former being slightly larger [92.67(8) – 94.00(6)°] than the latter [86.03(8) – 87.50(6)°]. A considerably larger distortion of the cube was observed in $[(2\text{-}Py_2Ph)PAgCl]_4$ [32] and $[Ph_3PAgCl]_4$ [33]. The Ag-P and Ag-Cl distances of 2.371(2), 2.383(4) and 2.645(3), 2.648(2), 2.690(2), 2.676(3) Å, respectively, in **2c** compare well to those found in related complexes such as $[(H_{11}C_6)_3PAuCl]_4$ [34] or $[Et_3PAgCl]_4$,[35] (see also references 29, 30).

2.4.3 Crystal structure of compound 2d

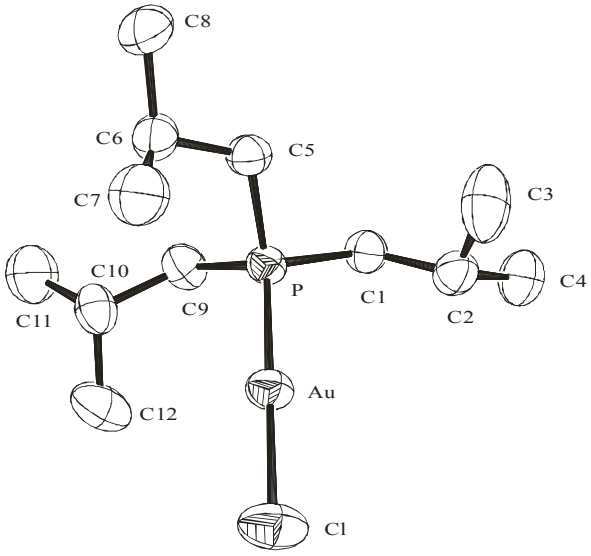

Figure 2a. Molecular structure of $[bu^{i}_{3}PAuCl]$ **2d**. Thermal ellipsoids are drawn on the 50% probability level. H atoms have been omitted for clarity.

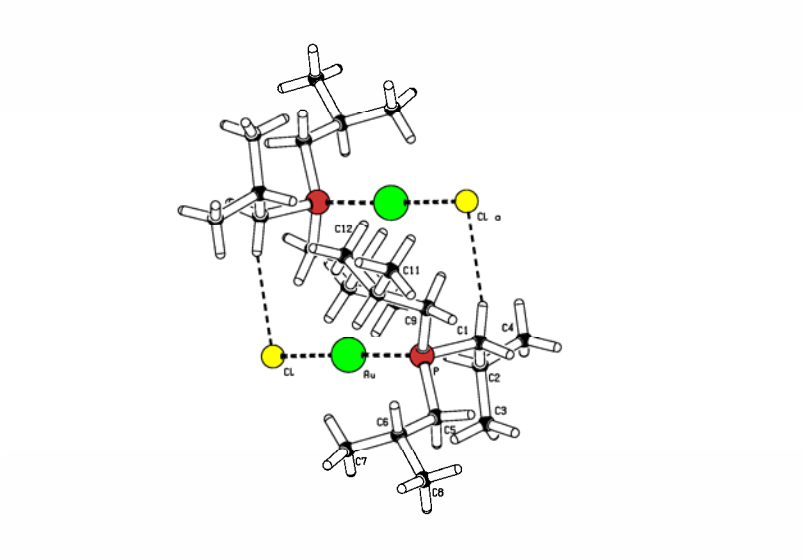

Figure 2b. Molecular structure of bu$^{i}_{3}$PAuCl showing CH···Cl contacts

Table 3. Selected bond distances (Å) and angles (°) for compound **2d**

Au-P	2.239(1)	Au-Cl	2.292(1)
P-C1	1.830(3)	P-C5	1.833(3)
P-C3	1.827(4)		
C1-H1···Cl'	2.82	C1···Cl	3.76
P-Au-Cl	178.41(3)	C1-H1-Cl'	164.96

[bu$^{i}_{3}$PAuCl] **2d** (cone angle for Pbu$^{i}_{3}$ is 143°) [31] is a monomer (shortest Au···Au contact 4.450 Å; Fig. 2a) in the solid state with a linear two coordinate gold atom [(P-Au-Cl 178.41(3)°]. The Au-P and Au-Cl bond distances of 2.239(1) and 2.292(1) Å are comparable to related complexes such as (c-$H_{11}C_6$)$_3$PAuCl, [36] (H_7C_{10})$_3$PAuCl, [37] (TPA)AuCl (TPA = 1,3,5-triaza-7-phosphaadamantane), [30] Et_3PAuCl, [38] (NCCH_2CH_2)$_3$PAuCl [39] , 2-Py_3PAuCl [40], Ph_3PAuCl [41] or Pr$^{i}_{3}$PAuCl [42] but slightly shorter than those in related silver complexes. This is thought to be a consequence of the relativistic contraction of gold [28, 43]. Two monomeric units of **2d** are linked via weak CH···Cl contacts (C1-H1···C1' 2.82 Å, Fig. 2b) between the Cl atom

and a CH_2 group of the neighbouring phosphine (Fig. 2b). $(c\text{-}H_{11}C_6)_3PAuCl$ was found to associate in a similar fashion to polymeric chains (Cl···HC 2.91 – 3.27 Å) [36a].

2.4.4 Crystal structure of compound 3c

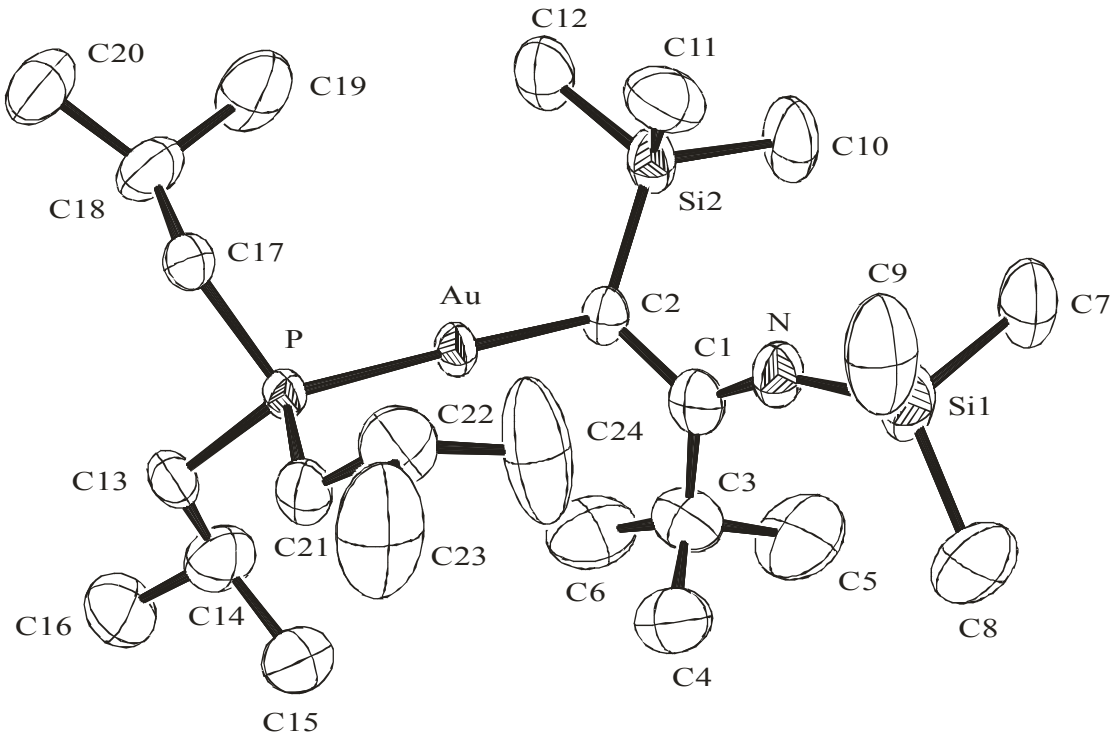

Figure 3. Molecular structure of [bu$^i_3$PAuLL'] **3c**. Thermal ellipsoids are drawn on the 50% probability level. H atoms have been omitted for clarity.

Table 4. Selected bond distances (Å) and angles (°) for compound **3c**

Au-P	2.284(1)	Au-C2	2.100(5)
N-C1	1.266(6)	C1-C2	1.493(7)
P-C13	1.842(5)	P-C17	1.830(5)
P-C21	1.825(5)		
C2-Au-P	178.3(1)		

Compound **3c** crystallises in the monoclinic space group $P2_1/n$ with one molecule in the asymmetric unit (Fig. 3). It is a monomer with a linear P-Au-C unit [P-Au-C2 178.3 (1)°] and represents the first example of a crystallographically characterised 1-azaallyl complex [44] that adopts an iminoalkyl configuration (II) and may be best compared to the enolate complex $Ph_3PAuCH_2C(O)Ph$ [45]. The Au-P distance of 2.284(1) Å is unexceptional as is the Au-C2 distance of 2.100(5) Å that is within the range expected for a Au-C σ bond to an sp^3-hybridised C-atom [$Ph_3PAuCH_2C(O)Ph$ [45] , $Ph_3PAuCH_2CH_2C(O)Ph$ [45], $Ph_3PAuC_5HPh_4$ [21], Ph_3PAuMe [46], Ph_3PAuCH_2Cl [18], Ph_3PAuCH_2SPh [18], $Ph_3PAuCH(SiMe_3)_2$ [17], $Ph_3PAuC_{13}H_9$ [19]] but slightly longer than those found in aryl gold complexes as for example $Ph_3PAuC_6H_3(OMe)_2$-2,6 [47], bu^t_3PAuPh [48], $Ph_3PAuC_4H_4O$ [49] or $Ph_3PAuC_6H_2Mes_3$-2,4,6 [50] (2.04 – 2.08 Å). The coordination geometry around C2 is a distorted tetrahedron with the angle C1-C2-Si1 (114.2°) between the bulkiest groups showing the largest deviation from 109.5°. The iminoalkyl configuration is further confirmed by the C1-C2 and C2-N bond distances of 1.493(7) and 1.266 (6) Å that correspond to C-C single and CN double bonds, respectively. The sum of angles is 360° around the N atom are in line with an sp^2-hybridisation at the N.

2.5 References

1 A. J. Pearson, *Syn. lett.*, **1990**, 10.

2 S. L. Blystone, *Chem. Rev.,* **1989**, 89, 1663.

3 J. W. Faller, K.-H. Chao, *J. Am. Chem. Soc.,* **1983,** 105, 3893.

4 K. Yamamoto, J. Tsuji, *Tetrahedron Lett.,* **1982**, 23, 3089.

5 B. M. Trost, *Tetrahedron,* **1977**, 33, 2615.

6 B. M. Trost, T. R. Verhoeven, *Comprehensive Organomet. Chem.,* **1982**, 8, 799 (and references therein).

7 C. F. Caro, M. F. Lappert, P. G. Merle, *Coord. Chem. Rev.,* **2001**, 605, 219.

8 J. K. Whitesell, M. A. Whitesell, *Synthesis*, **1983**, 517.

9 P.B. Hitchcock, M.F. Lappert, M. Layh, D.S. Liu, R. Sablong, T. Shun, *J. Chem. Soc., Dalton Trans*., **2000**, 2301.

10 P.B. Hitchcock, M.F. Lappert, D.S. Liu, *J. Chem. Soc., Chem. Commun*., **1994**, 2637.

11 R. I. Papasergio, C. L. Raston, A. H. White, *J. Chem. Soc., Chem. Commun.*, **1983**, 1419.

12 R. I. Papasergio, C. L. Raston, A. H. White, *J. Chem. Soc., Dalton Trans.*, **1987**, 3085.

13 P.B. Hitchcock, M.F. Lappert, M. Layh, *J. Chem. Soc., Dalton Trans.,* **1998**, 1619.

14 P.B. Hitchcock, M.F. Lappert, M. Layh, A. Klein*, J. Chem. Soc., Dalton Trans.,* **1999**, 1455.

15 P.B. Hitchcock, M.F. Lappert, D.-S. Liu, *J. Chem. Soc., Chem. Commun.,* **1994**, 1699.

16 P.B. Hitchcock, J. Hu, M.F. Lappert, M. Layh, J. Severn, *J. Chem. Soc., Chem. Commun.,* **1997**, 1189.

17 S. Bommers, H. Beruda, N. Dufour, M. Paul, A. Schier, H. Schmidbaur, *Chem. Ber.,* **1995**, 128, 137.

18 D. Steinborn, S. Becke, R. Herzog, M. Günther, R. Kircheisen, H. Stoeckli-Evans, C. Bruhn, *Z. Anorg. Allg. Chem.,* **1988**, 624, 1303.

19 Y.T. Struchkov, Y.L. Slovokhotov, D.N. Kravtsov, T.V. Baukova, *J. Organomet. Chem.,* **1988**, 338, 269.

20 H. Schmidbaur, A. Shiotani, *Chem. Ber.,* **1971**, 104, 2821.

21 T.V. Baukova, Y.L. Slovokhotov, Y.T. Struchkov, *J. Organomet. Chem.,* 1981, 220, 125.

22 E.L. Muetterties, C.W. Alegranti, *J. Am. Chem. Soc.,* **1972**, 94, 6386.

23 R.C. Gael, P. Pilon, *Inorg. Chem.*, **1978**, 17, 2876.

24 E.C. Alyea, S.A. Dias, S. Stevens, *Inorg. Chim.*, **1980**, 44, L203.

25 P.B. Hitchcock, M.F. Lappert, M. Layh, *Z. Anorg. Allg. Chem*., 2000, 626, 1081.

26 (a) R.G. Pearson, *J. Am. Chem. Soc.,* **1963**, 85, 3533. (b) R.G. Pearson, *Inorg. Chem.*, **1988**, 27, 734. (c) R.G. Pearson, *Inorg. Chim. Acta,* **1995**, 240, 93.

27 P.D. Akrivos, H.J. Katsikis, A. Koumoutsi, *Coord. Chem. Rev.,* **1997**, 167, 95.

28 P. Schwerdtfeger, H.L. Hermann, H. Schmidbaur, *Inorg. Chem.,* **2003**, 42, 1334.

29 P. Pyykkö *Chem. Rev.,* **1997**, 97, 597.

30 Z. Assefa, B.G. McBurnett, R.J. Staples, J.P. Jr Fackler, B. Assmann, K. Angermaier, H. Schmidbaur, *Inorg. Chem.,* **1995**, 34, 75.

31 C.A. Tolman, *Chem. Rev.*, **1977**, 315.

32 Y. Inoguchi, B. Milewski-Mahrla, D. Neugebauer, P.G. Jones, H. Schmidbaur, *Chem. Ber.,* **1983**, 116, 1487.

33 B.-K. Teo, J. Calabrese, *Inorg. Chem.,* **1976**, 15, 2467.

34 G.A. Bowmaker, Effendy, P.J. Harvey, P.C. Healy, B.W. Skelton, A.H. White, *J. Chem. Soc., Dalton Trans.,* **1996**, 2459.

35 M.R. Churchill, J. Donahue, F. Rotella, *Inorg. Chem.,* **1976**, 15, 2752.

36 (a) R.C. Bott, G.A. Bowmaker, R.W. Buckley, P.C. Healy, M.C.S. Perera, *Aust. J. Chem.,* **1999**, 52, 271. (b) J.A. Muir, M.M. Muir, L.B. Pulgar, *Acta Cryst.,* **1985**, C41, 1174.

37 T.E. Müller, J.C. Green, D.M.P. Mingos, C.M. McPartlin, C. Wittingham, D.J. Williams, T.M. Woodroffe, *J. Organomet. Chem.,* **1998**, 551, 313.

38 E.R.T. Tiekink, *Acta Cryst.,* **1989**, C45, 1233.

39 J.P. Jr Fackler, R.J. Staples, M.N.L. Khan, R.E.P. Winpenny, *Acta Cryst.,* **1994**, C50, 1020.

40 C.J.L. Lock, M.A. Turner, *Acta Cryst.,* **1987**, C43, 2096.

41 N.C. Baenzinger, W.E. Bennet, D.M. Soboroff, *Acta Cryst.,* **1976,** B32, 962.

42 K. Angermaier, E. Zeller, H. Schmidbaur, *J. Orgnomet. Chem.,* **1994**, 472, 371.

43 Bayler, A. Schier, G.A. Bowmaker, H. Schmidbaur, *J. Am. Chem. Soc.,* **1996**, 118, 7006.

44 Cambridge Structural Databese, Version 5.22.

45 Y. Ito, M. Inouye, M. Suginome, M. Murakami, *J. Organomet. Chem.,* **1988**, 342, C41.

46 P.G. Gavens, J.J. Guy, M.J. Mays, G.M. Sheldrick, *Acta Cryst.,* **1977**, B33, 137.

47 P.E. Riley, R. E. Davis, *J. Organomet. Chem.,* **1980**, 192, 283.

48 A. Sladek, S. Hofreiter, M. Paul, H. Schmidbaur, *J. Organomet. Chem.,* **1995**, 501, 47.

49 K.A. Porter, A. Schier, H. Schmidbaur, *Organometallics,* **2003**, 22, 4922.

50 G.W. Rabe, N.W. Mitzel, *Inorg. Chim. Acta*, **2001**, 316, 132.

Chapter Three

3.0 Results and discussion of tin complexes

3.1 Synthesis of 2,3-bis(diphenylphosphino)maleic anhydride (dpma)

2,3-bis(diphenylphosphino)maleic anhydride (dpma) was synthesed according to route (**i**) in Scheme 1 [1, 2a]. The product was obtained in good yield.

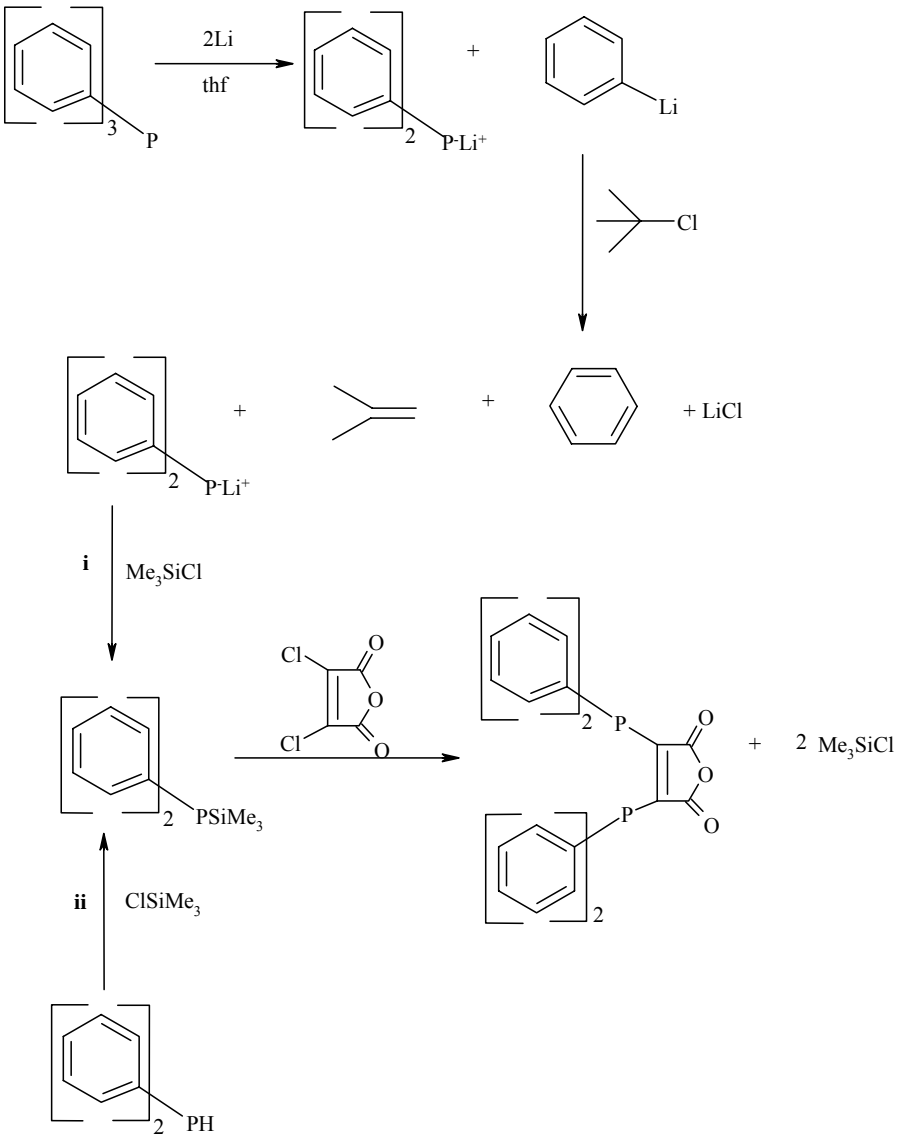

Scheme 2

Alternatively, the intermediate diphenylphosphinotrimethylsilane was prepared by reacting diphenylphosphine with an equivalent amount of trimethylchorosilane under argon [2b] (**ii** in Scheme 2). This route is advantageous to (**i**) as it does not require the use of lithium metal in the reaction mixture and also avoids the repeated filtering, necessary in method (**i**), to remove lithium chloride. The anhydride was then ring-opened to dpmaa following the procedure by Avey *et al*. [3].

3.2 Synthesis of ClAuSMe2

$ClAuSMe_2$ was synthesized following a literature procedure [4] (3) with a slight modification. Finely divided gold powder was used instead of pieces of gold metal. The powder was obtained by dissolving gold metal in aqua regia (a mixture of hydrochloric acid and nitric acid in a ratio of 3:1) and then reducing the ionic gold with zinc powder. The increased surface area of the finely divided gold reduced the reaction time from several hours to 2.5 hours and increased the yield from 86% to 94%.

$$4\,Au + 3\,Me_2SO + 6\,H^+ + 3\,Cl^- \longrightarrow 3\,[ClAuSMe_2] + 3H_2O + Au^{3+} \qquad 3$$

3.3 Tin complexes

3.3.1 Synthesis

Tin and gold complexes of dpmaaH_2 were synthesized according to reaction Scheme 3.

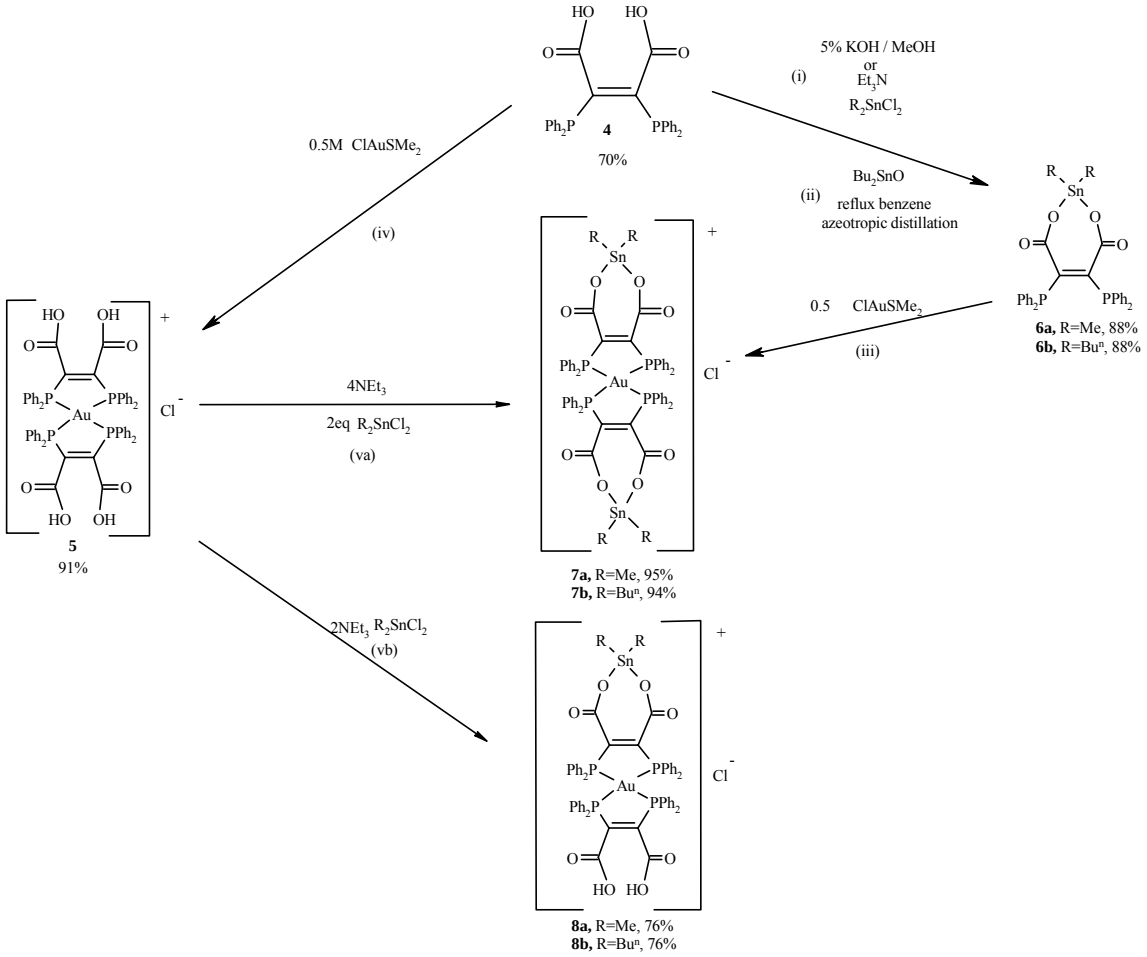

Scheme 3

The tin complexes **6** were synthesised from dpmaaH_2 (**4)** and one equivalent of R_2SnCl_2 (R = Me, Bu^n) in the presence of two equivalents of base (Et_3N or KOH) in benzene at room temperature (**i**). After an aqueous work-up the product was isolated from the organic phase as a light yellow solid in high yield. **6b** was alternatively obtained by refluxing **4** and an excess of Bu_2SnO in benzene (**ii**). The azeotropic distillation

(benzene/water) was completed after 30 minutes and removal of the solvent under reduced pressure gave the product in high yield.

The gold complex **5** was obtained following a previously described procedure (iv) [5a] by the reaction of half an equivalent of dimethyl sulfide gold chloride ($ClAuSMe_2$) and one equivalent of **4** in thf at room temperature as a brick red solid in good yield.

The mixed complexes **7** and **8** were either synthesized from one equivalent of dimethyl sulfide gold chloride ($ClAuSMe_2$) and two equivalents of **6** (iii) or from stoichiometric amounts of **5** and R_2SnCl_2 (R= Me, Bu^n) in the presence of the mild organic base triethylamine (va). The products (**7** and **8**) were obtained as pale yellow solids in high yield after removal of the solvent in *in vacuo* and washing of the residue with de-ionized water.

Complexes **6**, **7** and **8** are yellow (**6**) or pale yellow (**7**, **8**) solids that are moderately stable in moist air. The tin complexes **6** are soluble in most organic solvents while the mixed metal complexes **7** and **8** are insoluble in non polar solvent and only sparingly soluble in DMSO.

3.3.2 Spectroscopic studies

3.3.2.1 IR spectroscopy

Table 5 summarizes IR spectroscopic data of complexes **4** – **8.**

Table 5 spectroscopic data of complexes **4 - 8**

Complex	υ(OH)	υ(C-H)	υ_{as} (C=O)	υ_{s} (C-O)	Δυ
4	3425(b)	(3058-2866)*(w)	1725(s)	1216(s)	509
5	3426(b)	(3060-2745)*(w)	1728(s)	1247(s)	481
6a		3049-2912(m)	1587(s)	1323(s)	264
6b		3059-2856(m)	1595(s)	1342(s)	253
7a		3056-2927(m)	1625(s)	1327(s)	298
7b		3035-2839(m)	1620(s)	1315(s)	305
8a	3432(b&w)	3054-2927(m)	1720/1628(m)	1349/1292(m)	428/279
8b	3439(b&w)	3056-2860(m)	1720/1625(m)	1347/1242(m)	478/278

* Weak and broad signals due to the presence of coordinated solvent (Et_2O, thf) and C-H (Ph).

s = strong, m = medium, w = weak and b= broad

The formation of the metal complexes **6 - 8** from **4** and **5** was evident in the solid state IR spectrum (KBr-pellets) by the disappearance or weakening (complex **8**) of the intensities of the υ(OH) stretching frequency at around 3426 cm^{-1} and the appearance of absorption bands with medium intensity in the C-H region at around 3050-2950 cm^{-1} due to the introduction of alkyl groups in the complexes. Coordination of tin to the carboxylic acid groups was associated with a significant shift of the CO stretching frequency from around 1725-1728 cm^{-1} (C=O) and 1216-1292 cm^{-1} (C-O) in the uncoordinated carboxylic acid groups to around 1587-1628 cm^{-1} (C=O) and 1323-1349 cm^{-1} (C-O) in the metal coordinated species. The differences (Δυ, Table 5) between antisymmetric and symmetric carboxylate streching frequencies have previously been used to deduct the bonding mode of metal carboxylates [6]. Large Δυ values were related to an unidentate bonding mode (Δυ > 200-260 cm^{-1}; *c.f* Δυ for dpmaaH_2 in Table 5) and a small Δυ (Δυ < 200 cm^{-1}) to a bidentate chelating or bridging bonding mode [6]. Between the two extremes exists a bonding mode that is commonly referred to as anisobidentate where one metal oxygen contact is significantly shorter than the other. This region is not very well defined and

was more recently shown to extend considerably beyond $\Delta\upsilon$ = 260 cm^{-1} [7]. The metal complexes were found to have a $\Delta\upsilon$ of around 260 cm^{-1} which is therefore consistent with an anisobidentate coordination of the metal atom.

3.3.2.2 NMR spectroscopic studies

The NMR spectroscopic data of complexes **4 - 8** are summarized in Table 6.

Table 6 NMR spectroscopy data at room temperature in $CDCl_3$ or d_6-DMSO (♦).

Complex	^{119}Sn	^{31}P	^{13}C	
			C=O	C=C
4		-11.7	170.1	150.9
5		28.0	165.0	151.2
6a	-83.3	-8.7	174.3	149.8
6b	-102.3 (-116.5♦)	-8.6, -10.1	174.2, 172.2	151.0
7a		25.7♦		
7b	153.0♦	28.5♦	166.4♦	150.0♦
8a		26.6♦		
8b		30.7♦		

*Ref [5a]

The synthesis of the dialkyl tin complexes **6 - 8** was evident in the ^{1}H-NMR spectrum of the products from the disappearance of the OH group at around 3 ppm and the appearance of new signals in the range of δ 0.79 to 1.24 corresponding to the protons of alkyl groups.

The ^{31}P-NMR data of complexes **4 - 8** (see Table 6) showed that the peripheral coordination of tin to the carboxylic acid groups of the ligand had a negligible influence on the ^{31}P-NMR shift values (nearly identical values for **4** and **6**) while the direct coordination of gold to the phosphine lead to a significant shift from around δ -10 in **4** and **6** to around δ +27 in the gold complexes of **5**, **7** and **8**. A similar effect had previously been described for the related tetracoordinate gold complexes $[Au(P\text{-}P)_2]Cl$ (P-P = d2pype (where d2pype is 2-pyridylphosphine) [5a], dppe and dppey (where dppe

and dppey are 1,2-bis(diphenylphosphino)ethane and *cis*-1,2-bis(diphenylphosphino)ethylene, respectively) [5b]).

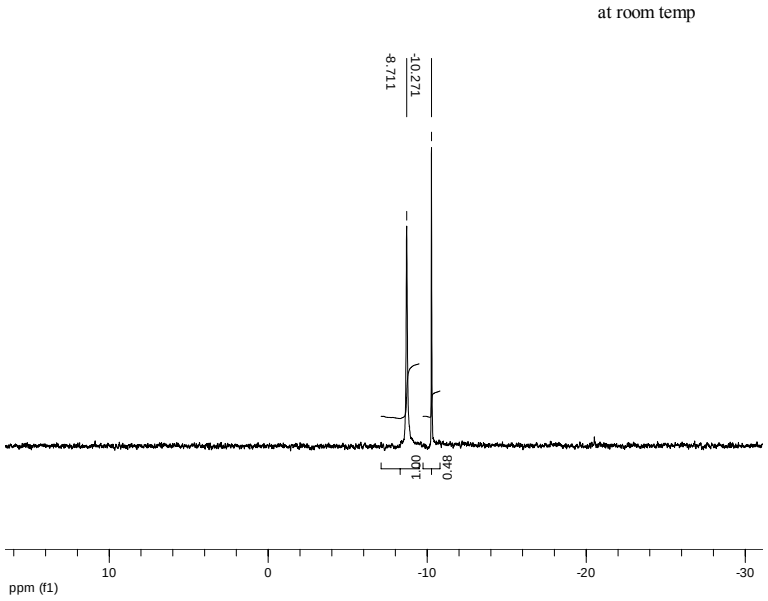

Figure 4 ^{31}P NMR of dibutyl tin dpmaa **6b** in $CDCl_3$

The chemical shift values in the ^{31}P-NMR spectrum of the complexes were not surprisingly similar to that of the free ligand (Table 6) indicating that tin coordination to the carboxylate had only a negligible effect on the electronic environment of the phosphorous atoms. The butyl-derivative **6b**, however, showed unexpectedly two distinct signals at δ -8.7 and δ -10.1 (Fig. 4). Repeated recrystallisation of **6b** and powder-XRD analysis (Fig. 5) confirmed the purity of **6b** and the absence of free dpmaa. Dilution experiments of a saturated solution of **6b**, in $CDCl_3$ that was stepwise diluted revealed that the ratio of the two peaks changed from 6:1 (saturated solution) to about 8:10. Variable temperature analysis (Fig. 6) showed further that the signal at δ -8.7 resolved into three broad signals at δ -7.4, δ -9.0 and δ -15.1 at 213 K (coalescence temperature 243 K) while the signal at δ -10.1 remained essentially unaffected. In a temptative interpretation of these results the broad signal at δ -8.5 was assigned to a trimeric species (**6b** was found to be a trimer in the solid state, Fig. 8a and 8b) whose different phosphous environments or different conformers (*c.f.* the existences of different polymorphs in the solid state) were partially resolved at lower temperature. The signal at δ – 10.1 is

consistent with a second species, possibly a monomer, in equilibrium with the trimer (equilibrium was established fast as there was no visible time dependence in the ratio of the intensities of the two signals at room temperature when a sample of **6b** was measured immediately after preparation and then again after a period of 15 h), whose ^{31}P NMR spectrum was not influenced by temperature and whose formation from the trimer, in agreement with the dilution experiments, should be favoured at lower total concentration of **6b**. The presence of several oligomers in solutions of tin carboxylates has been described previously [8, 9]. The latter explanation is also consistent with the fact that a sample of **6b** was converted in high yield to **7b** (**iii** in Scheme 3) indicating the presence of a single reagent in solution.

The ^{31}P NMR spectrum of the methyl derivative **6a** at room temperature showed in contrast only a single broad signal at δ -8.7 similar to the postulated trimeric species of **6b**. Cooling of the sample resulted in significant line broadening (64 Hz) at 223 K but gave no further evidence of the existence of more than species in solution.

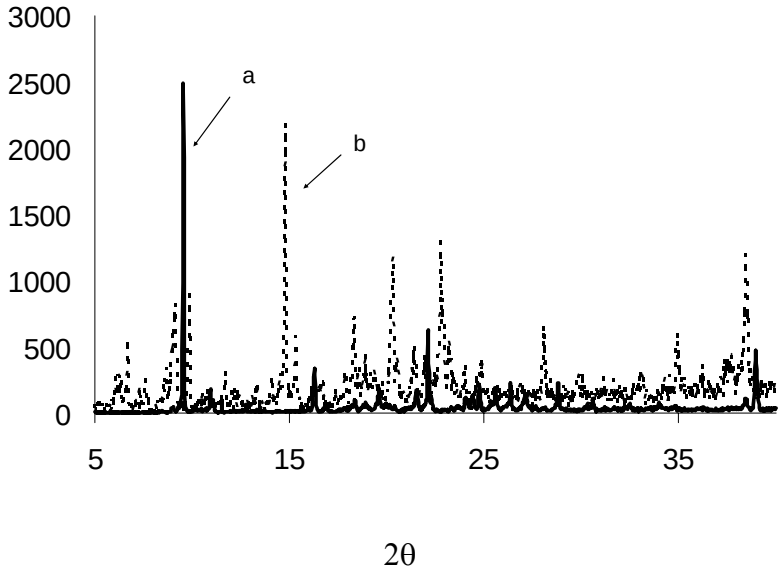

Figure 5 Powder XRD diffraction of dpmaaH_2 (**a**) and (Bu_2Sn)(O,O dpmaa)(**b**)

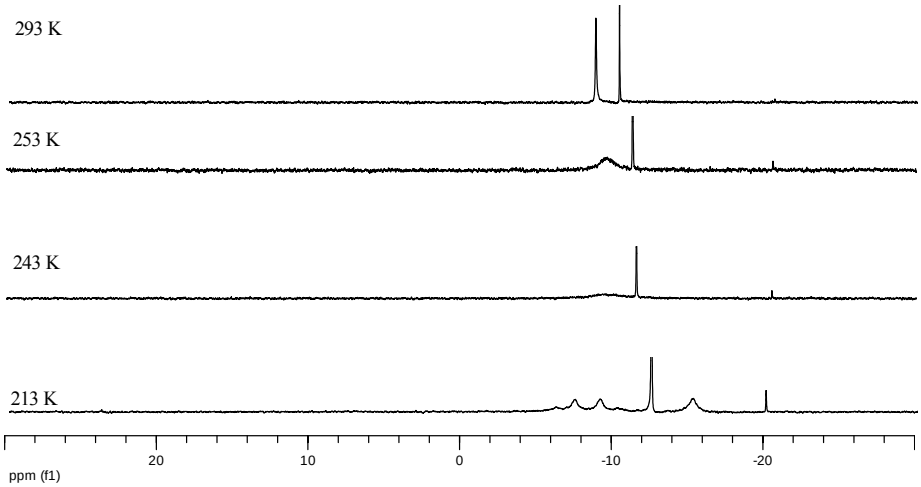

Figure 6 ^{31}P NMR of complex **6b** (Bu_2Sn)(O,O dpmaa) at variable temperature in $CDCl_3$

Due to the limited solubility of the majority of the metal complexes the spectroscopic data regarding ^{119}Sn and ^{13}C-NMR in Table 6 are incomplete, but the following observations are nevertheless worth mentioning. Increasing the chain length in the alkyl group from methyl to butyl resulted in a high field shift in the ^{119}Sn-NMR from δ -83.3 in **6a** to -102.3 in **6b** (both are in $CDCl_3$) in agreement with previously reported results [10, 11]. Coordination of **6** to gold caused a significant low field shift to δ +153 in the mixed metal complex **7b**.

It was also noted that at room temperature the ^{119}Sn-NMR spectrum of **6b** showed in contrast to the above discussed ^{31}P-NMR spectrum only a single peak. On cooling the sample to -60°C the signal resolved into three broad signals at δ -96.9, -104.2 and -169.3 in agreement with the complex behavior in the low temperature of ^{31}P-NMR spectrum. Similarly the ^{13}C-NMR spectrum of **6b** showed two distinct CO environments at room temperature which may mirror the two signals in the ^{31}P-NMR spectrum and support the previously discussed notion of **6b** existing in solution as a mixture of monomer and trimer.

3.3.3 Solid state structures

3.3.3.1 Crystallographic studies of **6**

A considerable number of diorganotin(IV) carboxylates has been crystallographically characterized in the last two decades and several structural types have been identified. These included (i) monomeric structures [12] with a six-coordinated tin atom and chelating carboxyate groups, (ii) polymeric structures [7, 8, 12b, 13] with bridging carboxylate groups, (iii) dimeric structures [14] similar to the monomeric type but with an additional interaction between tin and oxygen atoms of adjacent monomers and, (iv) more recently a cyclic trimer [8].

The repeated recrystallisation of **6b** in diethyl ether gave several batches of the dibutyltin derivative, two of which were characterized by X-ray crystallography and found to represent two different polymorphs of **6b**. While numerous attempts to obtain crystals of **6a** suitable for X-ray diffraction from solvents such as Et_2O, CH_2Cl_2 or $CHCl_3$ were unsuccessful, co-crystals **6a** $[Ph_2P(O)(CH_2)_2P(O)Ph_2]_{1/6}$ of **6a** and $Ph_2P(O)(CH_2)_2P(O)Ph_2$ (Fig 7) were obtained from diethyl ether solution by slow evaporation of the solvent. All three structures are cyclic trimers (in the case of **6a** bridged by $Ph_2P(O)(CH_2)_2P(O)Ph_2$) and crystallize with one molecule of diethyl ether per trimer. The molecular structures of **6a** and **6b** are illustrated in Fig. 7 and Fig. 8, respectively. Selective bond distances and angles are listed in Table 7.

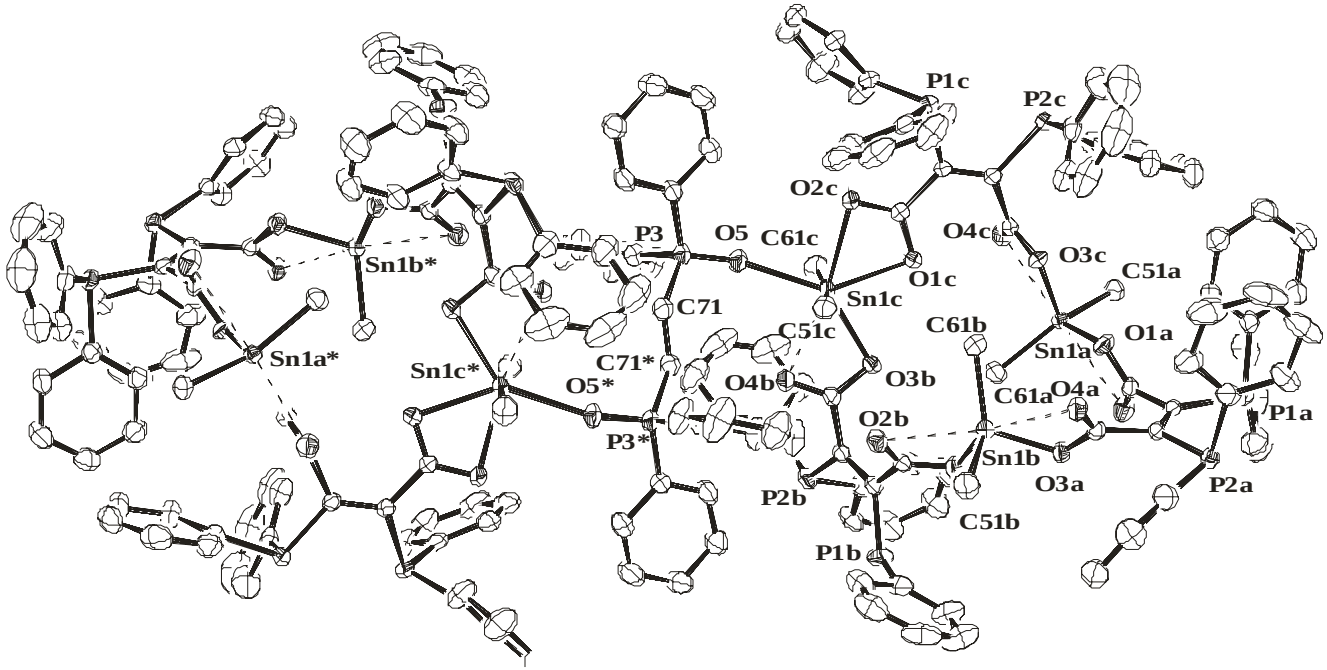

Figure 7 Molecular structure of (Me_2Sn)(O,O dpmaa) (**6a**). The thermal ellipsoids are drawn at 50 % probability level. Hydrogen atoms have been omitted for clarity.

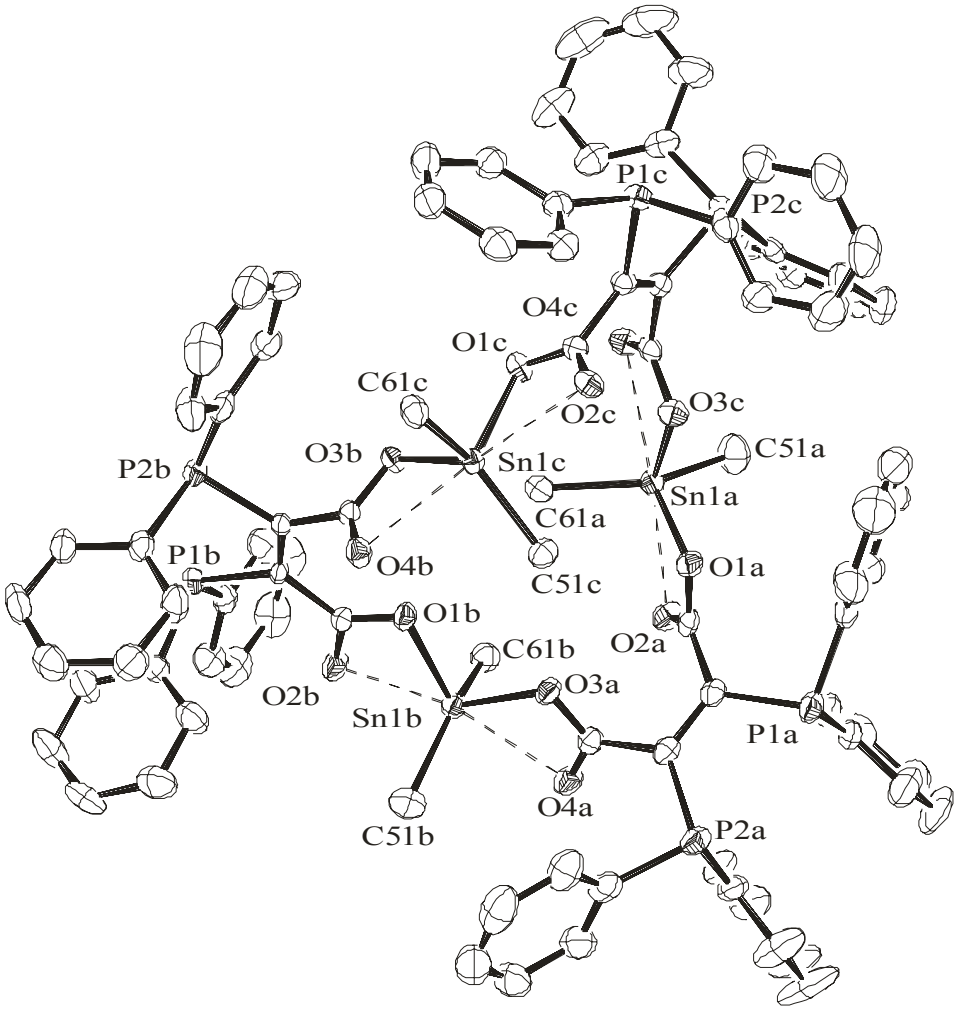

Figure 8a Molecular structure of (Bu_2Sn)(O,O dpmaa) (**6b**) (polymorph **1**). The thermal ellipsoids are drawn at 50 % probability level. Hydrogen atoms and β-,γ-and δ- carbon atoms of the Sn-butyl groups have been omitted for clarity.

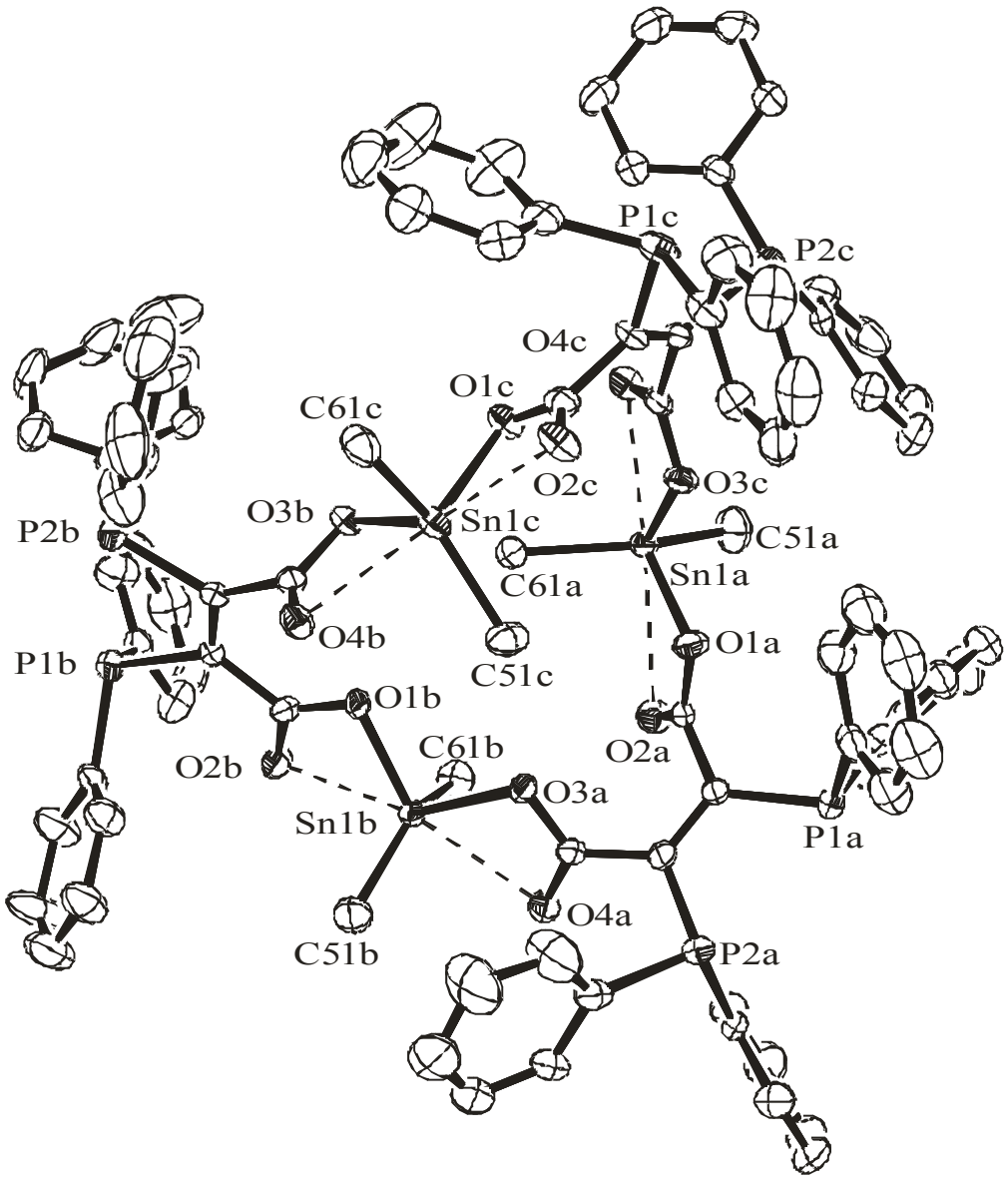

Figure 8b Molecular structure of (Bu_2Sn)(O,O dpmaa) (**6b**) (polymorph **2**). The thermal ellipsoids are drawn at 50 % probability level. Hydrogen atoms and β-,γ-and δ- carbon atoms of the Sn-butyl groups have been omitted for clarity.

Table 7 Selected bond lengths [Å] and angles [°]

	6a	Polymorph **1** of **6b**	Polymorph **2** of **6b**
Sn1a-O1a	2.069(2)	2.070(3)	2.093(3)
Sn1a-O3c	2.071(2)	2.092(3)	2.096(3)
Sn1a-C51a	2.097(3)	2.130(5)	2.104(4)
Sn1b-O1b	2.081(2)	2.166(3)	2.165(3)
Sn1b-O3a	2.117(2)	2.122(3)	2.134(3)
Sn1b-C51b	2.104(3)	2.117(5)	2.108(5)
Sn1c-O1c	2.258(2)	2.166(3)	2.119(3)
Sn1c-O3b	2.251(2)	2.129(3)	2.130(3)
Sn1c-C51c	2.108(4)	2.116(5)	2.118(4)
Sn1c-O5	2.346(2)	-	-
Sn1a-O2a	2.723(2)	2.846(3)	2.574(3)
Sn1a-O4c	2.673(2)	2.596(3)	2.637(3)
Sn1a-C61a	2.101(3)	2.120(5)	2.094(4)
Sn1b-O2b	2.737(2)	2.374(3)	2.350(3)
Sn1b-O4a	2.445(2)	2.561(3)	2.536(3)
Sn1b-C61b	2.102(3)	2.114(5)	2.121(4)
Sn1c-O2c	2.341(2)	2.414(3)	2.551(3)
Sn1c-O4b	2.518(2)	2.566(3)	2.566(3)
Sn1c-C61c	2.106(4)	2.105(5)	2.120(4)
O1a-C1a	1.304(4)	1.295(5)	1.296(5)
O3a-C4a	1.300(4)	1.307(5)	1.290(5)
O1b-C1b	1.297(4)	1.298(5)	1.299(4)
O3b-C4b	1.271(4)	1.297(5)	1.283(4)
O1c-C1c	1.268(4)	1.292(6)	1.298(5)
O3c-C4c	1.292(4)	1.297(5)	1.296(5)
O2a-C1a	1.225(4)	1.230(6)	1.255(5)
O4a-C4a	1.244(4)	1.238(5)	1.247(5)
O2b-C1b	1.228(4)	1.241(5)	1.260(5)
O4b-C4b	1.254(4)	1.209(5)	1.239(5)
O2c-C1c	1.258(4)	1.251(6)	1.234(5)
O4c-C4c	1.228(4)	1.241(6)	1.248(5)
O1a-Sn1a-O3c	80.7(1)	79.4(1)	82.5(1)
O1a-Sn1a-C51a	107.5(1)	104.2(2)	110.2(2)
O1a-Sn1a-C61a	109.4(1)	107.7(2)	108.4(1)
O3c-Sn1a-C51a	109.0(1)	111.8(2)	102.6(1)
O3c-Sn1a-C61a	110.1(1)	107.3(3)	104.7(2)
C51a-Sn1a-C61a	129.4(1)	133.0(2)	134.9(2)
O1b-Sn1b-O3a	81.5(1)	85.6(1)	86.2(1)
O1b-Sn1b-C51b	104.7(1)	101.0(2)	106.1(2)
O1b-Sn1b-C61b	105.0(1)	110.2(2)	103.7(1)
O3a-Sn1b-C51b	110.5(1)	102.9(2)	102.2(2)
O3a-Sn1b-C61b	106.2(1)	100.4(2)	102.3(1)
C51b-Sn1b-C61b	135.5(2)	142.1(2)	142.3(2)
O1c-Sn1c-O3b	79.3(1)	86.4(1)	84.0(1)
O1c-Sn1c-C51c	93.9(1)	104.1(2)	104.3(1)
O1c-Sn1c-C61c	94.0(1)	102.0(2)	104.0(1)
O3b-Sn1c-C51c	95.9(1)	102.6(2)	101.8(1)
O3b-Sn1c-C61c	91.3(1)	100.3(2)	105.3(1)
C51c-Sn1c-C61c	170.2(2)	146.5(2)	142.4(2)
O2c-Sn1c-C51c	89.1(1)	-	-
O2c-Sn1c-C61c	90.5(1)	-	-
O4b-Sn1c-C51c	86.1(1)	-	-
O4b-Sn1c-C61c	92.6(1)	-	-
O5-Sn1c-C51c	87.8(1)	-	-
O5-Sn1c-C61c	82.5(1)	-	-

The backbone of all three structures is a trimeric 21-membered macrocycle which is formed as a result of the dpmaa binding to the tin atoms in a bridging anisobidentate bonding mode. The coordination geometry of the tin atoms (except Sn1c of **6a**) may be described as highly distorted octahedral or bicapped tetrahedral with the coordinative bound carbonyl oxygen atoms O2a, O4a, O4b, O2c and O4c capping the faces. The Sn-O bond distances to the latter are much longer [ranging from 2.350(0) – 2.846(3) Å] than that to the covalently bound oxygen atoms [ranging from 2.070(3) – 2.166(3) Å]. The 'normal' tetrahedral angles around the tin atoms are in the range of 100.3(2)° to 111.8(2)°, while the remaining two sets of angles show the effect of the capping resulting in much more acute [79.4(1) – 86.4(1)°] and obtuse angles [129.4(1) – 146.5(2)°]. The octahedral view of the geometry is evident from the planarity of the SnO_4 fragment (largest deviation from planarity ranging from 0.018 to 0.081 Å calculated for **6a** and the large C-Sn-C angles. The covalent Sn-C and Sn-O distances show little variations and are similar to those described in the literature [7, 8, 12-14]. The coordinative Sn-O distances (Table 7) show much larger variations which are in agreement with the wide range of values (2.46 – 3.11 Å) reported for that type of bond in trialkyl- and dialkyltin carboxylates [12 – 14, 15]. The differences in Sn-O bond distances are also reflected in the disparity of the two associated CO distances of the carboxylate groups, one representing a C-O single [1.283(4) – 1.307(5) Å] and one a C=O double bond [1.209(5) – 1.260(5) Å].

In the case of **6a** two trimers are bridged via the O atoms of a $Ph_2P(O)(CH_2)_2P(O)Ph_2$ molecule that has an inversion center in the middle of the central C-C bond. This additional coordination results in a pentagonal bipyramidal coordination of Sn1c with five oxygen atoms in the equatorial plane (largest deviation from plane for O4b calculated 0.126 Å) and the two methyl groups (C51c, C61c) in axial position [C61c-Sn1c-C61c 170.2(2)°]. The bonding mode of the carbocyclic acid group is approximately bidentate as is evident from the similarity of the Sn-O bonds [2.518(2) – 2.251(2)] and the close to identical CO bond distances [1.271(4) – 1.254(4)] that are in agreement with delocalization in those groups.

A comparison of the two polymorph of **6b** reveals the main difference to be the different contact distances for Sn1a-O2a (2.848 versus 2.574 Å) and Sn1c-O2c (2.413 versus 2.549 Å) and a different arrangement of the phenyl groups of the phosphine ligand (Fig. 8).

The molecular structure of the related trimeric dibutyltin(IV) isophthalate $[C_6H_4(CO_2SnBu_2)_2\text{-}1,3]_3$ [8] differs from that of **6b** in ring size (24-membered) and the flatness of the ring that creates a cavity that can be occupied by a butyl group of a trimer from a different layer while adjacent trimers in the same layer form chains by an interaction between the tin atoms in one trimer with a carbonyl group of an adjacent trimer hereby increasing the coordination number around tin to seven (*c.f.* **6a**). The macrocycle in **6b** is in contrast twisted in such a way that the cavity is occupied by the alkyl substituents of each trimer hereby minimizing steric interactions between the butyl and the phenyl groups. This also prevents interaction between adjacent trimers and as result no close contacts other than van der Waals interactions are found in both polymorphs of **6b**.

3.3.3.2 Crystal structure of $[Au(dpmaaH_2)(dpmaaH)]$

The molecular structure of $[Au(dpmaaH_2)(dpmaaH)]$ and the atom numbering scheme used in corresponding tables is illustrated in Fig. 9. Selected bond distances and angles are presented in Table 8. Comprehensive crystallographic data can be found in Appendix 8.

X-Ray quality crystals of $[Au(dpmaaH_2)(dpmaaH)]$ were obtained during an attempt to grow crystals of a mixed Au/Sn complex **7b** from ethanol at room temperature. The Sn-O bond hydrolysed during the crystallization process to form an interesting zwitter ionic complex (Fig. 10) in which the Cl^- counter ion of $Au(dpmaaH_2)_2Cl$ has been replaced with a deprotonated carboxylic acid group. $[Au(dpmaaH_2)(dpmaaH)]$ crystallizes in the monoclinic space group $P2_1/n$ with one molecule of the complex and 1.5 molecules of ethanol in the asymmetric unit. The absence of the Cl^- anion and the presence of ethanol

molecules lead to an extended H-bonding pattern involving carboxylic acid groups, carboxylate groups and bridging ethanol molecules hereby forming an infinite chain along the axis (Fig. 10 and Table 9). The gold atom is surrounded by four phosphorus atoms in a distorted tetrahedral fashion; with all P-Au-P angles exhibiting deviations from the ideal angles of 109.5° (see Table 8). The smaller bite angles of 87.09(7) ° and 86.63(7)° for P(2)-Au-P(1) and P(3)-Au-P(4), respectively, are values largely imposed by the geometry of the five membered ring formed by chelating $dpmaaH_2$ ligands. These angles are a slightly bigger than those observed in $Au(dpmaaH_2)_2Cl{\cdot}H_2O{\cdot}CH_3OH$ [16]. Bond distances and angles in $[Au(dpmaaH_2)(dpmaaH)]$ compare well with those in the parent complex $[Au(dpmaaH_2)_2Cl{\cdot}H_2O{\cdot}CH_3OH]$ [16] or related four coordinated gold-phosphine complexes ranging from 2.36(1)-2.417(9) Å and 84.4(1)-137.5(3)°, respectively [17, 18-23]. Previously, the flexibility of the C-C-P angles in $dpmaaH_2$ has been noted [3]. The angles are 131.1(3) and 130.2(3)° in the free ligand, while upon coordination to Au(I) the angles average 120.3(6) and 120.7(7)° in $[Au(dpmaaH_2)(dpmaaH)]$ and 127.25(9) and 122.0(1)° in $[Au(dpmaaH_2)_2Cl{\cdot}H_2O{\cdot}CH_3OH$[[16]. The CO bond distances in the carboxylic acid groups C1, C4 and C8 differ considerably indicating the expected localization of the C=O double and C-O single bonds. The CO bond distances in the anionic carboxylate group C5 [C5-O5 1.22(1), C5-O6 1.23(1) Å] are in contrast identical within experimental errors indicating a complete delocalization of the negative charge.

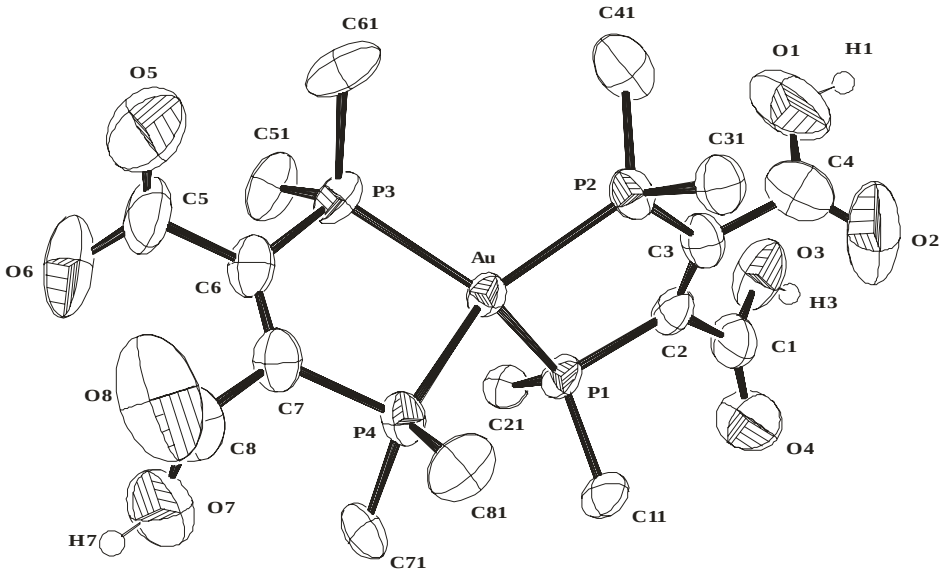

Figure 9 Molecular structure of [Au(dpmaaH_2)(dpmaaH)]. The thermal ellipsoids are drawn on 50 % probability level. Hydrogen atoms (except O-H) and phenyl groups (except *ipso*-C atoms) have been omitted for clarity.

Table 8 Selected bond lengths [Å] and angles [°] for [Au(dpmaaH_2)(dpmaaH)]

O(1)-C(4)	1.29 (1)
O(2)-C(4)	1.18 (1)
O(3)-C(1)	1.29(1)
O(4)-C(1)	1.20(1)
O(5)-C(5)	1.22 (1)
O(6)-C(5)	1.23 (1)
O(7)-C(8)	1.32(1)
O(8)-C(8)	1.17 (1)
Au-P(2)	2.373(2)
Au-P(3)	2.375 (2)
Au-P(1)	2.384 (2)
Au-P(4)	2.388 (2)
P(2)-Au-P(3)	111.9(8)
P(2)-Au-P(1)	87.1(7)
P(3)-Au-P(1)	134.0(7)
P(2)-Au-P(4)	135.6 (7)
P(3)-Au-P(4)	86.6 (7)
P(1)-Au-P(4)	109.1(7)

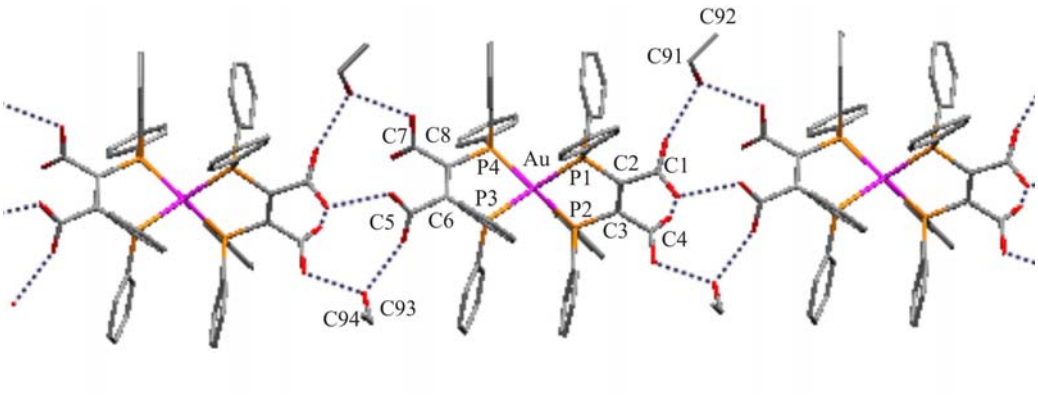

Figure 10 H-bonding pattern of [Au(dpmaaH_2)(dpmaaH)] in the solid state

Table 9 Hydrogen bonds distances [Å] and angles [°] for [Au(dpmaaH_2)(dpmaaH)]

D-H…A	d(D-H)	d(H…A)	d(D…A)	<(DHA)
O(10)-H(10)…O(5)	0.84	1.80	2.63(2)	175.6
O(9)-H(9)…O(4)#1	0.84	1.89	2.70(1)	161.6
O(7)-H(7)…O(9)	0.84	1.74	2.54(1)	159.5
O(3)-H(3)…O(6)#2	0.84	1.68	2.47(9)	155.4
O(1)-H(1)…O(10)#2	0.84	1.65	2.44(2)	156.3

Symmetry transformations used to generate equivalent atoms:

#1 x+1,y,z #2 x-1,y,z

3.4 References

1. G. W. Gluther, G. Beyerle, *Inorg. Syn.,* **1977**, 17, 186.
2. (a) D. Fenske, H. J. Becher, *Chem. Ber.,* **1974**, 107, 117. (b) *c.f.* F. Uhlig, B. Puschner, E. herrmann, B. Zobel, H. Bernhartd, W. Uhlig, *Phosphorous, Sulfur, Silcon Relat. Elem.,* **1993**, 81, 155.
3. A. Avey, D. M. Schut, J. R. Wae, D. R. Tyler, *Inorg. Chem.,* **1993**, 32, 233.
4. T. E. Müller, J. C. Green, D. M. P. Mingos, C. M. McPartlin, C. Whittingham, D. J. Williams, T. M. Woodroffe, *J. Organomet. Chem.,* **1998**, 551, 313.
5. (a) R. J. Bowen, PhD Thesis, Griffith University, Australia, **1999**. (b) S. J. Berners-Price, P. J. Sadler, *Inorg. Chem.,* **1986**, 25, 3822.
6. (a) G. B. Deacon, R. J. Phillips, *Coord. Chem. Rev.,* **1980**, 33, 227; (b) A. Glowacki, F. Huber, H. Preut, *Recl. Trav. Chim. Pays-Bas.,* **1988**, 107, 278.
7. N. W. Alcock, J. Culver, S. M. Roe, *J. Chem. Soc., Dalton Trans.,* **1992**, 1477.
8. R. Garcĭa-Zarracino, J. Ramos-Quiňones, H. Hőpfl, *Inog. Chem.,* **2003**, 42, 3835.
9. J. H. Wengrovius, M. F. Garbauskas, *Organometallics,* **1992**, 11, 1334.
10. C. R. Lassigne, E. J. Wells, *Can. J. Chem.,* **1977**, 55, 927.
11. J. Otera, T. Yano, K. Kusakabe, *Bull. Chem. Soc. Jpn.,* **1983**, 56, 1057.
12. (a) E. Mistry, S. J. Rettig, J. Trotter, F. Aubke, Z. Anorg, *Allg. Chem.,* **1995**, 621, 1875; (b) S.-G. Teoh, S.-H. Ang, E.-S. Looi, C.-A. Keok, S.-B. Teo, J.-P. Declercq, *J. Organomet. Chem.*, **1996**, 523, 75; T. P. Lockhart, J. C. Calabrese, F. Davidson, *Organometallics*, **1987**, 6, 2479; (d) S.–G. Teoh, S.–H. Ang, J.–P. Declercq, *Polyhedron,* **1997**, 16, 3729; (e) M. F. Garbauskas, J. H. Wengrovius, *Acta Cryst.,* **1991**, C47, 1969; (f) S. P. Narula, S. K. Bharadwaj, H. K. Sharma, Y. Sharda, *J. Organomet. Chem.,* **1991**, 415, 203; (g) V. Chandrasekhar, R. O. Day, J. M. Holmes, *Inorg. Chem.,* **1988**, 27, 958; (h) P. Harston, R. A. Howie, J. L. Wardell, S. M. S. V. Doidge-Harrison, P. J. Cox, *Acta Cryst.,***1992**, C48, 279; (i) C. Ma, Y. Han, R. Zhang, *J. Organomet. Chem.,* **2004**, 689, 1675.
13. F. Mistry, S. J. Rettig, J. Trotter, F. Aubke, *Acta Cryst.,* **1990**, C46, 2091.

14. (a) E. R. T. Tiekink, *J. Organomet. Chem.,* **1991**, 408, 323; (b) S. W. Ng, V. G. K. Das, W.-H. Yip, R. –J. Wang, T. C. W. Mak, *J. Organomet. Chem.,* **1990,** 393, 201; (c) S. P. Narula, S. K. Bharadwaj, Y. Sharda, *Organometallics,* **1992**, 11, 2206.
15. V. Chandrasekhar, S. Nagendran, V. Baskar, *Coord. Chem. Rev.,* **2002**, 235, 1.
16. S. J. Berners-Price, R. J. Bowen, M. A. Fernandes, W. Leseur, M. M. Mtotywa, M. Layh, R. E. Sue, *et al*. submitted to *Inorg. Chim. Acta*.
17. S. J. Berners-Price, R. J. Bowen, T. W. Hambley and P. C. Healy, *J. Chem. Soc., Dalton Trans.,* **1999**, 1337.
18. S. J. Berners-Price, M. A. Mazid, P. J. Sadler, *J. Chem. Soc., Dalton Trans.,* **1984**, 969.
19. P. A. Bates and J. M. Waters, *Inorg. Chim. Acta,* **1984**, 81, 151.
20. C. S. W. Harker, E. R. T. Tiekink, M. W. Whitehouse, *Inorg. Chim. Acta,* **1991**, 181, 23.
21. S. J. Berners-Price, L. A. Colquhoun, P. C. Healy, K. A. Byriel, J. V. Hanna, *J. Chem. Soc. Dalton Trans.,* **1992**, 3357.
22. D. E. Berning, K. V. Katti, C. L. Barnes, W. A. Volkert, A. R. Ketring, *Inorg. Chem.,* **1997**, 36, 2765.
23. F. P. Gabbai, S.-C. Chung, A. Schier, S. Kruger, N. Rosch, H. Schmidbaur, *Inorg. Chem.,* **1997**, 36, 5699.

Chapter Four

4 Biological tests on selected compounds

4.1 Introduction

Cytotoxicity assays were performed on cell cultures to determine the level of sensitivity of cancer cells and normal healthy cells in comparison to the experimental compounds. Various concentrations of the drug will be added to the cells in the wells of the culture plate and incubated for a period of time that may range from few hours to a week. Based on the results obtained in this experiment the concentration of the drug that inhibits 50% of cell growth (IC50) was calculated. The quantity of proliferating cells within each well of the culture plate was determined by adding MTTT (3-(4,5-dimethylthiazol-yl)-2,5-diphenyl tetrazolium bromide) to wells of the culture plate [1]. MTT is a pale yellow substance that is metabolised to dark blue formazan crystals by metabolically active cells. The amount of formazan produced is directly proportional to the amount of cells over a wide range.

4.2 Result and Discussions

Biological tests were not conducted on monodentate phosphine halides and 1-azaallyls complexes. The latter were found to be too sensitive to oxygen and moisture and also insoluble in polar solvents. The results of *in vitro* biological tests of bidentate phosphine complexes presented in chapter 3 are summarized in Table 10.

Table 10 IC50 (in μ mol) value of the complexes on different cell-lines

Complex	MCF-7	MCF-12A	Hela	Colo	A2780	A2780cis	Fibroblast	B16
5	91.2	>200	164.3	>200	>200	>200	>200	>200
6b	-	-	0.029	-	-	-	-	-
6a	6.5	16.6	12.3	26.2	17.3	20.0	8.0	2.7
7a	5.3	25.6	11.5	31.1	13.0	10.0	11.9	5.0
7b	-	-	0.027	-	-	-	-	-
8b	-	-	0.094	-	-	-	-	-
9a	-	-	28.035	-	-	-	-	-
9b	-	-	0.113	-	-	-	-	-
9c	-	-	20.431	-	-	-	-	-
Cisplatin	-	-	0.719	-	-	-	-	-

IC50 values indicate 50% survival of cells at the corresponding concentration. The test was conducted with a cell concentration of 500 cells per well and an incubation period of 7 days. Biological tests were conducted at the Department of Pharmacology of the University of Pretoria

The relatively high anti-tumour activity (small IC50 values) shown by the mixed gold/tin (**7** and **8**) complexes as compared to the parent gold complex **5** is believed to be a result of hydrolysis of the tin-ligand bond. The hydrolytic cleavage of Sn-O bonds resulting in highly active tin species was also observed previous studies [2, 3]. Although the mode of action of organotin species is still not fully understood due to the paucity of information concerning the cellular targets of these compounds it is largely believed that inhibition of mitochondrial oxidative phosphorylation plays an important role in the cytotoxicty of these compounds [4].

The higher activity (Hela cell line, Table 10) of dibutyl- as compared to dimethyl-complexes (**7a** versus **7b**, **8a** versus **8b**) is consistent with previous reports in the literature [5] that have shown dibutyltin species to be more active than dimethyl tin species. The dibutyltin- complexes **7b** and **8b** are both found to be more active than cisplatin. Previous studies on dialkyl tin derivatives have shown similar results for simple alkyl tin compounds [6, 7].

The anti-tumour activity of Sn(IV) alkyls has previously been related to the coordination number of the tin atom with five-coordiante tin complexes showing a higher activity than six-coordinate ones, possibly as a result of the additional free coordination site on the five-coordinate tin species [6]. The IR spectra of the metal complexes **6** – **9** were consistent with an anisobidentate bonding mode in these complexes (*c.f.* Section 2.3.2.1) representing approximately an average coordination number of five. This may be part of the reason for the high activity of these complexes.

Complexes **9a** and **9c** also showed higher activity than their parent gold complex (**5**). This may be the result of the presence of Ru in these complexes. Studies on ruthenium(III) compounds have revealed in some cases anti-tumour activity [8, 9, 10].

4.3References

1 T. Mosmann, *J. Immunological Methods,* **1983**, 65, 55.

2 A. K. Saxena, F. Huber, *Coord. Chem. Rev.,* **1989**, 95, 109.

3 R. Barbieri, L. Pellerito, G. Ruisi, M. T. Lo Giudice, F. Huber, G. Atassi, *Inorg. Chim. Acta*, **1982**, 66, 39.

4 A. K. Saxena, *Appl. Organomet. Chem.*, **1987**, 1, 39.

5 M. Gielen, *Coord. Chem. Rev.*, **1996**, 151, 41.

6 M. N. Xanthopoulou, S. K. Hadjikakou, N. Hadjiliadis, M. Scurmann, K. Jurkschat, A. Michaelides, S. Skoulika, T. Bakas, J. Binolis, S. Karkabounas, K. Charalabopoulos, *J. Inorg. Biochem.*, **2003**, 96, 425.

7 A. H. Pennink, M. Bol-Schooenmakers, M. Gellen, W. Sienen, *Main Group Met. Chem.*, **1989**, 12, 1.

8 C.A. Smith, A. J. Surland Smith, B. K. Keppler, F. Kratz, E. N. Baker, *J. Bio. Inorg. Chem.*, **1996**, 1, 424.

9 D. Frasca, J. Ciampa, J. Emerson, R. S. Umans, M. J. Clarke, *Metal-Based Drugs*, **1996**, 3, 197.

10 M. J. Clarke, in *Metal Complexes in Cancer Chemotherapy,* B. K. Keppler, Ed; VCH: Weinhem, **1993**.

Chapter Five

5 Conclusion

The monodentate phosphine complexes $bu^{i}_{3}PMX$ (**2a**: M = Cu, X = Cl, **2b**: M = Cu, X = I, **2c**: M = Ag, X = Cl, **2d**: M = Au, X = Cl) were synthesised in high yields from $bu^{i}_{3}P$ and MX. Further reaction of the phosphine complexes with $[Li\{\mu\text{-}N(R)C(bu^{t})C(H)R\}]_2$ (R = $SiMe_3$) gave the monomeric complexes $bu^{i}_{3}PCuN(R)C(bu^{t})=C(H)R$ (**3a**) and $bu^{i}_{3}PMC(H)RC(bu^{t})=NR$ (**3b**: M = Ag, **3c**: M = Au) in moderate to high yields.

A single crystal X-ray diffraction study of **2c** showed it to be a tetramer with a cubic AgCl core of three-fold rotation symmetry.

Compound **2d** is monomeric in the solid state with a linear two coordinate gold atom. Two monomeric units of **2d** are linked via weak CH···Cl contacts between the Cl atom and a CH_2 group of the neighbouring phosphine.

Compound **3c** crystallizes as monomer with a linear P-Au-C unit and represents to the best of our knowledge the first example of a crystallographically characterised 1-azaallyl complex that adopts an iminoalkyl configuration.

The bonding mode in the 1-azaallyl complexes **3a-c** was found to depend strongly on the metal ion, with **3a** being an enamide complex and **3b** and **3c** iminoalkyl complexes.

The reaction of $dpmaaH_2$ with a suitable metal precursor led to the bidentate metal complexes $Au[dpmaa]_2Cl$ (**5**) and (R_2Sn)(O,O dpmaa) (**6**) (where **6a**, R = Me; **6b**, R = Bu). Further reaction of **6** with $ClAuSMe_2$ yielded the mixed metal complexes $\{Au[(dpmaaO,O)(SnR_2)]_2\}Cl$ (**7**), $\{Au[(dpmaaO,O)(SnR_2)][dpmaa]\}Cl$ (**8**) (where **7a** and **8a**, R = Me; **7b** and **8b**, R = Bu). The reaction of **5** with ruthenium trichloride and dichlorotindibutyl gave $\{Au[(dpmaaO,O)(RuCl)]_2\}Cl$ (**9a**) $\{Au[(dpmaaO,O)(SnBu_2)(dpmaaO,O)RuCl)]\}Cl$ (**9b**) and

{Au[(dpmaaO,O)(RuCl)][dpmaa]}Cl (**9c**). The characterization of the latter complexes was unsatisfactory due to the difficulty of purifying the products and the low solubility of the compounds in common solvents.

The solid state structures of **6a** and **6b** (two polymorphs, of space group P$\bar{1}$ and $P2_1/n$) as determined by X-ray crystallography were found to be trimeric. The backbone of all three structures shows a trimeric 21-membered macrocycle which is formed as the result of the dpmaa binding to the tin atoms in a bridging anisobidentate bonding mode. The two polymorphs of **6b** differ in some of the Sn-O contact distances and a different orientation of the phenyl groups of the phosphine ligands. In the case of **6a** two trimers are bridged via the O atoms of a $Ph_2P(O)(CH_2)_2P(O)Ph_2$ molecule that has an inversion center in the middle of the central C-C bond. This additional coordination results in a pentagonal bipyramidal coordination at one of the tin atoms in the trimer.

The bidentate mixed metal complexes **7** and **8** were obtained from the reaction of $ClAuSMe_2$ and **6** or **5** and R_2SnCl_2 (R = Me, Bu^n). These complexes were insoluble in most solvents (except **7b** which is slightly soluble in ethanol) but sparingly soluble in polar solvents such as DMSO. Attempts to grow crystals of **7b** from ethanol led to the hydrolysis of the Sn-O bond and the formation of the an interesting zwitter ionic complex, [Au(dpmaaH_2)(dpmaaH)].

The metal complexes (**6**-**9**) were tested on a single cell-line (except **7a** and **8a** on eight cell-lines) and the complexes were found to show an activity comparable to cisplatin. Changing the R groups from methyl to butyl as exemplified by **7** and **8** led to an increase in activity.

Chapter Six

6.0 Experimental

6.1 General procedures

All manipulations were carried out under argon, using standard Schlenk techniques. Solvents were distilled from drying agents and degassed. The NMR spectra (chemical shift data in ppm) were recorded in d_6-DMSO, C_6D_6 or $CDCl_3$ at ambient probe temperature using the following Bruker instruments: DRX 400 (^{1}H, 400.32 MHz; ^{31}P, 161.9 MHz; ^{119}Sn, 149.2 MHz), Avance 300 (^{1}H, 300.13; ^{13}C 75.5 MHz; ^{31}P, 121.4 MHz) and referenced internally to residual solvent resonances (^{1}H and ^{13}C). ^{31}P and ^{119}Sn spectra were referenced externally to H_3PO_4 and $SnMe_4$. ^{13}C NMR spectra were all proton-decoupled. Elemental analyses were determined by the Institute for Soil, Climate and Water, Pretoria, South Africa. The following abbreviations are used throughout the experimental section: bs = broad singlet, d = doublet, dd = doublet of doublet, m = multiplet, s = singlet. Coupling constants (*J*) are given in Hz. Infrared-spectra were recorded on a Bruker Vectro 22 spectrometer using KBr discs. Absorption values are reported on the wave number (cm^{-1}) scale in the range of 400 - 4000 cm^{-1}. Mass spectra were collected using a VG70-SEQ instrument in a positive ion mode using FAB ionization.

Diffraction data were collected on a Bruker SMART 1K CCD area detector diffractometer with graphite monochromated Mo K_α radiation (50kV, 30mA). The collection method involved ω-scans of width 0.3°. Data reduction was carried out using the program *SAINT+*[1] and face indexed absorption corrections were made using the program *XPREP* [1]. The crystal structures were solved by direct methods using *SHELXTL* **[**2]. Non-hydrogen atoms were first refined isotropically followed by anisotropic refinement by full matrix least-squares calculation based on F^2 using *SHELXTL*. Hydrogen atoms were located from the difference map and then positioned geometrically and allowed to ride on their respective parent atoms. The isobutyl groups of compound **2c** exhibited very large thermal vibration as indicated by the large thermal

ellipsoids. Attempts to apply a disorder model proved to be unsuccessful. Several low temperature collections were attempted on crystals grown from various solvents without success due to a phase transition at around -70 °C. A data collection at -50 °C was found to be of lower quality than the presented room temperature data. Bond lengths and angles from **2d** were used as restraints in the final structure solution of **2c**. Compound **3c** was found to be disordered in a ratio of 0.9379(8): 0.0621(8) although only a partial refinement on the minor component was possible. Only the equivalent atoms of Au, P, C2, C13, C17 and C21 were refined as a rigid body on the disordered component, with the occupancies of the two components being summed to unity. This was necessary as a refinement of the major component only would lead to a residual peak of about 9 eÅ^{-3} corresponding to the Au atom from the minor component. In **6a** ($P2_1/n$) one of the phenyl groups was found to be disordered (C11b-C16b). This was refined isotropically over two positions as C11b-C16b and C11d-C16d with site occupancies of 0.60(2) and 0.40(2), respectively. In addition, one of the diethyl ether molecules was also found to be disordered and was refined anisotropically in two positions with site occupancies of 0.501(11) and 0.499(11), respectively. Polymorph **1** ($P\bar{1}$) of compound **6b** contains disordered ether molecules (1 per main molecule). A treatment of squeeze accounted for 53 electrons per unit cell, less than the 84 electrons two ether molecules would account for, but not unexpected as the data collection was done at room temperature allowing some of the solvent molecules to escape. Though coordinates of the ether molecules has not been added to the final structure, their contribution to F000, the sum formula and density has been accounted for as two ether molecules with full occupancy. Polymorph **2** ($P2_1/n$) of compound **6b** contains several disordered butyl groups. These have each been refined over two positions, using free variables for the occupancy of each position (the occupancies of the two positions being summed up to unity), as well as SADI and DFIX restraints on the molecular geometries of each disordered fragment. [Au (dpmaaH_2)(dpmaaH)] ($P2_1/n$) contains several disordered phenyl groups. Phenyl ring 6 was refined over 3 positions with the aid of AFIX constraints on bond lengths, and angles and DELU and SIMU restraints on the ADPs, using free variables for the occupancy of each position. The occupancies of the three positions were being summed unity. Phenyl ring 4 was refined over two positions in a similar way to ring 6. Further crystallographic

data are summarized in Appendix 2-8. Diagrams and publication materials were generated using *SHELXTL* [2], *PLATON* [3] and *ORTEP3* [4].

6.2 Synthesis

6.2.1 Preparation of finely divided gold powder

In a 1000 ml beaker 4.60 g of gold were dissolved in aqua regia and the solution was concentrated to a thick syrup. The nitric acid was removed by evaporation with five 20 ml aliquots of diluted hydrochloric acid (1:4) on a hot plate. The viscous residue was dissolved in 800 ml of deionized water and digested until all soluble material had dissolved. The solution was allowed to cool to room temperature. A stoichiometric amount of zinc powder was added to reduce the cationic gold to gold metal that precipitated as a dark brown powder. The fine gold powder was collected by filtration and washed repeatedly with hydrochloric acid (diluted 1:10) to remove zinc and other metal ions. 4.03 g (87.6 %) of finely divided gold metal was obtained.

6.2.2 Synthesis of $ClAuSMe_2$

This complex was synthesized following literature [8] but replacing gold granules with finely divided gold powder. Gold powder (4.23 g, 0.022 mol) was added to a mixture of 100 ml fuming hydrochloric acid and 50 ml DMSO and the reaction mixture was stirred and refluxed at 95 °C for 2.5 hours. The reaction mixture was allowed to cool to room temperature and kept overnight at -20 °C. The mixture of crystalline $ClAuSMe_2$ and unreacted gold metal was filtered and repeatedly washed with methanol. $ClAuSMe_2$ was then extracted in 100, 50 and 50 ml portions of dichloromethane. Hexane (80 ml) was added to the extracted solution until a white precipitate formed which was isolated. The remaining solution was concentrated to yield further fractions of $ClAuSMe_2$. The combined yield was 5.95 g (94%).

6.2.3 Synthesis Synthesis of bu^i_3PCuCl (2a)

a) bu^i_3P (0.64 cm^3, 2.53 mmol) was added to a suspension of CuCl (0.25 g, 2.53 mmol) in thf (20 cm^3). The initially yellow, later colourless solution was stirred for 3 h at room temperature. The solvent was removed *in vacuo* and the residue extracted into hexane. The solution was filtered of some dust and the solvent was then removed

from the filtrate to give a colourless, viscous oil that was sufficiently pure for further reactions.

b) $bu^{i}_{3}P$ (0.80 cm^3, 3.16 mmol) was added to acetonitrile (25 cm^3) followed by the addition of CuCl (0.38 g, 3.84 mmol). The resulting mixture was stirred overnight to give a colourless solution. After keeping the reaction mixture for two days at – 20 °C colourless crystals of $bu^{i}_{3}PCuCl$ **2a** (0.35 g, 30 %) were isolated. ^1H NMR (C_6D_6): δ = 1.02 [d, $CHMe_2$, 18H, $^3J_{H-H}$ = 6.6 Hz], 1.22 [dd, CH_2, 6H, $^1J_{P-H}$ = 10.5 Hz; $^3J_{H-H}$ = 6.6 Hz], 2.03 (m, $CHMe_2$, 3H); ^{13}C NMR (C_6D_6): δ = 24.0 (s, $CHMe_2$), 26.3 (br s, $CHMe_2$), 37.5 (br s, CH_2); ^{31}P NMR (C_6D_6): δ = -25.1.

6.2.4 Synthesis of $bu^{i}_{3}PCuI$ (2b)

CuI (0.38 g, 2.00 mmol) was dissolved in 25 cm^3 acetonitrile. The solution was cooled to 0 °C and 0.50 cm^3 (2.00 mmol) $bu^{i}_{3}P$ was added. Immediately a colourless precipitate formed that was isolated by removing all volatiles *in vacuo* to give 0.82 g of crude material. Recrystallisation from diethyl ether (25 cm^3) at – 60 °C gave colourless crystals of $bu^{i}_{3}PCuI$ **2b** (0.53 g, 67%). (Found: C, 36.48; H, 6.97. $C_{12}H_{27}CuI$ requires C, 36.70; H, 6.93 %); ^1H NMR (C_6D_6): δ = 1.05 [d, $CHMe_2$, 18H, $^3J_{H-H}$ = 8.8 Hz], 1.39 [dd, CH_2, 6H, $^1J_{P-H}$ = 9.6 Hz; $^3J_{H-H}$ = 9.4 Hz], 2.05 (m, $CHMe_2$, 3H); ^{13}C NMR (C_6D_6): δ = 25.3 [d, $CHMe_2$, $^3J_{C-P}$ = 7.8 Hz], 26.0 [d, $CHMe_2$, $^2J_{C-P}$ = 3.8 Hz], 36.7 [d, CH_2, $^1J_{C-P}$ = 36.7 Hz]; ^{31}P NMR (C_6D_6): δ = -29.6.

6.2.5 Synthesis of $bu^{i}_{3}PAgCl$ (2c)

A mixture of AgCl (0.29 g, 2.00 mmol) and $bu^{i}_{3}P$ (0.50 cm^3, 2.00 mmol) was stirred in 25 cm^3 acetonitrile overnight. After filtration and cooling the filtrate to – 20 °C colourless crystals of $bu^{i}_{3}PAgCl$ **2c** (0.61 g, 87 %) were obtained. (Found: C, 42.14; H, 8.10. $C_{12}H_{27}AgCl$ requires C, 41.70; H, 7.87 %); ^1H NMR (C_6D_6): δ = 1.08 [d, $CHMe_2$, 18H, $^3J_{H-H}$ = 8.4 Hz], 1.30 [dd, CH_2, 6H, $^2J_{P-H}$ = 9.7 Hz; $^3J_{H-H}$ = 9.6 Hz], 2.02 (m, $CHMe_2$, 3H); ^{13}C NMR (C_6D_6): δ = 25.0 (m, $CHMe_2$), 26.9 (br s, $CHMe_2$), 37.8 (m, CH_2); ^{31}P NMR

(C_6D_6): δ = -15.6 [d, ^1J = 599.4 Hz]; ^{31}P NMR (C_7D_8) (-15 °C): δ = -16.1 [dd, ^1J(^{31}P-^{107}Ag) 592.2 Hz; ^1J(^{31}P-^{109}Ag) 683.3 Hz].

6.2.6 Synthesis of bu$^i_3$PAuCl (2d)

Me_2SAuCl (1.00 g, 3.4 mmol) was dissolved in thf (approx. 25 cm^3) at room temperature and 0.87 g (4.3 mmol) bu$^i_3$P was added. The resulting mixture was stirred for 2 hours. The solution was concentrated to 2/3 of its volume and stored at –20 °C to give colourless crystals of bu$^i_3$PAuCl **2d** (1.31g, 89 %). (Found: C, 33.34; H, 6.29. $C_{12}H_{27}AuCl$ requires C, 33.15; H, 6.26 %); ^{1}H NMR (C_6D_6): δ = 0.86 [d, $CHMe_2$, 18H, $^3J_{H-H}$ = 6.7 Hz], 1.09 [dd, CH_2, 6H, $^2J_{P-H}$ = 10.4 Hz; $^3J_{H-H}$ = 6.7 Hz**]**, 1.56 (m, $CHMe_2$, 3H); ^{13}C NMR (C_6D_6): δ = 24.6 [d, $CHMe_2$ $^3J_{C-P}$ = 19.0 Hz], 26.3 (s, $CHMe_2$), 36.7 [d, CH_2, $^1J_{C-P}$ =74.5 Hz]; ^{31}P NMR (C_6D_6): δ = 11.9.

6.2.7 Synthesis of [bu$^i_3$PCuN(R)C(bu^t)=CHR] (3a)

a) bu$^i_3$P (0.29 cm^3, 1.18 mmol) was dissolved in hexane (12 cm^3) and added dropwise at – 40 °C to a solution of [CuN(R)C(bu^t)=CHR]$_2$ (0.36 g, 0.58 mmol). The reaction mixture was allowed to warm up to room temperature and stirred for 1.5 hours to give a yellow reaction mixture that was filtered. The filtrate was concentrated and cooled to –60 °C to give colourless crystals of [bu$^i_3$PCuN(R)C(bu^t)=CHR] **3a** (0.29 g, 48 %).

b) A solution of LiCH(R)C(bu^t)NR (0.40 g, 1.60 mmol) in hexane (10 cm^3) was added to a solution of bu$^i_3$PCuCl (0.48 g, 1.60 mmol) in hexane (20 cm^3) at -20 °C. The reaction mixture was allowed to warm up to room temperature and stirred for 6 h to give a pale yellow, slightly turbid solution. Filtration of the reaction mixture and concentration of the filtrate gave after cooling to -60 °C colourless crystals of **3a** (0.51 g, 63%). Isolation of the crystals by removal of the mother liquor led to a slow decomposition of the sample as evident by the crystals turning brown and becoming sticky. ^{1}H NMR (C_6D_6): δ = 0.45 (s, $SiMe_3$, 9H), 0.49 (s, $SiMe_3$, 9H), 0.94 [d, $CHMe_2$, 18H, $^3J_{H-H}$ = 6.6 Hz], 1.38 [dd, CH_2, 6H, $^2J_{P-H}$ = 16.8 Hz; $^3J_{H-H}$ = 3.4 Hz], 1.41 (s, CMe_3, 9H), 1.66 (m, $CHMe_2$, 3H), 4.95 (s, CH, 1H); ^{13}C NMR (C_6D_6) δ = 2.3

(s, $NSiMe_3$), 5.1 (s, $CSiMe_3$), 25.0 [d, $CHMe_2$, $^3J_{C\text{-}P}$ = 8.3 Hz], 26.2 [d, $CHMe_2$, $^2J_{C\text{-}P}$ = 3.0 Hz], 32.0 (s, CMe_3), 37.0 [d, CH_2, $^1J_{C\text{-}P}$ = 24.5 Hz], 40.0 (s, CMe_3), 103.1 (s, CH), 177.8(s, CN); ^{31}P NMR (C_6D_6) δ = -19.2.

6.2.8 Synthesis [bu$^i_3$PAgCH(R)C(bu^t)=NR] (3b)

A solution of LiCH(R)C(bu^t)NR (0.38 g, 1.52 mmol) in hexane (10 cm^3) was added dropwise to a solution of (bu^i)$_3$PAgCl **2c** (0.45 g, 1.3 mmol) in hexane (10 cm^3) at – 60 °C. The reaction mixture was kept at that temperature for 20 minutes and then slowly warmed to room temperature. The reaction mixture was stirred for 6 hours at room temperature to give a yellow solution with a fine black precipitate. The solvent was removed *in vacuo* to give a blackish/white solid that was found to be light and temperature sensitive. The solid was extracted with hexane (30 cm^3), it was filtered and the pale brown filtrate was concentrated (to approx. 4 cm^3) and cooled to – 60 °C to give after a several days slightly brownish, highly sensitive crystals of **3b** (0.42 g, 58 %). ^{1}H NMR (C_6D_6): δ = 0.51 (s, $SiMe_3$, 9H), 0.54 (s, $SiMe_3$, 9H), 0.92 [d, $CHMe_2$, 18H, $^3J_{H\text{-}H}$ = 6.5 Hz], 1.05 (bs, CH_2, 6H), 1.43 (s, CMe_3, 9H), 1.63 (bs, $CHMe_2$, 3H), 3.50 (s, CH, 1H); ^{13}C NMR (C_6D_6): δ = 2.8 (s, $CSiMe_3$), 4.6 (bs, $NSiMe_3$), 24.6 [d, $CHMe_2$, $^3J_{C\text{-}P}$ = 9.0 Hz], 26.7 [d, $CHMe_2$, $^2J_{C\text{-}P}$ = 5.9 Hz], 31.5 (s, CMe_3), 37.5 [d, CH_2, $^1J_{C\text{-}P}$ = 15.1 Hz], 41.7 (s, CMe_3), 60.1 (s, CH), 189.8 (s, CN); ^{31}P NMR (C_6D_6): δ = -17.4 (bs).

6.2.9 Synthesis [(bu^i)$_3$PAuCH(R)C(bu^t)=NR] (3c)

To a solution of (bu^i)$_3$PAuCl **2d** (0.68 g, 1.56 mmol) in diethyl ether (40 cm^3) was added dropwise a solution of LiCH(R)C(bu^t)NR (0.39 g, 1.56 mmol) in diethyl ether (20 cm^3) at – 60 °C. Initially a white precipitate was formed that redissolved at – 40 °C to give a colourless solution after allowing to warm up to room temperature. After stirring for 1 h at room temperature a fine colourless precipitate started to form. The reaction mixture was stirred overnight, the solvent removed *in vacuo* to give a colourless solid. Extraction with hexane (30 cm^3) and filtration gave a colourless solution that was concentrated and cooled to – 20 °C. A first crop of crystals (0.18 g, 0.4 mmol, 26 %) was identified as starting material **2d**. Concentration of the mother liquor and cooling to – 60 °C gave

colourless crystals of **3c** (0.68 g, 68 %). (Found: C, 44.03; H, 7.61; N 2.05. $C_{24}H_{55}AuNPSi_2$ requires C, 44.91; H, 8.64; N 2.18 %); ^{1}H NMR (C_6D_6): δ = 0.45 (s, $SiMe_3$, 9H), 0.49 (s, $SiMe_3$, 9H), 0.98 [d, $CHMe_2$, 18H, $^3J_{H-H}$ = 8.0 Hz], 1.15 [dd, CH_2, 6H, $^2J_{P-H}$ = 9.6 Hz; $^3J_{H-H}$ = 6.8 Hz], 1.39 (s, CMe_3, 9H), 1.88 (m, $CHMe_2$, 3H), 3.01 [d, CH, 1H, $^3J_{P-H}$ = 10.9 Hz]; ^{13}C NMR (C_6D_6): δ = 2.1 (s, $CSiMe_3$), 3.0 (bs, $NSiMe_3$), 24.9 [d, $CHMe_2$, $^3J_{C-P}$ = 8.05 Hz], 26.4 (s, $CHMe_2$), 30.7 (s, CMe_3), 38.3 [d, CH_2, $^1J_{C-P}$ = 47.2 Hz], 42.3 (s, CMe_3), 50.3 [d, CH, $^2J_{C-P}$ = 56.3 Hz], 193.7(s, CN); ^{31}P NMR (C_6D_6): δ = 21.4.

6.2.10 Synthesis of Ph_2PSiMe_3

2,3-bis(diphenylphosphino)maleic anhydride was synthesised following a literature procedure [5, 6] with slight modifications. Granular lithium (1.39 g, 0.2 mol) was added to a solution of triphenylphosphine (26.23 g, 0.1 mol) in 100 ml of thf under argon. The mixture was stirred for 3 days at room temperature resulting in a dark red solution. The solution was cooled to 0 ^{o}C where upon freshly distilled tert-butyl chloride (9.26 g, 0.1 mol) was added to give a bright red solution. After stirring for 1 hour trimethylchorosilane (10.86 g, 0.1 mol), freshly distilled and neutralized with pyridine, was then added dropwise causing the red colour to discharge and a white precipitate to form. The mixture was stirred overnight, filtered using a canula, and the solvent was removed at room temperature *in vacuo.* Hexane (50 ml) was added to the remaining solution to precipitate all LiCl that had dissolved in thf. It was filtered under argon and the solvent was removed under reduced pressure. Distillation in vacuum gave 20.2 g of Ph_2PSiMe_3 (81%). ^{1}H NMR (C_6D_6): δ 0.26 (s, CH_3, 9H), 7.22-7.58 (m, Ar-*H*, 10H); ^{31}P NMR (C_6D_6): δ -56.2; Boiling point 126-127 °C at 200 mTorr.

6.2.11 Synthesis of 2,3-bis(diphenylphosphino)maleic anhydride (dpma) [7]

A solution of 2,3-dichloromaleic anhydride (5.41 g, 32.5 mmol) in diethylether (30 ml) was added dropwise over a period of 1 hour to Ph_2PSiMe_3 (14.8 g, 65 mmol) at 0 ^{o}C while stirring continuously. A yellow precipitate formed when the anhydride was added. The mixture was cooled to -80 ^{o}C for 20 hours. The precipitate was filtered under argon

by means of a frit. The precipitate was immediately washed four times with nearly freezing diethyl ether (20 ml x 4) and then dried under high vacuum to remove Me_3SiCl to give 23.15 g of 2,3-bis(diphenylphosphino)maleic anhydride (80%). ^1H NMR (C_6D_6): δ 7.01-7.50 (m, Ar-*H*, 20H); ^{31}P NMR (C_6D_6): δ -19.9

6.2.12 Synthesis of 2,3-bis(diphenylphosphino)maleic acid (dpmaaH_2)·2Et_2O (4)

2,3-bis(diphenylphosphino)maleic acid·2Et_2O was synthesized using the same method as described by Avey *et al* [7]. NaOH (1.74 g, 0.045 mmol) was added to 380 ml of boiling deionised water, followed by addition of dpma (6.74 g, 14.7 mmol). The mixture was refluxed for 45 minutes until all the yellow solid had disappeared. The resulting solution was cooled to room temperature and washed three times with diethyl ether (~ 50 ml). The aqueous layer was acidified with 5% H_2SO_4 (v/v) to give a cloudy yellow solution. This solution was extracted three times with of diethyl ether (~ 50 ml) and the combined fractions were dried over $MgSO_4$. The solution was concentrated and kept at -20 ^oC overnight. Yellow–orange crystals of **1** were collected by filtration (6.54 g, 70%). ^1H NMR ($CDCl_3$): δ 3.02 (s, OH, 2H), 7.17-7.37 (m, Ar-*H*, 20H); ^{31}P NMR ($CDCl_3$): δ -11.7; IR (KBr, cm^{-1}): 1216 s [ν_s(C-O)], 1725 s [ν_{as}(C=O)], 3425 b [ν(OH)].

6.2.13 Synthesis of [Au(dpmaa)$_2$Cl·2thf] (5)

Au(dpmaaH_2)$_2$Cl was synthesized by the method of Bowen *et al.* [9]. 2,3-bis(diphenylphosphino)maleic acid (dpmaa) **(4)** (2.15 g, 3.4 mmol) was dissolved in thf (~ 30 ml) and $ClAuSMe_2$ (0.50 g, 1.7 mmol) was added. The colour of the solution turned from yellow to brick red. After stirring for 15 minutes a brick red precipitate started to form. The solid was filtered and dried under reduced pressure to give **2** (2.38 g, 91%). ^1H NMR ($CDCl_3$): δ 1.7 (q, thf, 8H), 3.39 (s, OH, 4H), 3.60 (q, thf, 8H), 7.17-7.37 (m, Ar-*H*, 20H); ^{31}P NMR ($CDCl_3$): δ 28.0; IR (KBr, cm^{-1}): 1247 s [ν_s(C-O)], 1728 s [ν_{as}(C=O)], 3426 b [ν(OH)], 2745-3060 w [ν(C-H)].

6.2.14 Synthesis of [(Me_2Sn)(O,O dpmaa)] (6a)

NEt_3 (0.16 g, 1.58 mmol), was added to a benzene (25 ml) solution of 2,3-bis(diphenylphosphino)maleic acid (0.50 g, 0.79 mmol) and the solution was stirred for 15 minutes. A benzene solution of dimethyltindichloride (0.17 g, 0.79 mmol) was then added dropwise to the dpmaa solution at room temperature over a period of 15 minutes. The reaction mixture was stirred overnight. The solvent was evaporated and the residue dried *in vacuo*. The remaining yellow powder was dissolved in chloroform (15 ml) and washed twice with de-ionized water (~20 ml). The chloroform solution was dried over $MgSO_4$ and the solvent removed under reduced pressure to give a light yellow product (0.56 g, 88%). Elemental analysis: Calcd. for $C_{30}H_{26}O_4P_2Sn$: C 57.09, H 4.15 %. Found: C 56.88, H 4.62 %. ^{1}H NMR ($CDCl_3$): δ 0.25 [s, CH_3, $^2J(^{119}Sn\text{-}^1H)$ 77.8 Hz, 6H], 7.32-7.23 (m, *o* and *m*- Ar, 16H), 7.43 (bs, *p*-Ar, 4H); ^{13}C NMR ($CDCl_3$): δ 3.3 (s, CH_3), 128.3 [t, Ar, $^2J(^{19}P\text{-}^{13}C)$ 3.6 Hz], 128.8 [s, (*p*-Ar-C)], 133.9 [t, Ar, $^1J(^{19}P\text{-}^{13}C)$ 10.7 Hz], 134.5 [t, Ar, $^2J(^{19}P\text{-}^{13}C)$ 2.4 Hz], 149.8 (s, C=C), 174.3 [t, C=O, $^2J(^{19}P\text{-}^{13}C)$ 3.7 Hz]; ^{31}P NMR ($CDCl_3$): δ -8.7 (s); ^{119}Sn NMR ($CDCl_3$): δ -83.3; FAB-MS: (M^++H) 632 m/z (8%); IR (KBr, cm^{-1}): 1323 s [ν_s(C-O)], 1580 s [ν_{as}(C=O)], 2912 m, 2930 m, 3000 m, 3049 m [ν (C-H)].

Synthesis of compound **6a[$Ph_2P(O)(CH_2)_2P(O)Ph_2$]$_{1/6}$** was obtained from a solution of **6a** (0.172 g, 0.77 mmol) and a slight excess (stoichiometric ratio of **6a**:P-oxide =6:1.13) of $Ph_2P(O)(CH_2)_2P(O)Ph_2$ (0.022 g, 0.055 mmol) in a 1:1 mixture of Et_2O and CH_2Cl_2. Slow evaporation of the solvents resulted in the formation of yellow crystals of the adduct (0.14 g, 74%) M.P (decomp.) 135-140^{o}C. Elemental analysis: Calc. for $C_{206}H_{180}O_{26}P_{24}Sn_6(CH_2Cl_2)$ C 57.79, H4.26%. Found: C57.3, H4.47%

6.2.15 Synthesis of [(Bu_2Sn)(O,O dpmaa)] (6b)

a) An excess of dibutyl tin oxide **(**0.60 g, 2.4 mmol) was added to a benzene solution (90 ml) of dpmaa·$2Et_2O$ (1.00 g, 1.58 mmol). The reaction mixture was brought to reflux and the water was removed by means of an azeotropic distillation in a Dean Stark apparatus. The reaction mixture was refluxed for about 30 minutes and then allowed to cool down to room temperature. The yellow solution was filtered and the

product was isolated as yellow crystals (1.2 g, 88%) by removal of the solvent *in vacuo* and re-crystallization of the residue from diethyl ether.

b) A solution of KOH (0.027 g, 0.85 mmol) in methanol was added to a solution of 2,3-bis(diphenylphosphino)maleic acid (0.25 g, 0.42 mmol) in thf (~15 ml). The reaction mixture was stirred for 15 minutes. A thf solution of dibutyltindichloride (0.13 g, 0.42 mmol) was added dropwise to the dpmaa solution over a period of 15 minutes at room temperature. The reaction mixture was stirred overnight. The solvent was evaporated and the residue dried *in vacuo*. The remaining yellow powder was dissolved in chloroform (20 ml) and washed twice with de-ionized water (~20 ml). The chloroform solution was dried over $MgSO_4$ and the solvent removed under reduced pressure to give a light yellow product (0.22 g, 76%).

Elemental analysis: Calcd. for $C_{36}H_{38}O_4P_2Sn$: C 60.42, H 5.31 %. Found: C 60.37, H 5.34 %. ^{1}H NMR ($CDCl_3$): δ 0.73 (m, CH_3, Bu, 6H), 0.92-1.13 (mm, (CH_2), Bu, 12H), 7.07-7.31 (mm, *m,* p/*o*, Ar, 20H). ^{13}C NMR ($CDCl_3$): δ 13.51, 13.8 (s, CH_3), 26.1, 26.35, 26.43, 27.0 (s, CH_2), 127.9-128.1 (mm, m-Ar-C), 128.6-128.7 (mm, *p*-Ar-C), 133.9-134.3 (mm, *o*-Ar-C), 134.9, 135.3 (*ipso*-Ar-C) 151.0 (s, C=C), 172.2 [t, C=O, $^2J(^{31}P\text{-}^{13}C)$ 4.1 Hz] 174.2 [t, C=O $^2J(^{31}P\text{-}^{13}C)$ 3.6 Hz]; ^{31}P NMR ($CDCl_3$): δ - 8.6 (s) and -10.1(s); ^{119}Sn NMR ($CDCl_3$) : δ -102.3 (s), ^{119}Sn NMR (d_6-DMSO): δ -116.5(s), ^{119}Sn NMR ($CDCl_3$, at 213K) : δ 96.9, -104.2 and -169.3; FAB-MS: (M^+-Bu) 660.06 m/z (12%); IR (KBr, cm^{-1}): 1342 s [ν_s(C-O)], 1594 s [ν_{as}(C=O)], 2856 m, 2915 m, 2959 m, 3055 m [ν (C-H)].

6.2.16 Synthesis of{Au[(dpmaaO,O)($SnMe_2$)]$_2$}Cl·H_2O·Et_2O (7a)

a) NEt_3 (0.15 g, 1.49 mmol) was added to a suspension of Au(dpmaa)$_2$Cl·2thf (0.5 g, 0.37 mmol) in thf (~30 ml) at room temperature. The resulting brick red solution was cooled (0 ^{o}C) and Me_2SnCl_2 (0.16 g, 0.74 mmol) was added dropwise as a thf solution over a period of 15 minutes. The reaction mixture was allowed to warm to room temperature and stirred overnight. The solvent was removed *in vacuo,* the residue was washed with de-ionized water (~15 ml) and thoroughly dried *in vacuo* to give 0.53 g (95%) of **7a**.

b) Solid Me_2SAuCl (0.12 g, 0.42 mmol) was added to a thf (20 ml) solution of **(6a)** (0.53 g, 0.83 mmol) resulting in a colour change from yellow to pale orange. The reaction mixture was stirred overnight. The solvent was removed *in vacuo* and the residue was washed three times with de-ionized water (~15 ml) and then dried *in vacuo* to give 0.55 g (94%) of **7b**.

Elemental analysis: Calcd. for $C_{64}H_{64}AuClO_{10}P_4Sn_2$: C 48.41, H 4.03 %. Found: C 48.35, H 4.13 %. ^{1}H NMR (d_6-DMSO) δ: 0.52 (bs, CH_3, 12H), 1.01 (t, Et_2O, CH_3, 6H), 3.32 (s, H_2O, OH), 3.6 (q, CH_2, Et_2O, 4H), 7.09 (m, *o, m*-Ar, 32H), 7.32 (bs, *p*-Ar, 8H). ^{31}P NMR (d_6-DMSO) δ: 25.7 (s); IR (KBr, cm^{-1}): 1327 s [ν_s(C-O)], 1625 s [ν_{as}(C=O)], 2492 w, 2611 w, 2675 w, [ν(C-H), Et_2O], 2927 m, 2990 m, 3056 m [ν(C-H), CH_3], 3438 br [ν(O-H),H_2O)].

6.2.17 Synthesis of {Au[(dpmaaO,O) $SnBu_2$]$_2$}Cl (7b)

a) Solid Me_2SAuCl (0.06 g, 0.116 mmol) was added to a diethyl ether (~ 20 ml) solution of **6b** (0.4 g, 0.23 mmol) resulting in a colour change from yellow to orange. The reaction mixture was stirred overnight. The solvent was removed *in vacuo* and the residue was washed three times with de-ionized water (~15 ml) and then dried *in vacuo* to give 0.21 g (94%) of **7b**.

b) **7b** was synthesized using the same procedure as described for **7a** in **5.2.16 (a)** from NEt_3 (0.093 g, 0.92 mmol), $Au(dpmaa)_2Cl{\cdot}2thf$ (0.31 g, 0.23 mmol) and Bu_2SnCl_2 (0.095 g, 0.46 mmol) yielding 0.39 g (92%) of **7b**.

Elemental analysis found: Calcd. for $C_{72}H_{76}AuClO_8P_4Sn_2$: C 51.97, H 4.61 %. Found: C 51.16, H 4.71 %. ^{1}H NMR (d_6-DMSO) : δ 0.72 (bs, CH_3, 12H), 0.90-1.21 (bs, butyl, CH_2 , 24H), 1.01 (t, Et_2O, CH_3, 6H), 3.37 (q, Et_2O, CH_2, 4H), 7.05 (m, *o* or *m*-Ar, 16H), 7.35-7.64 (bs, *o* or *m/p*-Ar, 24H); ^{13}C NMR (d_6-DMSO) : δ 13.4 (s, CH_3, butyl), 15.0 (s, CH_3, Et_2O), 25.4-26.6 (s, CH_2, butyl), 64.7 (s, CH_2, Et_2O), 127.9-132.6 (Ar-C), 150.0 (s, C=C), 166.4 (s, C=O); ^{31}P NMR (d_6-DMSO) : δ 28.5 (s); ^{119}Sn NMR(d_6-DMSO) : δ 153.0; IR (KBr, cm^{-1}): 1315 s [ν_s(C-O)], 1607s [ν_{as}(C=O)], 2839 m, 2892 m, 2946 m, 3035 m [ν(C-H)].

6.2.18 Synthesis of {Au[(dpmaaO,O)($SnMe_2$)][dpmaa]}Cl·$Et_2O_{(0.5)}$ (8a)

NEt_3 (0.074 g, 0.74 mmol) was added to a suspension of $Au(dpmaa)_2Cl·2thf$ (0.5 g, 0.37 mmol) in thf (~30 ml) resulting in a brick red solution. The reaction mixture was stirred for 15 min at room temperature, after which period Me_2SnCl_2 (0.08 g 0.37 mmol) was dissolved in thf (~20 ml) and added dropwise at 0 ^oC over a period of 15 minutes. The colour of the solution changed to light yellow. The reaction mixture was stirred overnight and the solvent removed *in vacuo*. The residue was washed with de-ionized water (~15 ml) and thoroughly dried *in vacuo* to give 0.42 g (76%) of **8a**. Elemental analysis: Calcd. for $C_{60}H_{53}AuClO_{8.5}P_4$ Sn: C 52.28, H 4.02 %. Found: C 52.65, H 4.04 %. ^1H NMR (d_6-DMSO): δ 0.61 (bs, CH_3, 6H), 1.24 (t, CH_3, Et_2O, 3H), 3.10 (q, CH_2, Et_2O, 2H), 5.82-5.08 (bs, OH, 2H), 7.07 (m, *o* and *m*-Ar, 32H), 7.50 (bs, *p*-Ar, 8H); ^{31}P NMR (d_6-DMSO): δ 25.1 and 26.6; FAB-MS: (M^+-Cl^-) 1312.6 m/z (5%); IR (KBr, cm^{-1}): 1292 s [ν_s(C-O), COOH], 1349 s [ν_s(C-O), COO], 1628 s [ν_{as}(C=O), COO], 1719 m [ν_{as}(C=O),COOH], 2494 w, 2607 w, 2675 w, 2739 w [ν(C-H), Et_2O], 2927 w, 2981 w, 3054 w [ν(C-H), CH_3], 3432 br [ν(O-H)].

6.2.19 Synthesis of {Au[(dpmaaO,O)($SnBu_2$)][dpmaa]}Cl·Et_2O (8b)

8b was synthesized using the same procedure as described for **8a** from NEt_3 (0.044 g, 0.44 mmol), $Au(dpmaa)_2Cl·2thf$ (0.30 g, 0.22 mmol) and Bu_2SnCl_2 (0.046 g. 0.22 mmol) yielding 0.22 g (76%) of **8b**. Elemental analysis: Calcd. for $C_{68}H_{68}AuClO_9P_4Sn$: C 54.27, H 4.54 %. Found: C 54.15, H 4.72 %. ^1H NMR:(d_6-DMSO): δ 0.65 (bs, CH_3, 6H), 0.98-1.13 (mm, CH_2, 12H), 4.54 (bs, OH), 7.16 (m, *o* and *m*-Ar, 32H), 7.49 (bs, *p*-Ar, 8H);.^{31}P NMR: (d_6-DMSO): δ 26.6 and δ 25.1; MS-FAB: (M^+-Cl^-) 1396.1 m/z (5%); IR(KBr, cm^{-1}): 1242 s [ν_s(C-O), COOH], 1347 s [ν_s(C-O), COO], 1625 s [ν_{as}(C=O), COO], 1720 s [ν_{as}(C=O), COOH], 2860 m, 2918 m, 2958 m, 3055 m [ν(C-H), Butyl], 3440 br [ν(O-H)].

6.2.20 Synthesis of {Au[(dpmaaO,O)(RuCl)]$_2$}Cl (9a)

KOH (0.08 g, 1.43 mmol, 0.89 M solution in ethanol) was added to a suspension of Au(dpmaa)$_2$Cl·2thf (0.41g, 0.305 mmol) in thf (25ml) and the mixture was stirred for about 15 minutes. Ru(III)Cl$_3$ (0.13g, 0.61 mmol) was then added to the solution and the colour changed to green, over a period of two days. The reaction mixture was stirred for a total of four days, the solvent was removed *in vacuo* and the residue washed three times with de-ionized water (~ 15 ml) and dried to give 0.34 g (76%) of **9a**. ^{1}H NMR (d$_6$-DMSO) : δ 3.78 (bs, H$_2$O), 7.03-7.10 (mm, *o* and *m*-Ar, 32H), 7.32 (bs, *p*-Ar, 8H); ^{31}P NMR (d$_6$-DMSO) : δ 32.5; IR (KBr, cm^{-1}): 1353 s [ν_s(C-O), COO], 1605 s [ν_{as}(C=O)], 3407 br [ν(O-H), H$_2$O].

6.2.21 Synthesis of {Au[(dpmaaO,O)(SnBu$_2$)(dpmaaO,O)RuCl)]}Cl·(H$_2$O)$_2$ ·(NEt$_3$)$_{1.5}$ (9b)

Excess NEt$_3$ (0.4 ml, 2.8 mmol) was added to a suspension of Au(dpmaa)$_2$Cl·2thf (0.5 g, 0.37 mmol) in thf (25ml) and stirred for about 30 minutes. Ru(III)Cl$_3$ (0.077 g, 0.37 mmol) was then added. The reaction mixture was stirred for an additional two hours. Bu$_2$SnCl$_2$ (0.112 g, 0.37 mmol) was dissolved in thf (~ 15 ml) and added dropwise over a period of 15 minutes to the solution at room temperature. The reaction mixture was stirred for four days to give a green solution. The solvent was then removed *in vacuo* to give a green powder, which was washed three times with de-ionised water (~15 ml). The powder was dried *in vacuo* to give **9b** (0.55 g, 89%). Elemental analysis: Calcd. for C$_{73}$H$_{84.5}$AuCl$_2$N$_{1.5}$O$_{10}$P$_4$RuSn: C 49.98, H 4.82, N 1.19 %. Found: C 48.49, H 4.78, N 1.07 %. ^{1}H NMR (d$_6$-DMSO): δ 0.68 (bs, CH$_3$, butyl, 6H), 1.14 (t, NEt$_3$, CH$_3$, 13.5H), 1.31-1.01(m, CH$_2$, butyl, 12H), 3.60 (q, CH$_2$, NEt$_3$, 6H), 3.90(bs, H$_2$O), 7.03-7.10 (mm, *o* or *m*-Ar, 16H), 7.32-7.34 (bs, *o* or m/*p*-Ar, 24H); ^{31}P NMR (d$_6$-DMSO): δ 28.6 and 30.4; ^{119}Sn NMR (d$_6$-DMSO): δ 18.91; IR (KBr, cm^{-1}): 1324 s, br [ν_s(C-O), COO], 1621 s [ν_{as}(C=O)], 2492 w, 2612 w, 2743 w [ν(C-H), NEt$_3$], 2860 m, 2958 m, 3058 m [ν(C-H), butyl], 3342 br [H$_2$O].

6.2.22 Synthesis of {Au[(dpmaaO,O)(RuCl)][dpmaa]}Cl (9c)

KOH (0.34 g, 0.60 mmol, 0.89M solution in ethanol) was added to a suspension of $Au(dpmaa)_2Cl{\cdot}2thf$ (0.40 g, 0.29 mmol) in thf (~25 ml) and the reaction mixture was stirred for a period of 15 minutes. A light orange precipitate formed. $Ru(III)Cl_3$ (0.06 g, 0.29 mmol) was added to the reaction mixture and it was stirred for three days. The solvent was removed *in vacuo* to give a dark green powder, which was washed three times with de-ionised water (~ 15 ml) and dried to give **9c** (0.30 g, 77%) as a green powder. Elemental analysis: Calcd. for $C_{56}H_{48}AuCl_2O_8P_4Ru$: C 51.80, H 3.60%. Found: C 49.77, H 3.55 %. ^{1}H NMR (d_6-DMSO): δ 1.76 (t, thf,), 3.60 (q, thf,), 7.04-7.45 (m, Ar, 40H); ^{31}P NMR (d_6-DMSO): δ 28.3 (bs); IR (KBr, cm^{-1}): 1241 s [ν_s(C-O), COOH], 1348 s [ν_s(C-O), COO], 1626 s [ν_{as}(C=O), COO], 1720 s [ν_{as}(C=O), COOH], 3399- 3458 br [ν(O-H), OH/ H_2O].

6.2.23 General method for Cytotoxicity assay

Cells (100 µl) was plated in 96 well plates and incubated for 24 hours at 37^{o}C with 5%CO_2. Different concentrations of the drugs were prepared (between 0.08 mM to 3 mM) and 20 µl of a drug concentration was added to the wells in quadruplicate. The range of values was subjected to change depending on the IC50 values of the drugs. After supplemented medium (80 µl) was added to each well then the cell was incubated at 37^{o}C with 5% CO_2 with the drug until the controls confluented. After the incubation period, MTT solution (20 µl) was added to each well the plate was re-incubated for three and a half hours at 37^{o}C in a 5%CO_2 incubator. Then the cell was centrifuged for 10 minute at 2000 rpm and the supernatant was discarded. Pellets were washed with PBS (150 µl) and the cells were centrifuged again for 10 minutes at 2000 rpm. DMSO (100 µl) was added to each well. The plates were put onto a shaker for about 2 hours and then measured the absorbance on a UV 900 Micro-ELISA reader at 540 nm wavelength.

6.3 References

1. Bruker, SAINT+ Version 6.02 (includes XPREP and SADABS). Bruker AXS INC., Madison, Wisconsin, USA, **1999**; G. M. Sheldrick, SADABS, University of Göttingen, **1996**.
2. Bruker (1999). SHELXTL, Version 5.1 (includes XS, XL, XP, XSHELL), Bruker AXS INC., Madison, Wisconsin, USA, **1999**.
3. A. L. Spek, *J. App. Cryst.*, **2003**, *36*, 7.
4. L. J. Farrugia, *J. Appl. Cryst.*, **1997**, *30*, 565.
5. G. W. Gluther, G. Beyerle, *Inorg. Syn.,* **1977**, 17, 186.
6. D. Fenske, H. J. Becher, *Chem. Ber.,* **1974**, 107, 117.
7. A. Avey, D. M. Schut, J. R. Weakly, D. R. Tyler, *Inorg. Chem.,* **1993**, 32, 233.
8. T. E. Müller, J. C. Green, D. M. P. Mingos, C. M. McPartlin, C. Whittingham, D. J. Williams, T. M. Woodroffe, *J. Organomet. Chem.* **1998**, 551, 313.
9. R. J. Bowen, PhD Thesis, Griffith University, Australia, **1999**.

Appendix 1

A1.1. Mixed gold, tin and ruthenium complexes

A1.1.1 Synthesis

Mixed gold-tin and gold-ruthenium complexes were synthesized according to Scheme 4.

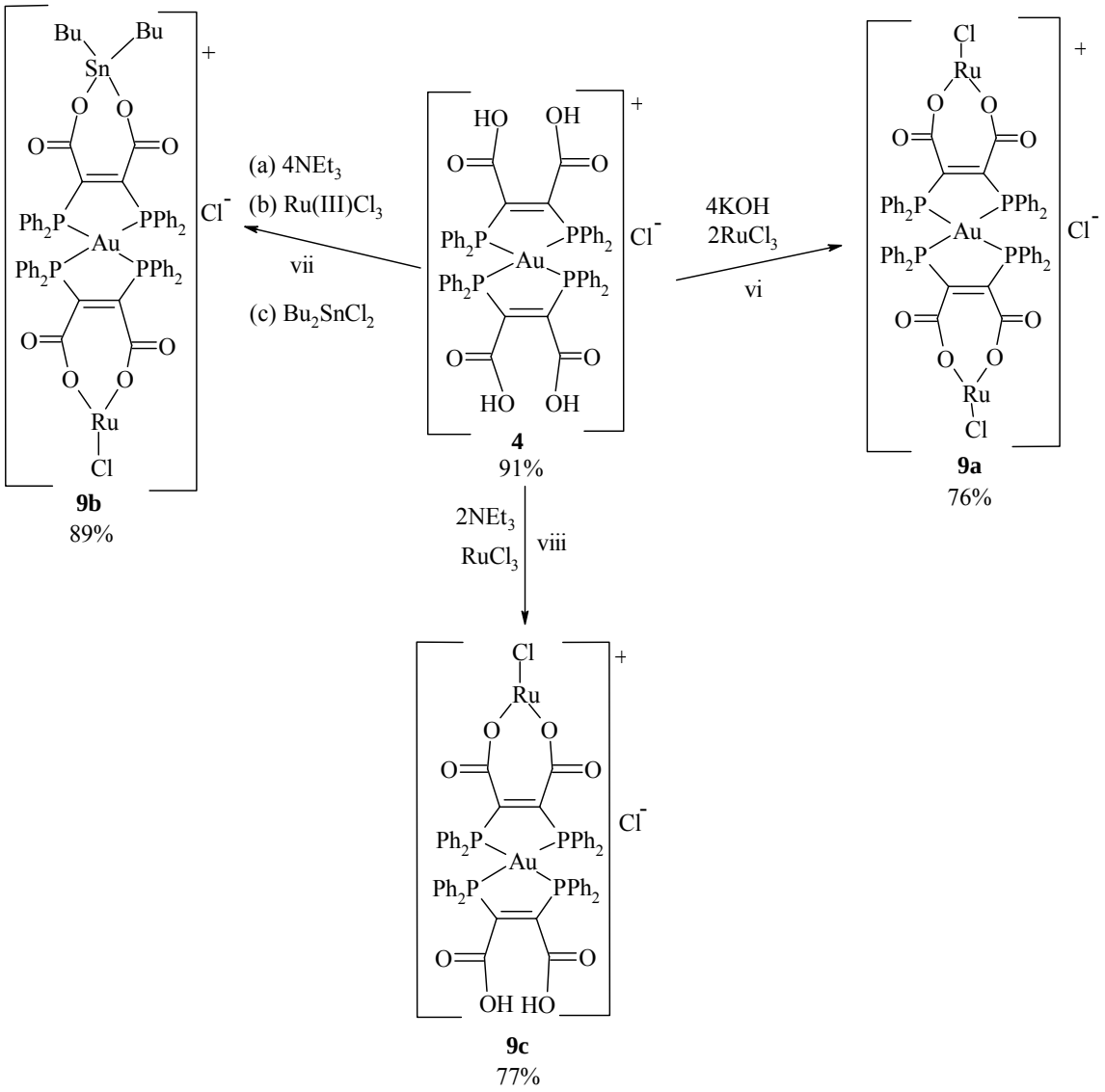

Scheme 4

Complexes **9a** and **9c** were synthesized from **4** and two or one equivalents of Ru(III)Cl_3 in the presence of four or two equivalents of KOH in thf at room temperature (**vi** and

viii). Complex **9b** was synthesized from **4** and one equivalent of $Ru(III)Cl_3$ and dibutyltindichloride, in a one-pot reaction in thf at room temperature in the presence of NEt_3 by adding the ruthenium and tin precursor sequentially (**vii**). The products (**9**) were obtained as light green solids in good yield after removal of the solvent *in vacuo* and washing with de-ionized water.

Complexes **9** are moderately stable in moist air, insoluble in non polar solvents but sparingly soluble in DMSO.

A1.1.2 Spectroscopic studies

Table 11 summarizes IR and NMR spectroscopic data of complexes **9**

Complex	NMR		IR				
	^{117}Sn	^{31}P	υ(OH)	υ(C-H)	υ_{as}(C=O)	υ_{as}(C-O)	Δυ
4		28.0	3426(b)	3060-2745* (w)	1728(s)	1216(s)	512
9a		32.5	-	-	1605(s)	1353(s)	252
9b	18.9	28.6, 30.4	-	3058-2612 (m)	1621(s)	1324(s)	297
96c		28.3	3458(b)	-	1720/1625(s)	1241/1348(m)	479/277

* Weak and broad signals due to the presence of coordinated solvent (thf) and C-H (Ph).

s = strong, m = medium, w = weak and b= broad

The absorption bands in the solid state IR spectrum (KBr-pellets) indicated the formation of the complexes **9** by the disappearance or weakening (**9c**) of the intensities of the υ(OH) stretching frequency above 3400 cm^{-1} and the appearance of absorption bands with medium intensity in the C-H region around 3050-2950 cm^{-1} due to the introduction of alkyl groups in the complex of **9b**. As discussed in section 2.3.2.1 the differences Δυ (Table 11) between antisymmetric and symmetric carboxylate streching frequencies, have been related to three possible bonding modes, a unidentate bonding mode (Δυ > 200-260 cm^{-1}; *c.f* Δυ for dpmaa in Table 11) and to a bidentate chelating or bridging bonding mode (Δυ < 200 cm^{-1}) [1, 2]. The last bonding mode is called anisobidentate (see discussion in section 2.3.2.1) and defined the region between the two extremes as discussed above. The metal complexes were found to be around 260 cm^{-1} which is therefore consistent with an anisobidentate coordination of the metal atom.

NMR spectroscopy gave additional confirmation for the formation of the complexes of **9** by the disappearance of the OH signal at around 3 ppm (in the formation of **9a** and **9b**) and the appearance of new signals in the range of δ 0.79 to 1.24 corresponding to the protons of alkyl groups (**9b**).

There was no significant shift of the signals in the ^{31}P NMR spectrum of complexes **9** as compared to **4**. Two ^{31}P NMR signals were recorded for **9b** as a result of the two different phosphorous environments in the heterometallic complexes. The presence of tin in complex **9b** was confirmed by ^{119}Sn NMR spectroscopy with a peak at δ 18.9.

A1.1.3 References

1. G. B. Deacon, R. J. Phillips, *Coord. Chem. Rev.,* **1980**, 33, 227.
2. Glowacki, F. Huber, H. Preut, *Recl. Trav. Chim. Pays-Bas.* **1988**, 107, 278.

Appendix 2

Table **12** Crystal data and summary of data collection and refinement for compound

Compound	2c	2d	3c
Empirical formula	$C_{48}H_{108}Ag_4Cl_4P_4$	$C_{12}H_{27}AuClP$	$C_{24}H_{55}AuNPSi_2$
M	1382.50	434.72	641.81
T(K)	293(2) K	293(2)	173(2)
Wavelength (Å)	0.71073 Å	0.71073	0.71073
Crystal system	Rhombohedral	Monoclinic	Monoclinic
Space group	R3	*P*2(1)/n	*P*2(1)/n
a(Å)	a = 22.654(4) Å	9.296(2)	8.9678(11)
b(Å)	b = 22.654(4) Å	9.2668(19)	17.093(2)
c(Å)	c = 11.656(2) Å	19.291(4)	20.747(3)
α(°)	90	90	90
β(°)	90	101.299(4)	94.337(2)
γ	120	90	90
V(Å^3)	5180.8(15)	1629.6(6)	3171.1(7)
Z	3	4	4
D (calc.) Mg/m^3	1.329	1.772	1.344
μ (mm^{-1})	1.390	9.264	4.776
F(000)	2136	840	1312
Crystal size (mm^3)	0.38 x 0.29 x 0.13	0.29 x 0.20 x 0.09	0.22 x 0.22 x 0.12
Theta range for data collection (°)	1.80 to 25.97.	2.15 to 28.35	1.55 to 26.00
Index ranges	-27<=h<=27, -23<=k<=27, -13<=l<=14	-11<=h<=12, -12<=k<=11, -25<=l<=17	-10<=h<=11, -21<=k<=11, -25<=l<=25
Reflections collected	10302	11009	18588
Independent reflections	4379 [R(int) = 0.0597]	4019 [R(int) = 0.0380]	6226 [R(int) = 0.0330]
Completeness to theta	100	98.3	100.0
Absorption correction	Semi-empirical from equivalents	Integration	Integration
Max. and min. transmission	0.8399 and 0.6201	0.4894 and 0.1742	0.5405 and 0.3648
Refinement method	Full-matrix least-squares on F^2	Full-matrix least-squares on F^2	Full-matrix least-squares on F^2
Data / restraints / parameters	4379 / 33 / 181	4019 / 0 / 143	6226 / 12 / 288
Goodness-of-fit on F^2	0.958	1.042	1.085
Final R indices [I>2sigma(I)]	R1 = 0.0512, wR2 = 0.1326	R1 = 0.0236, wR2 = 0.0510	R1 = 0.0334, wR2 = 0.0658
R indices (all data)	R1 = 0.0931, wR2 = 0.1571	R1 = 0.0348, wR2 = 0.0538	R1 = 0.0471, wR2 = 0.0695
Extinction coefficient	-0.04(6)	0.00106(9)	-
Largest diff. peak and hole (eÅ^{-3})	0.321 and -0.322	0.739 and -0.567	0.837 and -0.595

Appendix 3

Comprehensive crystallographic data for compound **2c**

Table **13**.Bond lengths [Å] **I2c**

Ag(1)-P(1)	2.371(2)
Ag(1)-Cl(1)	2.645(3)
Ag(1)-Cl(2)	2.648(2)
Ag(1)-Cl(1)#1	2.690(2)
Ag(2)-P(2)	2.383(4)
Ag(2)-Cl(1)	2.676(3)
Ag(2)-Cl(1)#2	2.676(3)
Ag(2)-Cl(1)#1	2.676(3)
Cl(1)-Ag(1)#2	2.690(2)
Cl(2)-Ag(1)#1	2.648(2)
Cl(2)-Ag(1)#2	2.648(2)
P(1)-C(21)	1.809(5)
P(1)-C(11)	1.812(5)
P(1)-C(31)	1.813(5)
P(2)-C(41)	1.819(5)
P(2)-C(41)#1	1.819(5)
P(2)-C(41)#2	1.819(5)
C(11)-C(12)	1.513(5)
C(12)-C(14)	1.515(5)
C(12)-C(13)	1.522(5)
C(21)-C(22)	1.512(5)
C(22)-C(24)	1.516(5)
C(22)-C(23)	1.523(5)
C(31)-C(32)	1.511(5)
C(32)-C(33)	1.519(5)
C(32)-C(34)	1.520(5)
C(41)-C(42)	1.524(5)
C(42)-C(44)	1.516(5)
C(42)-C(43)	1.519(5)

Table **14** Angles [°] **2c**

P(1)-Ag(1)-Cl(1)	119.48(8)
P(1)-Ag(1)-Cl(2)	134.98(9)
Cl(1)-Ag(1)-Cl(2)	94.00(6)
P(1)-Ag(1)-Cl(1)#1	112.61(8)
Cl(1)-Ag(1)-Cl(1)#1	93.04(11)
Cl(2)-Ag(1)-Cl(1)#1	92.99(6)
P(2)-Ag(2)-Cl(1)	123.36(6)
P(2)-Ag(2)-Cl(1)#2	123.36(6)
Cl(1)-Ag(2)-Cl(1)#2	92.67(8)
P(2)-Ag(2)-Cl(1)#1	123.36(6)
Cl(1)-Ag(2)-Cl(1)#1	92.67(8)
Cl(1)#2-Ag(2)-Cl(1)#1	92.67(8)
Ag(1)-Cl(1)-Ag(2)	87.50(6)
Ag(1)-Cl(1)-Ag(1)#2	86.03(8)
Ag(2)-Cl(1)-Ag(1)#2	86.60(6)
Ag(1)#1-Cl(2)-Ag(1)#2	86.81(8)
Ag(1)#1-Cl(2)-Ag(1)	86.81(8)
Ag(1)#2-Cl(2)-Ag(1)	86.81(8)
C(21)-P(1)-C(11)	92.7(10)
C(21)-P(1)-C(31)	102.5(12)
C(11)-P(1)-C(31)	96.9(10)
C(21)-P(1)-Ag(1)	121.4(4)
C(11)-P(1)-Ag(1)	124.1(4)
C(31)-P(1)-Ag(1)	114.3(4)
C(41)-P(2)-C(41)#1	101.3(5)
C(41)-P(2)-C(41)#2	101.3(5)
C(41)#1-P(2)-C(41)#2	101.3(5)
C(41)-P(2)-Ag(2)	116.7(4)
C(41)#1-P(2)-Ag(2)	116.7(4)

C(41)#2-P(2)-Ag(2)	116.7(4)
C(12)-C(11)-P(1)	119.4(5)
C(11)-C(12)-C(14)	111.4(5)
C(11)-C(12)-C(13)	110.6(5)
C(14)-C(12)-C(13)	110.9(5)
C(22)-C(21)-P(1)	119.8(5)
C(21)-C(22)-C(24)	111.5(5)
C(21)-C(22)-C(23)	110.8(5)
C(24)-C(22)-C(23)	110.6(5)
C(32)-C(31)-P(1)	119.8(5)
C(31)-C(32)-C(33)	111.2(5)
C(31)-C(32)-C(34)	111.1(5)
C(33)-C(32)-C(34)	110.6(5)
C(42)-C(41)-P(2)	117.8(5)
C(44)-C(42)-C(43)	110.8(5)
C(44)-C(42)-C(41)	110.8(5)
C(43)-C(42)-C(41)	110.5(5)

Symmetry transformations used to generate equivalent atoms:

#1 -x+y+1,-x+2,z #2 -y+2,x-y+1,z

Table **15** Torsion angles [°] for **2c**

P(1)-Ag(1)-Cl(1)-Ag(2)	-121.51(8)	Cl(1)#1-Ag(1)-P(1)-C(11)	165.3(10)
Cl(2)-Ag(1)-Cl(1)-Ag(2)	89.89(7)	Cl(1)-Ag(1)-P(1)-C(31)	30.6(12)
Cl(1)#1-Ag(1)-Cl(1)-Ag(2)	-3.33(8)	Cl(2)-Ag(1)-P(1)-C(31)	163.3(12)
P(1)-Ag(1)-Cl(1)-Ag(1)#2	151.73(8)	Cl(1)#1-Ag(1)-P(1)-C(31)	-77.0(12)
Cl(2)-Ag(1)-Cl(1)-Ag(1)#2	3.12(8)	Cl(1)-Ag(2)-P(2)-C(41)	147.8(6)
Cl(1)#1-Ag(1)-Cl(1)-Ag(1)#2	-90.09(9)	Cl(1)#2-Ag(2)-P(2)-C(41)	27.8(6)
P(2)-Ag(2)-Cl(1)-Ag(1)	136.94(4)	Cl(1)#1-Ag(2)-P(2)-C(41)	-92.2(6)
Cl(1)#2-Ag(2)-Cl(1)-Ag(1)	-89.46(2)	Cl(1)-Ag(2)-P(2)-C(41)#1	27.8(6)
Cl(1)#1-Ag(2)-Cl(1)-Ag(1)	3.34(8)	Cl(1)#2-Ag(2)-P(2)-C(41)#1	-92.2(6)
P(2)-Ag(2)-Cl(1)-Ag(1)#2	-136.89(4)	Cl(1)#1-Ag(2)-P(2)-C(41)#1	147.8(6)
Cl(1)#2-Ag(2)-Cl(1)-Ag(1)#2	-3.29(8)	Cl(1)-Ag(2)-P(2)-C(41)#2	-92.2(6)
Cl(1)#1-Ag(2)-Cl(1)-Ag(1)#2	89.51(2)	Cl(1)#2-Ag(2)-P(2)-C(41)#2	147.8(6)
P(1)-Ag(1)-Cl(2)-Ag(1)#1	129.72(11)	Cl(1)#1-Ag(2)-P(2)-C(41)#2	27.8(6)
Cl(1)-Ag(1)-Cl(2)-Ag(1)#1	-90.15(6)	C(21)-P(1)-C(11)-C(12)	114.1(16)
Cl(1)#1-Ag(1)-Cl(2)-Ag(1)#1	3.11(8)	C(31)-P(1)-C(11)-C(12)	-143.0(16)
P(1)-Ag(1)-Cl(2)-Ag(1)#2	-143.29(11)	Ag(1)-P(1)-C(11)-C(12)	-17.4(19)
Cl(1)-Ag(1)-Cl(2)-Ag(1)#2	-3.17(8)	P(1)-C(11)-C(12)-C(14)	62.3(15)
Cl(1)#1-Ag(1)-Cl(2)-Ag(1)#2	90.09(6)	P(1)-C(11)-C(12)-C(13)	-173.9(15)
Cl(1)-Ag(1)-P(1)-C(21)	154.2(11)	C(11)-P(1)-C(21)-C(22)	-142.5(18)
Cl(2)-Ag(1)-P(1)-C(21)	-73.1(11)	C(31)-P(1)-C(21)-C(22)	119.8(18)
Cl(1)#1-Ag(1)-P(1)-C(21)	46.6(11)	Ag(1)-P(1)-C(21)-C(22)	-9(2)
Cl(1)-Ag(1)-P(1)-C(11)	-87.1(10)	P(1)-C(21)-C(22)-C(24)	56(2)
Cl(2)-Ag(1)-P(1)-C(11)	45.6(10)	P(1)-C(21)-C(22)-C(23)	179.4(18)

C(21)-P(1)-C(31)-C(32)	-121(2)
C(11)-P(1)-C(31)-C(32)	144(2)
Ag(1)-P(1)-C(31)-C(32)	12(3)
P(1)-C(31)-C(32)-C(33)	126(4)
P(1)-C(31)-C(32)-C(34)	-110(4)
C(41)#1-P(2)-C(41)-C(42)	107.0(15)
C(41)#2-P(2)-C(41)-C(42)	-148.8(12)
Ag(2)-P(2)-C(41)-C(42)	-20.9(13)
P(2)-C(41)-C(42)-C(44)	-67.0(15)
P(2)-C(41)-C(42)-C(43)	169.8(15)

Symmetry transformations used to generate equivalent atoms:

#1 -x+y+1,-x+2,z #2 -y+2,x-y+1,z

Appendix 4

Comprehensive crystallographic data for compound **2d**

Table **16** Bond lengths [Å] for **2d**

Au-P	2.2386(10)
Au-Cl	2.2920(11)
P-C(9)	1.827(4)
P-C(1)	1.830(3)
P-C(5)	1.833(3)
C(1)-C(2)	1.529(5)
C(2)-C(3)	1.519(6)
C(2)-C(4)	1.531(5)
C(5)-C(6)	1.528(5)
C(6)-C(7)	1.489(6)
C(6)-C(8)	1.538(5)
C(9)-C(10)	1.542(5)
C(10)-C(12)	1.514(6)
C(10)-C(11)	1.530(6)

Table **18** Angles [°] for **2d**

P-Au-Cl	178.41(3)
C(9)-P-C(1)	102.13(16)
C(9)-P-C(5)	104.64(17)
C(1)-P-C(5)	105.46(16)
C(9)-P-Au	115.74(12)
C(1)-P-Au	112.94(12)
C(5)-P-Au	114.61(12)
C(2)-C(1)-P	117.0(2)
C(3)-C(2)-C(1)	112.5(3)
C(3)-C(2)-C(4)	110.4(4)
C(1)-C(2)-C(4)	108.8(3)
C(6)-C(5)-P	117.9(2)
C(7)-C(6)-C(5)	113.0(3)
C(7)-C(6)-C(8)	110.4(3)
C(5)-C(6)-C(8)	108.9(3)
C(10)-C(9)-P	117.6(3)
C(12)-C(10)-C(11)	109.8(4)
C(12)-C(10)-C(9)	111.6(3)
C(11)-C(10)-C(9)	110.1(4)

Table **17**. Torsion angles [°] for **2d**

C(9)-P-C(1)-C(2)	-163.1(3)
C(5)-P-C(1)-C(2)	87.8(3)
Au-P-C(1)-C(2)	-38.1(3)
P-C(1)-C(2)-C(3)	-70.1(4)
P-C(1)-C(2)-C(4)	167.2(3)
C(9)-P-C(5)-C(6)	63.1(3)
C(1)-P-C(5)-C(6)	170.4(3)
Au-P-C(5)-C(6)	-64.8(3)
P-C(5)-C(6)-C(7)	68.7(4)
P-C(5)-C(6)-C(8) -	168.3(3)
C(1)-P-C(9)-C(10)	158.2(3)
C(5)-P-C(9)-C(10)	-92.0(3)
Au-P-C(9)-C(10)	35.1(3)
P-C(9)-C(10)-C(12)	-80.4(4)
P-C(9)-C(10)-C(11)	157.4(3)

Appendix 5

Comprehensive crystallographic data for compound **3c**

Table **18** Bond lengths [Å] for **3c**

Au-C(2)	2.100(5)
Au-P	2.2840(12)
N-C(1)	1.266(6)
N-Si(1)	1.692(4)
P-C(21)	1.825(5)
P-C(17)	1.830(5)
P-C(13)	1.842(5)
Si(1)-C(7)	1.859(6)
Si(1)-C(9)	1.862(7)
Si(1)-C(8)	1.876(8)
Si(2)-C(11)	1.845(7)
Si(2)-C(2)	1.863(5)
Si(2)-C(12)	1.871(6)
Si(2)-C(10)	1.878(6)
C(1)-C(2)	1.493(7)
C(1)-C(3)	1.558(8)
C(3)-C(6)	1.515(9)
C(3)-C(5)	1.538(9)
C(3)-C(4)	1.574(9)
C(13)-C(14)	1.511(8)
C(14)-C(16)	1.510(8)
C(14)-C(15)	1.538(8)
C(17)-C(18)	1.515(7)
C(18)-C(19)	1.505(8)
C(18)-C(20)	1.519(7)
C(21)-C(22)	1.516(8)
C(22)-C(24)	1.476(9)
C(22)-C(23)	1.533(8)
Au'-C(2')	2.110(0)
Au'-P'	2.284(0)
P'-C(13')	1.840(0)
P'-C(17')	1.840(0)
P'-C(21')	1.840(0)

Table 19. Angles [°] for **3c**

C(2)-Au-P	178.33(14)
C(1)-N-Si(1)	153.8(5)
C(21)-P-C(17)	102.3(3)
C(21)-P-C(13)	103.4(3)
C(17)-P-C(13)	101.4(2)
C(21)-P-Au	116.23(17)
C(17)-P-Au	117.48(16)
C(13)-P-Au	113.92(18)
N-Si(1)-C(7)	107.8(3)
N-Si(1)-C(9)	106.8(3)
C(7)-Si(1)-C(9)	108.4(3)
N-Si(1)-C(8)	120.8(3)
C(7)-Si(1)-C(8)	106.7(4)
C(9)-Si(1)-C(8)	105.8(4)
C(11)-Si(2)-C(2)	114.0(3)
C(11)-Si(2)-C(12)	108.0(3)
C(2)-Si(2)-C(12)	108.4(3)
C(11)-Si(2)-C(10)	109.1(4)
C(2)-Si(2)-C(10)	110.9(3)
C(12)-Si(2)-C(10)	106.1(3)
N-C(1)-C(2)	119.0(5)
N-C(1)-C(3)	124.5(5)
C(2)-C(1)-C(3)	116.4(5)
C(1)-C(2)-Si(2)	114.2(4)
C(1)-C(2)-Au	107.1(3)
Si(2)-C(2)-Au	110.5(2)
C(6)-C(3)-C(5)	109.6(6)

C(6)-C(3)-C(1)	117.0(6)
C(5)-C(3)-C(1)	106.8(5)
C(6)-C(3)-C(4)	107.0(6)
C(5)-C(3)-C(4)	109.2(6)
C(1)-C(3)-C(4)	107.0(5)
C(14)-C(13)-P	118.8(4)
C(16)-C(14)-C(13)	110.4(5)
C(16)-C(14)-C(15)	108.8(5)
C(13)-C(14)-C(15)	111.8(5)
C(18)-C(17)-P	118.8(4)
C(19)-C(18)-C(17)	113.1(5)
C(19)-C(18)-C(20)	109.8(5)
C(17)-C(18)-C(20)	111.6(5)
C(22)-C(21)-P	118.4(4)
C(24)-C(22)-C(21)	114.0(6)
C(24)-C(22)-C(23)	109.2(5)
C(21)-C(22)-C(23)	109.9(5)
C(2')-Au'-P'	176.9
C(13')-P'-C(17')	102.8
C(13')-P'-C(21')	102.4
C(17')-P'-C(21')	102.6
C(13')-P'-Au'	115.7
C(17')-P'-Au'	115.7
C(21')-P'-Au'	115.7

Table **20**. Torsion angles [°] for **3c**.

C(2)-Au-P-C(21)	27(5)	N-C(1)-C(3)-C(5)	-56.6(7)
C(2)-Au-P-C(17)	148(5)	C(2)-C(1)-C(3)-C(5)	123.8(6)
C(2)-Au-P-C(13)	-94(5)	C(1)-C(3)-C(4)	60.3(7)
C(1)-N-Si(1)-C(7)	114.0(9)	C(2)-C(1)-C(3)-C(4)	-119.3(5)
C(1)-N-Si(1)-C(9)	-129.6(9)	C(21)-P-C(13)-C(14)	-96.5(5)
C(1)-N-Si(1)-C(8)	-8.9(10)	C(17)-P-C(13)-C(14)	157.8(4)
Si(1)-N-C(1)-C(2)	178.6(7)	Au-P-C(13)-C(14)	30.6(5)
Si(1)-N-C(1)-C(3)	-1.0(12)	P-C(13)-C(14)-C(16)	-177.8(4)
N-C(1)-C(2)-Si(2)	27.4(6)	P-C(13)-C(14)-C(15)	60.9(6)
C(3)-C(1)-C(2)-Si(2)	-153.0(4)	C(21)-P-C(17)-C(18)	-177.0(4)
N-C(1)-C(2)-Au	-95.3(5)	C(13)-P-C(17)-C(18)	-70.4(5)
C(3)-C(1)-C(2)-Au	84.4(4)	Au-P-C(17)-C(18)	54.4(5)
C(11)-Si(2)-C(2)-C(1)	-73.3(4)	P-C(17)-C(18)-C(19)	-72.6(6)
C(12)-Si(2)-C(2)-C(1)	166.5(4)	P-C(17)-C(18)-C(20)	163.0(4)
C(10)-Si(2)-C(2)-C(1)	50.4(4)	C(17)-P-C(21)-C(22)	-73.6(5)
C(11)-Si(2)-C(2)-Au	47.6(4)	C(13)-P-C(21)-C(22)	-178.7(5)
C(12)-Si(2)-C(2)-Au	-72.7(3)	Au-P-C(21)-C(22)	55.7(5)
C(10)-Si(2)-C(2)-Au	171.2(3)	P-C(21)-C(22)-C(24)	-70.2(7)
P-Au-C(2)-C(1)	-7(5)	P-C(21)-C(22)-C(23)	166.8(5)
P-Au-C(2)-Si(2)	-132(5)	C(2')-Au'-P'-C(13')	118.7
N-C(1)-C(3)-C(6)	-179.8(6)	C(2')-Au'-P'-C(17')	-1.5
C(2)-C(1)-C(3)-C(6)	0.6(7)	C(2')-Au'-P'-C(21')	-121.5

Appendix 6

Table **21**Crystal data and summary of data collection and refinement

Compound	**6a** compound	**6b** Polymorph 1	**6b** Polymorph 2	$Au(dpmaaH_2)(dpmaaH)$
Empirical formula	$C_{218}H_{210}O_{29}P_{14}Sn_6$	$C_{112}H_{124}O_{13}P_6\ Sn_3$	$C_{112}H_{124}O_{13}P_6\ Sn_3$	$C_{59}\ H_{52}\ Au\ O_{9.5}\ P_4$
Formula weight	4439.58	2220.00	2220.00	1233.85
Temperature, (K)	173(2)	293(2)	173(2)	173(2)
Wavelength (Å)	0.71073	0.71073	0.71073 Å	0.71073
Crystal system	Monoclinic	Triclinic	Monoclinic	Monoclinic
Space group	$P2_1/n$	Pī	$P2_1/n$	$P2_1/n$
a(Å)	13.5228(13)	15.1482(7)	a = 15.4779(5) Å	13.323(3) Å
b(Å)	25.780(3)	15.8531(8)	b = 19.4003(3) Å	22.101(4) Å
c(Å)	29.962(3)	24.6201(12)	c = 35.4638(11) Å	18.362(3) Å
α(°)	90	86.851(4)	90	90
β(°)	93.518(4)	80.508(3)	91.585(2)	93.266(4)°.
γ	90	63.835(3)	90	90
V($Å^3$)	10425.5(18)	5232.9(5)	10644.9(6)	5398.1(17)
Z	2	2	4	4
ρ (calc.) Mg/m^3	1.414	1.409	1.385	1.518
μ (mm^{-1})	0.882	0.863	0.848	2.902
F(000)	4520	2280	4560	2484
Crystal size (mm^3)	0.44 x 0.22 x 0.22	0.26 x 0.20 x 0.18	0.30 x 0.30 x 0.22	0.36 x 0.16 x 0.14
Theta range for data collection (°)	1.04 to 27.00	0.84 to 26.00	1.15 to 25.00.	1.44 to 26.00°.
Index ranges	-16<=h<=16, -31<=k<=32, -34<=l<=38	-18<=h<=18, -19<=k<=19, -26<=l<=30	-18<=h<=18, -22<=k<=22, -42<=l<=39	-16<=h<=15, -27<=k<=27, -22<=l<=14
Reflections collected	66839	36940	45573	31230
Independent reflections	22499[R(int) = 0.0626]	20292 [R(int) = 0.0630]	18496[R(int) = 0.0602]	10616 [R(int) = 0.0520]
Completeness to theta	98.8	98.6	98.7	99.9 %
Absorption correction	integration	Semi-empirical from equivalents	integration	Semi-empirical from equivalents
Max. and min. transmission	0.8296 and 0.6976	0.8602 and 0.8068	0.8331 and 0.7880	0.6868 and 0.4214
Refinement method	Full-matrix least-squares on F^2	Full-matrix least-squares on F^2	Full-matrix least-squares on F^2	Full-matrix least-squares on F^2
Data / restraints / parameters	22499 / 108 / 1206	20292 / 0 / 1169	18496/ 67 / 1253	10616 / 398 / 770
Goodness-of-fit on F^2	1.048	1.001	1.061	1.030
Final R indices [I>2sigma(I)]	R1 = 0.0371, wR2 = 0.0890	R1 = 0.0452, wR2 = 0.1252	R1 = 0.0392, wR2 = 0.1018	R1 = 0.0494, wR2 = 0.1090
R indices (all data)	R1 = 0.0531, wR2 = 0.0981	R1 = 0.0723, wR2 = 0.1421	R1 = 0.553 wR2 = 0.1113	R1 = 0.0877, wR2 = 0.1246
Largest diff. peak and hole ($eÅ^{-3}$)	1.263 and -1.015	1.289 and -0.669	1.171 and -0.774	0.868 and -0.926

Appendix 7

Comprehensive crystallographic data for compound **6a**

Table **22** bond distances [Å] for **6a**

Sn(1A)-O(1A)	2.069(2)
Sn(1A)-O(3C)	2.071(2)
Sn(1A)-C(51A)	2.097(3)
Sn(1A)-C(61A)	2.101(3)
Sn(1B)-O(1B)	2.081(2)
Sn(1B)-C(61B)	2.102(3)
Sn(1B)-C(51B)	2.104(3)
Sn(1B)-O(3A)	2.117(2)
Sn(1B)-O(4A)	2.445(2)
Sn(1B)-C(4A)	2.645(3)
Sn(1C)-C(61C)	2.106(4)
Sn(1C)-C(51C)	2.108(4)
Sn(1C)-O(3B)	2.251(2)
Sn(1C)-O(1C)	2.258(2)
Sn(1C)-O(2C)	2.341(2)
Sn(1C)-O(5)	2.346(2)
Sn(1C)-O(4B)	2.518(2)
Sn(1C)-C(1C)	2.654(3)
P(1A)-C(21A)	1.837(3)
P(1A)-C(11A)	1.840(4)
P(1A)-C(2A)	1.846(3)
P(2A)-C(41A)	1.839(4)
P(2A)-C(31A)	1.840(3)
P(2A)-C(3A)	1.853(3)
P(1B)-C(21B)	1.840(4)
P(1B)-C(2B)	1.847(3)
P(1B)-C(11D)	1.849(3)
P(1B)-C(11B)	1.851(3)
P(2B)-C(41B)	1.825(3)
P(2B)-C(31B)	1.834(4)
P(2B)-C(3B)	1.848(3)
P(1C)-C(21C)	1.824(3)
P(1C)-C(11C)	1.838(4)
P(1C)-C(2C)	1.843(3)
P(2C)-C(31C)	1.835(4)
P(2C)-C(41C)	1.841(3)
P(2C)-C(3C)	1.853(3)
P(3)-O(5)	1.500(2)
P(3)-C(91)	1.800(4)
P(3)-C(81)	1.807(4)
P(3)-C(71)	1.807(3)
O(1A)-C(1A)	1.304(4)
O(2A)-C(1A)	1.225(4)
O(3A)-C(4A)	1.300(4)
O(4A)-C(4A)	1.244(4)
O(1B)-C(1B)	1.297(4)
O(2B)-C(1B)	1.228(4)
O(3B)-C(4B)	1.271(4)
O(4B)-C(4B)	1.254(4)
O(1C)-C(1C)	1.268(4)
O(2C)-C(1C)	1.258(4)
O(3C)-C(4C)	1.292(4)
O(4C)-C(4C)	1.228(4)
C(1A)-C(2A)	1.499(4)
C(2A)-C(3A)	1.345(4)
C(3A)-C(4A)	1.497(4)
C(11A)-C(16A)	1.390(5)
C(11A)-C(12A)	1.391(5)
C(12A)-C(13A)	1.382(6)
C(13A)-C(14A)	1.372(8)
C(14A)-C(15A)	1.369(8)
C(15A)-C(16A)	1.397(6)
C(21A)-C(26A)	1.394(5)
C(21A)-C(22A)	1.402(5)
C(22A)-C(23A)	1.390(5)
C(23A)-C(24A)	1.381(6)

C(24A)-C(25A)	1.383(5)	C(33B)-C(34B)	1.361(8)
C(25A)-C(26A)	1.390(5)	C(34B)-C(35B)	1.361(8)
C(31A)-C(32A)	1.390(5)	C(35B)-C(36B)	1.402(7)
C(31A)-C(36A)	1.396(5)	C(41B)-C(46B)	1.390(5)
C(32A)-C(33A)	1.396(5)	C(41B)-C(42B)	1.394(5)
C(33A)-C(34A)	1.378(6)	C(42B)-C(43B)	1.383(5)
C(34A)-C(35A)	1.389(5)	C(43B)-C(44B)	1.379(6)
C(35A)-C(36A)	1.391(5)	C(44B)-C(45B)	1.378(6)
C(41A)-C(42A)	1.385(5)	C(45B)-C(46B)	1.377(6)
C(41A)-C(46A)	1.393(6)	C(1C)-C(2C)	1.506(4)
C(42A)-C(43A)	1.383(6	C(2C)-C(3C)	1.349(4)
C(43A)-C(44A)	1.351(8	C(3C)-C(4C)	1.505(4)
C(44A)-C(45A)	1.380(8	C(11C)-C(12C)	1.394(5)
C(45A)-C(46A)	1.385(6	C(11C)-C(16C)	1.395(5)
C(1B)-C(2B)	1.508(4)	C(12C)-C(13C)	1.377(6)
C(2B)-C(3B)	1.341(5)	C(13C)-C(14C)	1.386(7)
C(3B)-C(4B)	1.502(4)	C(14C)-C(15C)	1.383(7)
C(11B)-C(12B)	1.3900	C(15C)-C(16C)	1.386(6)
C(11B)-C(16B)	1.3900	C(21C)-C(22C)	1.380(6)
C(12B)-C(13B)	1.3900	C(21C)-C(26C)	1.389(5)
C(13B)-C(14B)	1.3900	C(22C)-C(23C)	1.392(6)
C(14B)-C(15B)	1.3900	C(23C)-C(24C)	1.382(7)
C(15B)-C(16B)	1.3900	C(24C)-C(25C)	1.359(7)
C(11D)-C(12D)	1.3900	C(25C)-C(26C)	1.389(5)
C(11D)-C(16D)	1.3900	C(31C)-C(32C)	1.385(6)
C(12D)-C(13D)	1.3900	C(31C)-C(36C)	1.394(6)
C(13D)-C(14D)	1.3900	C(32C)-C(33C)	1.392(6)
C(14D)-C(15D)	1.3900	C(33C)-C(34C)	1.362(8)
C(15D)-C(16D)	1.3900	C(34C)-C(35C)	1.362(9)
C(21B)-C(26B)	1.388(6)	C(35C)-C(36C)	1.399(8)
C(21B)-C(22B)	1.395(5)	C(41C)-C(46C)	1.390(5)
C(22B)-C(23B)	1.388(6)	C(41C)-C(42C)	1.398(5)
C(23B)-C(24B)	1.376(7)	C(42C)-C(43C)	1.385(6)
C(24B)-C(25B)	1.374(7)	C(43C)-C(44C)	1.370(7)
C(25B)-C(26B)	1.385(6)	C(44C)-C(45C)	1.374(
C(31B)-C(32B)	1.388(6)	C(45C)-C(46C)	1.396(
C(31B)-C(36B)	1.391(6)	C(71)-C(71)#1	1.548(7)
C(32B)-C(33B)	1.393(6)	C(81)-C(82)	1.384(5)

C(81)-C(86)	1.392(5)
C(82)-C(83)	1.389(6)
C(83)-C(84)	1.381(7)
C(84)-C(85)	1.373(6)
C(85)-C(86)	1.384(6)
C(91)-C(96)	1.388(5)
C(91)-C(92)	1.403(5)
C(92)-C(93)	1.381(5)
C(93)-C(94)	1.378(5)
C(94)-C(95)	1.386(6)
C(95)-C(96)	1.382(6)
C(110)-C(111)	1.573(11)
C(111)-O(101)	1.272(0
O(101)-C(112)	1.525(12)
C(112)-C(113)	1.439(
O(100)-C(102)#2	1.308(9)
O(100)-C(102)	1.308(9)
O(100)-C(101)#2	1.339(10)
O(100)-C(101)	1.339(10)
C(101)-C(103)	1.51(20
C(102)-C(104)	1.50(2

Table **23** bond angles [°] Compound **6a**

O(1A)-Sn(1A)-O(3C)	80.67(9)	C(51C)-Sn(1C)-O(4B)	86.14(11)
O(1A)-Sn(1A)-C(51A)	107.52(12)	O(3B)-Sn(1C)-O(4B)	54.62(7)
O(3C)-Sn(1A)-C(51A)	108.97(11)	O(1C)-Sn(1C)-O(4B)	133.57(7)
O(1A)-Sn(1A)-C(61A)	109.38(12)	O(2C)-Sn(1C)-O(4B)	168.83(7)
O(3C)-Sn(1A)-C(61A)	110.07(12)	O(5)-Sn(1C)-O(4B)	84.00(8)
C(51A)-Sn(1A)-C(61A)	129.44(14)	C(61C)-Sn(1C)-C(1C)	92.48(14)
O(1B)-Sn(1B)-C(61B)	105.02(12)	C(51C)-Sn(1C)-C(1C)	91.73(12)
O(1B)-Sn(1B)-C(51B)	104.67(13)	O(3B)-Sn(1C)-C(1C)	107.78(9)
C(61B)-Sn(1B)-C(51B)	135.46(16)	O(1C)-Sn(1C)-C(1C)	28.48(9)
O(1B)-Sn(1B)-O(3A)	81.45(8)	O(2C)-Sn(1C)-C(1C)	28.29(9)
C(61B)-Sn(1B)-O(3A)	106.18(12)	O(5)-Sn(1C)-C(1C)	114.01(9)
C(51B)-Sn(1B)-O(3A)	110.45(13)	O(4B)-Sn(1C)-C(1C)	161.79(8)
O(1B)-Sn(1B)-O(4A)	138.44(8)	C(21A)-P(1A)-C(11A)	103.23(16)
C(61B)-Sn(1B)-O(4A)	88.30(11)	C(21A)-P(1A)-C(2A)	100.00(14)
C(51B)-Sn(1B)-O(4A)	90.94(12)	C(11A)-P(1A)-C(2A)	103.04(15)
O(3A)-Sn(1B)-O(4A)	56.99(8)	C(41A)-P(2A)-C(31A)	104.54(16)
O(1B)-Sn(1B)-C(4A)	110.51(9)	C(41A)-P(2A)-C(3A)	102.08(14)
C(61B)-Sn(1B)-C(4A)	96.90(12)	C(31A)-P(2A)-C(3A)	100.30(14)
C(51B)-Sn(1B)-C(4A)	102.86(13)	C(21B)-P(1B)-C(2B)	100.17(15)
O(3A)-Sn(1B)-C(4A)	29.08(9)	C(21B)-P(1B)-C(11D)	104.85(17)
O(4A)-Sn(1B)-C(4A)	27.95(8)	C(2B)-P(1B)-C(11D)	112.26(18)
C(61C)-Sn(1C)-C(51C)	170.20(15)	C(21B)-P(1B)-C(11B)	101.62(15)
C(61C)-Sn(1C)-O(3B)	91.26(13)	C(2B)-P(1B)-C(11B)	104.74(17)
C(51C)-Sn(1C)-O(3B)	95.87(12)	C(41B)-P(2B)-C(31B)	100.74(17)
C(61C)-Sn(1C)-O(1C)	94.03(13)	C(41B)-P(2B)-C(3B)	101.98(15)
C(51C)-Sn(1C)-O(1C)	93.89(12)	C(31B)-P(2B)-C(3B)	104.40(15)
O(3B)-Sn(1C)-O(1C)	79.31(8)	C(21C)-P(1C)-C(11C)	106.65(16)
C(61C)-Sn(1C)-O(2C)	90.53(13)	C(21C)-P(1C)-C(2C)	102.71(15)
C(51C)-Sn(1C)-O(2C)	88.99(12)	C(11C)-P(1C)-C(2C)	103.39(15)
O(3B)-Sn(1C)-O(2C)	136.06(8)	C(31C)-P(2C)-C(41C)	102.65(15)
O(1C)-Sn(1C)-O(2C)	56.77(8)	C(31C)-P(2C)-C(3C)	101.55(15)
C(61C)-Sn(1C)-O(5)	82.46(13)	C(41C)-P(2C)-C(3C)	103.85(14)
C(51C)-Sn(1C)-O(5)	87.75(12)	O(5)-P(3)-C(91)	112.23(15)
O(3B)-Sn(1C)-O(5)	137.92(8)	O(5)-P(3)-C(81)	110.62(16)
O(1C)-Sn(1C)-O(5)	142.42(8)	C(91)-P(3)-C(81)	105.79(16)
O(2C)-Sn(1C)-O(5)	85.77(8)	O(5)-P(3)-C(71)	112.65(15)
C(61C)-Sn(1C)-O(4B)	92.56(13)	C(91)-P(3)-C(71)	107.75(16)

C(81)-P(3)-C(71)	107.44(16)	C(24A)-C(23A)-C(22A)	120.7
C(1A)-O(1A)-Sn(1A)	106.99(19)	C(23A)-C(24A)-C(25A)	119.5
C(4A)-O(3A)-Sn(1B)	98.64(18)	C(24A)-C(25A)-C(26A)	120.2
C(4A)-O(4A)-Sn(1B)	85.01(18)	C(25A)-C(26A)-C(21A)	121.2
C(1B)-O(1B)-Sn(1B)	107.7(2)	C(32A)-C(31A)-C(36A)	118.6(3)
C(4B)-O(3B)-Sn(1C)	98.03(19)	C(32A)-C(31A)-P(2A)	123.3(3)
C(4B)-O(4B)-Sn(1C)	86.08(18)	C(36A)-C(31A)-P(2A)	117.9(2)
C(1C)-O(1C)-Sn(1C)	93.38(18)	C(31A)-C(32A)-C(33A)	120.4
C(1C)-O(2C)-Sn(1C)	89.79(18)	C(34A)-C(33A)-C(32A)	120.6
C(4C)-O(3C)-Sn(1A)	105.35(19)	C(33A)-C(34A)-C(35A)	119.6
P(3)-O(5)-Sn(1C)	158.28(15)	C(34A)-C(35A)-C(36A)	119.9
O(2A)-C(1A)-O(1A)	121.8(3)	C(35A)-C(36A)-C(31A)	120.9
O(2A)-C(1A)-C(2A)	123.5(3)	C(42A)-C(41A)-C(46A)	118.8(4)
O(1A)-C(1A)-C(2A)	114.5(3)	C(42A)-C(41A)-P(2A)	116.3(3)
C(3A)-C(2A)-C(1A)	121.5(3)	C(46A)-C(41A)-P(2A)	124.8(3)
C(3A)-C(2A)-P(1A)	120.0(2)	C(43A)-C(42A)-C(41A)	120.6
C(1A)-C(2A)-P(1A)	118.0(2)	C(44A)-C(43A)-C(42A)	120.7
C(2A)-C(3A)-C(4A)	118.2(3)	C(43A)-C(44A)-C(45A)	119.5
C(2A)-C(3A)-P(2A)	121.7(2)	C(44A)-C(45A)-C(46A)	121.1
C(4A)-C(3A)-P(2A)	119.9(2)	C(45A)-C(46A)-C(41A)	119.3
O(4A)-C(4A)-O(3A)	119.2(3)	O(2B)-C(1B)-O(1B)	121.5(3)
O(4A)-C(4A)-C(3A)	122.1(3)	O(2B)-C(1B)-C(2B)	123.1(3)
O(3A)-C(4A)-C(3A)	118.6(3)	O(1B)-C(1B)-C(2B)	115.4(3)
O(4A)-C(4A)-Sn(1B)	67.04(17)	C(3B)-C(2B)-C(1B)	119.2(3)
O(3A)-C(4A)-Sn(1B)	52.29(15)	C(3B)-C(2B)-P(1B)	121.0(2)
C(3A)-C(4A)-Sn(1B)	169.6(2)	C(1B)-C(2B)-P(1B)	119.6(2)
C(16A)-C(11A)-C(12A)	117.9(4)	C(2B)-C(3B)-C(4B)	120.7(3)
C(16A)-C(11A)-P(1A)	116.7(3)	C(2B)-C(3B)-P(2B)	120.6(2)
C(12A)-C(11A)-P(1A)	125.3(3)	C(4B)-C(3B)-P(2B)	118.7(2)
C(13A)-C(12A)-C(11A)	121.4	O(4B)-C(4B)-O(3B)	121.3(3)
C(14A)-C(13A)-C(12A)	120.0	O(4B)-C(4B)-C(3B)	120.0(3)
C(15A)-C(14A)-C(13A)	120.1	O(3B)-C(4B)-C(3B)	118.7(3)
C(14A)-C(15A)-C(16A)	120.2	C(12B)-C(11B)-C(16B)	120.0
C(11A)-C(16A)-C(15A)	120.5	C(12B)-C(11B)-P(1B)	114.1(2)
C(26A)-C(21A)-C(22A)	117.9(3)	C(16B)-C(11B)-P(1B)	125.9(2)
C(26A)-C(21A)-P(1A)	123.8(2)	C(11B)-C(12B)-C(13B)	120.0
C(22A)-C(21A)-P(1A)	118.0(3)	C(14B)-C(13B)-C(12B)	120.0
C(23A)-C(22A)-C(21A)	120.5	C(13B)-C(14B)-C(15B)	120.0

C(16B)-C(15B)-C(14B)	120.0	O(1C)-C(1C)-Sn(1C)	58.14(16)
C(15B)-C(16B)-C(11B)	120.0	C(2C)-C(1C)-Sn(1C)	178.2(2)
C(12D)-C(11D)-C(16D)	120.0	C(3C)-C(2C)-C(1C)	121.0(3)
C(12D)-C(11D)-P(1B)	114.1(2)	C(3C)-C(2C)-P(1C)	117.4(2)
C(16D)-C(11D)-P(1B)	125.9(2)	C(1C)-C(2C)-P(1C)	121.5(2)
C(13D)-C(12D)-C(11D)	120.0	C(2C)-C(3C)-C(4C)	123.2(3)
C(12D)-C(13D)-C(14D)	120.0	C(2C)-C(3C)-P(2C)	120.5(2)
C(13D)-C(14D)-C(15D)	120.0	C(4C)-C(3C)-P(2C)	116.3(2)
C(16D)-C(15D)-C(14D)	120.0	O(4C)-C(4C)-O(3C)	122.3(3)
C(15D)-C(16D)-C(11D)	120.0	O(4C)-C(4C)-C(3C)	123.3(3)
C(26B)-C(21B)-C(22B)	118.6(4)	O(3C)-C(4C)-C(3C)	114.2(3)
C(26B)-C(21B)-P(1B)	124.1(3)	C(12C)-C(11C)-C(16C)	118.6(3)
C(22B)-C(21B)-P(1B)	117.2(3)	C(12C)-C(11C)-P(1C)	115.4(3)
C(23B)-C(22B)-C(21B)	120.0(4)	C(16C)-C(11C)-P(1C)	126.0(3)
C(24B)-C(23B)-C(22B)	120.6(4)	C(13C)-C(12C)-C(11C)	121.1(4)
C(25B)-C(24B)-C(23B)	119.8(4)	C(12C)-C(13C)-C(14C)	119.8(4)
C(24B)-C(25B)-C(26B)	120.2(5)	C(15C)-C(14C)-C(13C)	119.8(4)
C(25B)-C(26B)-C(21B)	120.8(4)	C(14C)-C(15C)-C(16C)	120.4(4)
C(32B)-C(31B)-C(36B)	118.6(4)	C(15C)-C(16C)-C(11C)	120.2(4)
C(32B)-C(31B)-P(2B)	124.3(3)	C(22C)-C(21C)-C(26C)	117.8(3)
C(36B)-C(31B)-P(2B)	116.8(3)	C(22C)-C(21C)-P(1C)	121.5(3)
C(31B)-C(32B)-C(33B)	120.3(5)	C(26C)-C(21C)-P(1C)	119.7(3)
C(34B)-C(33B)-C(32B)	120.2(5)	C(21C)-C(22C)-C(23C)	121.3(4)
C(33B)-C(34B)-C(35B)	120.8(5)	C(24C)-C(23C)-C(22C)	119.9(5)
C(34B)-C(35B)-C(36B)	119.9(5)	C(25C)-C(24C)-C(23C)	119.2(4)
C(31B)-C(36B)-C(35B)	120.1(5)	C(24C)-C(25C)-C(26C)	121.2(4)
C(46B)-C(41B)-C(42B)	118.1(3)	C(21C)-C(26C)-C(25C)	120.6(4)
C(46B)-C(41B)-P(2B)	116.9(3)	C(32C)-C(31C)-C(36C)	118.5(4)
C(42B)-C(41B)-P(2B)	125.0(3)	C(32C)-C(31C)-P(2C)	125.4(3)
C(43B)-C(42B)-C(41B)	120.7(4)	C(36C)-C(31C)-P(2C)	116.0(3)
C(44B)-C(43B)-C(42B)	120.0(4)	C(31C)-C(32C)-C(33C)	120.4(4)
C(45B)-C(44B)-C(43B)	120.0(4)	C(34C)-C(33C)-C(32C)	120.8(5)
C(46B)-C(45B)-C(44B)	120.0(4)	C(35C)-C(34C)-C(33C)	119.6(5)
C(45B)-C(46B)-C(41B)	121.2(4)	C(34C)-C(35C)-C(36C)	121.0(5)
O(2C)-C(1C)-O(1C)	120.1(3)	C(31C)-C(36C)-C(35C)	119.7(5)
O(2C)-C(1C)-C(2C)	119.7(3)	C(46C)-C(41C)-C(42C)	118.0(3)
O(1C)-C(1C)-C(2C)	120.2(3)	C(46C)-C(41C)-P(2C)	124.0(3)
O(2C)-C(1C)-Sn(1C)	61.91(16)	C(42C)-C(41C)-P(2C)	117.3(3)

C(43C)-C(42C)-C(41C)	120.9(4)
C(44C)-C(43C)-C(42C)	120.3(4)
C(43C)-C(44C)-C(45C)	120.0(4)
C(44C)-C(45C)-C(46C)	120.2(4)
C(41C)-C(46C)-C(45C)	120.6(4)
C(71)#1-C(71)-P(3)	111.1(3)
C(82)-C(81)-C(86)	119.4(4)
C(82)-C(81)-P(3)	118.6(3)
C(86)-C(81)-P(3)	121.9(3)
C(81)-C(82)-C(83)	119.7(4)
C(84)-C(83)-C(82)	120.7(4)
C(85)-C(84)-C(83)	119.5(4)
C(84)-C(85)-C(86)	120.5(4)
C(85)-C(86)-C(81)	120.1(4)
C(96)-C(91)-C(92)	119.0(3)
C(96)-C(91)-P(3)	118.7(3)
C(92)-C(91)-P(3)	122.1(3)
C(93)-C(92)-C(91)	120.4(3)
C(94)-C(93)-C(92)	119.9(4)
C(93)-C(94)-C(95)	120.2(4)
C(96)-C(95)-C(94)	120.2(4)
C(95)-C(96)-C(91)	120.2(4)
O(101)-C(111)-C(110)	119.1(8)
C(111)-O(101)-C(112)	108.3(7)
C(113)-C(112)-O(101)	99.8(11)
C(102)#2-O(100)-C(102)	180.0(11)
C(102)#2-O(100)-C(101)#2	55.8(6)
C(102)-O(100)-C(101)#2	124.2(6)
C(102)#2-O(100)-C(101)	124.2(6)
C(102)-O(100)-C(101)	55.8(6)
C(101)#2-O(100)-C(101)	180.0(11)
O(100)-C(101)-C(103)	115.3(10)
O(100)-C(102)-C(104)	114.5(10)

Symmetry transformations used to generate equivalent atoms:

#1 -x+1,-y+2,-z+1 #2 -x+2,-y+2,-z

Table **24** Bond distances [Å] for Compound **6b** polymorph 1

Sn(1A)-O(1A)	2.070(3)
Sn(1A)-O(3C)	2.092(3)
Sn(1A)-C(61A)	2.120(5)
Sn(1A)-C(51A)	2.130(5)
P(1A)-C(11A)	1.830(5)
P(1A)-C(21A)	1.835(5)
P(1A)-C(2A)	1.851(5)
P(2A)-C(31A)	1.835(5)
P(2A)-C(41A)	1.838(5)
P(2A)-C(3A)	1.842(5)
O(1A)-C(1A)	1.295(5)
O(2A)-C(1A)	1.230(6)
O(3A)-C(4A)	1.307(5)
O(3A)-Sn(1B)	2.122(3)
O(4A)-C(4A)	1.238(5)
C(1A)-C(2A)	1.502(6)
C(2A)-C(3A)	1.329(6)
C(3A)-C(4A)	1.510(6)
C(11A)-C(12A)	1.395(7)
C(11A)-C(16A)	1.409(7)
C(12A)-C(13A)	1.391(8)
C(13A)-C(14A)	1.381(9)
C(14A)-C(15A)	1.377(9)
C(15A)-C(16A)	1.382(8)
C(21A)-C(22A)	1.368(7)
C(21A)-C(26A)	1.400(7)
C(22A)-C(23A)	1.410(9)
C(23A)-C(24A)	1.334(9)
C(24A)-C(25A)	1.364(9)
C(25A)-C(26A)	1.433(8)
C(31A)-C(32A)	1.361(7)
C(31A)-C(36A)	1.389(7)
C(32A)-C(33A)	1.394(8)
C(33A)-C(34A)	1.338(9)
C(34A)-C(35A)	1.372(9)
C(35A)-C(36A)	1.383(7)
C(41A)-C(42A)	1.385(7)
C(41A)-C(46A)	1.410(8)
C(42A)-C(43A)	1.361(8)
C(43A)-C(44A)	1.391(10)
C(44A)-C(45A)	1.357(11)
C(45A)-C(46A)	1.350(9)
C(51A)-C(52A)	1.605(11)
C(52A)-C(53A)	1.461(11)
C(53A)-C(54A)	1.548(11)
C(61A)-C(62A)	1.516(6)
C(62A)-C(63A)	1.542(7)
C(63A)-C(64A)	1.511(8)
Sn(1B)-C(61B)	2.114(5)
Sn(1B)-C(51B)	2.117(5)
Sn(1B)-O(1B)	2.166(3)
Sn(1B)-O(2B)	2.374(3)
Sn(1B)-C(1B)	2.621(4)
P(1B)-C(21B)	1.832(5)
P(1B)-C(11B)	1.842(5)
P(1B)-C(2B)	1.845(4)
P(2B)-C(31B)	1.814(6)
P(2B)-C(41B)	1.855(5)
P(2B)-C(3B)	1.862(5)
O(1B)-C(1B)	1.298(5)
O(2B)-C(1B)	1.241(5)
O(3B)-C(4B)	1.297(5)
O(3B)-Sn(1C)	2.129(3)
O(4B)-C(4B)	1.209(5)
C(1B)-C(2B)	1.507(6)
C(2B)-C(3B)	1.343(6)
C(3B)-C(4B)	1.518(6)
C(11B)-C(12B)	1.355(7)
C(11B)-C(16B)	1.384(7)
C(12B)-C(13B)	1.416(8)
C(13B)-C(14B)	1.396(10)
C(14B)-C(15B)	1.360(9)

C(15B)-C(16B)	1.383(8)
C(21B)-C(26B)	1.357(7)
C(21B)-C(22B)	1.395(7)
C(22B)-C(23B)	1.380(7)
C(23B)-C(24B)	1.397(8)
C(24B)-C(25B)	1.393(9)
C(25B)-C(26B)	1.373(8)
C(31B)-C(32B)	1.376(8)
C(31B)-C(36B)	1.411(8)
C(32B)-C(33B)	1.370(9)
C(33B)-C(34B)	1.334(11)
C(34B)-C(35B)	1.409(12)
C(35B)-C(36B)	1.381(9)
C(41B)-C(42B)	1.360(7)
C(41B)-C(46B)	1.391(7)
C(42B)-C(43B)	1.387(8)
C(43B)-C(44B)	1.349(8)
C(44B)-C(45B)	1.437(8)
C(45B)-C(46B)	1.361(7)
C(51B)-C(52B)	1.506(9)
C(52B)-C(53B)	1.354(10)
C(53B)-C(54B)	1.499(10)
C(61B)-C(62B)	1.484(7)
C(62B)-C(63B)	1.539(8)
C(63B)-C(64B)	1.390(10)
Sn(1C)-C(61C)	2.105(5)
Sn(1C)-C(51C)	2.116(5)
Sn(1C)-O(1C)	2.166(3)
Sn(1C)-O(2C)	2.414(3)
Sn(1C)-C(1C)	2.642(5)
P(1C)-C(11C)	1.829(5)
P(1C)-C(21C)	1.832(5)
P(1C)-C(2C)	1.843(5)
P(2C)-C(41C)	1.819(5)
P(2C)-C(31C)	1.824(5)
P(2C)-C(3C)	1.857(5)
O(1C)-C(1C)	1.292(6)
O(2C)-C(1C)	1.251(6)
O(3C)-C(4C)	1.297(5)
O(4C)-C(4C)	1.241(6)
C(1C)-C(2C)	1.495(6)
C(2C)-C(3C)	1.350(6)
C(3C)-C(4C)	1.491(6)
C(11C)-C(12C)	1.395(7)
C(11C)-C(16C)	1.404(7)
C(12C)-C(13C)	1.354(8)
C(13C)-C(14C)	1.384(9)
C(14C)-C(15C)	1.369(10)
C(15C)-C(16C)	1.360(8)
C(21C)-C(22C)	1.367(8)
C(21C)-C(26C)	1.401(8)
C(22C)-C(23C)	1.401(10)
C(23C)-C(24C)	1.389(11)
C(24C)-C(25C)	1.363(10)
C(25C)-C(26C)	1.416(8)
C(31C)-C(36C)	1.395(7)
C(31C)-C(32C)	1.411(7)
C(32C)-C(33C)	1.396(9)
C(33C)-C(34C)	1.330(9)
C(34C)-C(35C)	1.406(9)
C(35C)-C(36C)	1.393(8)
C(41C)-C(42C)	1.379(7)
C(41C)-C(46C)	1.394(7)
C(42C)-C(43C)	1.394(7)
C(43C)-C(44C)	1.398(8)
C(44C)-C(45C)	1.362(8)
C(45C)-C(46C)	1.386(7)
C(51C)-C(52C)	1.518(7)
C(52C)-C(53C)	1.525(8)
C(53C)-C(54C)	1.494(9)
C(61C)-C(62C)	1.520(8)
C(62C)-C(63C)	1.498(9)
C(63C)-C(64C)	1.535(10)

Table **25**Bond angles [°] Compound **6b** polymorph **1**

O(1A)-Sn(1A)-O(3C)	79.39(12)	C(22A)-C(21A)-C(26A)	119.9(5)
O(1A)-Sn(1A)-C(61A)	107.74(16)	C(22A)-C(21A)-P(1A)	114.5(4)
O(3C)-Sn(1A)-C(61A)	107.31(16)	C(26A)-C(21A)-P(1A)	125.5(4)
O(1A)-Sn(1A)-C(51A)	104.16(19)	C(21A)-C(22A)-C(23A)	119.6(6)
O(3C)-Sn(1A)-C(51A)	111.80(19)	C(24A)-C(23A)-C(22A)	121.3(6)
C(61A)-Sn(1A)-C(51A)	133.0(2)	C(23A)-C(24A)-C(25A)	120.8(6)
C(11A)-P(1A)-C(21A)	105.3(2)	C(24A)-C(25A)-C(26A)	119.8(6)
C(11A)-P(1A)-C(2A)	102.0(2)	C(21A)-C(26A)-C(25A)	118.5(6)
C(21A)-P(1A)-C(2A)	106.5(2)	C(32A)-C(31A)-C(36A)	118.5(5)
C(31A)-P(2A)-C(41A)	104.8(2)	C(32A)-C(31A)-P(2A)	117.5(4)
C(31A)-P(2A)-C(3A)	104.1(2)	C(36A)-C(31A)-P(2A)	123.8(4)
C(41A)-P(2A)-C(3A)	101.5(2)	C(31A)-C(32A)-C(33A)	121.3(6)
C(1A)-O(1A)-Sn(1A)	110.6(3)	C(34A)-C(33A)-C(32A)	120.0(6)
C(4A)-O(3A)-Sn(1B)	101.0(3)	C(33A)-C(34A)-C(35A)	119.9(6)
O(2A)-C(1A)-O(1A)	123.2(4)	C(34A)-C(35A)-C(36A)	120.8(6)
O(2A)-C(1A)-C(2A)	124.0(4)	C(35A)-C(36A)-C(31A)	119.5(5)
O(1A)-C(1A)-C(2A)	112.8(4)	C(42A)-C(41A)-C(46A)	116.9(5)
C(3A)-C(2A)-C(1A)	120.3(4)	C(42A)-C(41A)-P(2A)	126.0(4)
C(3A)-C(2A)-P(1A)	118.5(3)	C(46A)-C(41A)-P(2A)	117.1(5)
C(1A)-C(2A)-P(1A)	121.1(3)	C(43A)-C(42A)-C(41A)	121.2(6)
C(2A)-C(3A)-C(4A)	119.7(4)	C(42A)-C(43A)-C(44A)	120.1(7)
C(2A)-C(3A)-P(2A)	121.4(4)	C(45A)-C(44A)-C(43A)	119.6(7)
C(4A)-C(3A)-P(2A)	118.9(3)	C(46A)-C(45A)-C(44A)	120.4(7)
O(4A)-C(4A)-O(3A)	121.0(4)	C(45A)-C(46A)-C(41A)	121.5(7)
O(4A)-C(4A)-C(3A)	121.0(4)	C(52A)-C(51A)-Sn(1A)	111.8(4)
O(3A)-C(4A)-C(3A)	118.1(4)	C(53A)-C(52A)-C(51A)	108.1(7)
C(12A)-C(11A)-C(16A)	118.5(5)	C(52A)-C(53A)-C(54A)	108.5(8)
C(12A)-C(11A)-P(1A)	123.4(4)	C(62A)-C(61A)-Sn(1A)	113.4(3)
C(16A)-C(11A)-P(1A)	117.4(4)	C(61A)-C(62A)-C(63A)	113.4(4)
C(13A)-C(12A)-C(11A)	120.3(5)	C(64A)-C(63A)-C(62A)	113.4(5)
C(14A)-C(13A)-C(12A)	120.8(6)	C(61B)-Sn(1B)-C(51B)	142.1(2)
C(15A)-C(14A)-C(13A)	119.0(6)	C(61B)-Sn(1B)-O(3A)	100.36(17)
C(14A)-C(15A)-C(16A)	121.6(6)	C(51B)-Sn(1B)-O(3A)	102.90(17)
C(15A)-C(16A)-C(11A)	119.8(5)	C(61B)-Sn(1B)-O(1B)	110.19(17)

C(51B)-Sn(1B)-O(1B)	101.04(17)	C(11B)-C(12B)-C(13B)	121.5(6)
O(3A)-Sn(1B)-O(1B)	85.59(11)	C(14B)-C(13B)-C(12B)	118.1(6)
C(61B)-Sn(1B)-O(2B)	90.88(16)	C(15B)-C(14B)-C(13B)	119.7(6)
C(51B)-Sn(1B)-O(2B)	88.10(17)	C(14B)-C(15B)-C(16B)	121.4(6)
O(3A)-Sn(1B)-O(2B)	143.15(11)	C(15B)-C(16B)-C(11B)	120.0(6)
O(1B)-Sn(1B)-O(2B)	57.66(11)	C(26B)-C(21B)-C(22B)	117.9(5)
C(61B)-Sn(1B)-C(1B)	103.26(18)	C(26B)-C(21B)-P(1B)	123.4(4)
C(51B)-Sn(1B)-C(1B)	93.34(18)	C(22B)-C(21B)-P(1B)	117.9(4)
O(3A)-Sn(1B)-C(1B)	115.13(14)	C(23B)-C(22B)-C(21B)	122.1(5)
O(1B)-Sn(1B)-C(1B)	29.54(13)	C(22B)-C(23B)-C(24B)	118.8(5)
O(2B)-Sn(1B)-C(1B)	28.21(13)	C(25B)-C(24B)-C(23B)	118.7(5)
C(21B)-P(1B)-C(11B)	107.6(2)	C(26B)-C(25B)-C(24B)	120.7(6)
C(21B)-P(1B)-C(2B)	100.8(2)	C(21B)-C(26B)-C(25B)	121.6(5)
C(11B)-P(1B)-C(2B)	104.9(2)	C(32B)-C(31B)-C(36B)	115.5(6)
C(31B)-P(2B)-C(41B)	101.1(2)	C(32B)-C(31B)-P(2B)	127.5(5)
C(31B)-P(2B)-C(3B)	105.9(2)	C(36B)-C(31B)-P(2B)	116.2(5)
C(41B)-P(2B)-C(3B)	100.6(2)	C(33B)-C(32B)-C(31B)	124.6(7)
C(1B)-O(1B)-Sn(1B)	95.1(3)	C(34B)-C(33B)-C(32B)	118.6(8)
C(1B)-O(2B)-Sn(1B)	87.0(3)	C(33B)-C(34B)-C(35B)	121.4(7)
C(4B)-O(3B)-Sn(1C)	100.1(3)	C(36B)-C(35B)-C(34B)	118.4(8)
O(2B)-C(1B)-O(1B)	119.8(4)	C(35B)-C(36B)-C(31B)	121.5(7)
O(2B)-C(1B)-C(2B)	119.7(4)	C(42B)-C(41B)-C(46B)	120.3(5)
O(1B)-C(1B)-C(2B)	120.5(4)	C(42B)-C(41B)-P(2B)	117.5(4)
O(2B)-C(1B)-Sn(1B)	64.7(2)	C(46B)-C(41B)-P(2B)	122.1(4)
O(1B)-C(1B)-Sn(1B)	55.4(2)	C(41B)-C(42B)-C(43B)	119.8(5)
C(2B)-C(1B)-Sn(1B)	172.3(3)	C(44B)-C(43B)-C(42B)	121.6(6)
C(3B)-C(2B)-C(1B)	123.2(4)	C(43B)-C(44B)-C(45B)	118.4(6)
C(3B)-C(2B)-P(1B)	117.4(3)	C(46B)-C(45B)-C(44B)	119.6(5)
C(1B)-C(2B)-P(1B)	119.3(3)	C(45B)-C(46B)-C(41B)	120.2(5)
C(2B)-C(3B)-C(4B)	124.5(4)	C(52B)-C(51B)-Sn(1B)	115.5(4)
C(2B)-C(3B)-P(2B)	119.0(3)	C(53B)-C(52B)-C(51B)	122.3(8)
C(4B)-C(3B)-P(2B)	116.0(3)	C(52B)-C(53B)-C(54B)	119.0(8)
O(4B)-C(4B)-O(3B)	123.0(4)	C(62B)-C(61B)-Sn(1B)	120.0(4)
O(4B)-C(4B)-C(3B)	120.1(4)	C(61B)-C(62B)-C(63B)	116.8(5)
O(3B)-C(4B)-C(3B)	116.8(4)	C(64B)-C(63B)-C(62B)	114.3(6)
C(12B)-C(11B)-C(16B)	119.3(5)	C(61C)-Sn(1C)-C(51C)	146.5(2)
C(12B)-C(11B)-P(1B)	114.1(4)	C(61C)-Sn(1C)-O(3B)	100.27(18)
C(16B)-C(11B)-P(1B)	126.6(4)	C(51C)-Sn(1C)-O(3B)	102.06(16)

C(61C)-Sn(1C)-O(1C)	101.98(18)	C(12C)-C(11C)-P(1C)	125.6(4)
C(51C)-Sn(1C)-O(1C)	104.10(18)	C(16C)-C(11C)-P(1C)	117.5(4)
O(3B)-Sn(1C)-O(1C)	86.39(12)	C(13C)-C(12C)-C(11C)	121.3(6)
C(61C)-Sn(1C)-O(2C)	82.04(17)	C(12C)-C(13C)-C(14C)	120.7(6)
C(51C)-Sn(1C)-O(2C)	94.66(17)	C(15C)-C(14C)-C(13C)	119.6(6)
O(3B)-Sn(1C)-O(2C)	142.87(11)	C(16C)-C(15C)-C(14C)	119.6(6)
O(1C)-Sn(1C)-O(2C)	57.27(11)	C(15C)-C(16C)-C(11C)	122.2(6)
C(61C)-Sn(1C)-C(1C)	92.04(18)	C(22C)-C(21C)-C(26C)	118.3(5)
C(51C)-Sn(1C)-C(1C)	100.65(18)	C(22C)-C(21C)-P(1C)	116.8(5)
O(3B)-Sn(1C)-C(1C)	115.16(13)	C(26C)-C(21C)-P(1C)	124.9(4)
O(1C)-Sn(1C)-C(1C)	29.07(13)	C(21C)-C(22C)-C(23C)	123.1(7)
O(2C)-Sn(1C)-C(1C)	28.19(13)	C(24C)-C(23C)-C(22C)	117.4(7)
C(11C)-P(1C)-C(21C)	105.1(2)	C(25C)-C(24C)-C(23C)	121.6(7)
C(11C)-P(1C)-C(2C)	104.6(2)	C(24C)-C(25C)-C(26C)	119.9(7)
C(21C)-P(1C)-C(2C)	99.2(2)	C(21C)-C(26C)-C(25C)	119.6(6)
C(41C)-P(2C)-C(31C)	104.2(2)	C(36C)-C(31C)-C(32C)	118.9(5)
C(41C)-P(2C)-C(3C)	102.2(2)	C(36C)-C(31C)-P(2C)	125.5(4)
C(31C)-P(2C)-C(3C)	99.3(2)	C(32C)-C(31C)-P(2C)	115.4(4)
C(1C)-O(1C)-Sn(1C)	96.4(3)	C(33C)-C(32C)-C(31C)	119.5(6)
C(1C)-O(2C)-Sn(1C)	86.1(3)	C(34C)-C(33C)-C(32C)	121.2(6)
C(4C)-O(3C)-Sn(1A)	102.7(3)	C(33C)-C(34C)-C(35C)	120.8(6)
O(2C)-C(1C)-O(1C)	120.3(4)	C(36C)-C(35C)-C(34C)	119.5(6)
O(2C)-C(1C)-C(2C)	118.7(4)	C(35C)-C(36C)-C(31C)	120.0(5)
O(1C)-C(1C)-C(2C)	120.9(4)	C(42C)-C(41C)-C(46C)	118.7(5)
O(2C)-C(1C)-Sn(1C)	65.7(3)	C(42C)-C(41C)-P(2C)	124.9(4)
O(1C)-C(1C)-Sn(1C)	54.6(2)	C(46C)-C(41C)-P(2C)	116.3(4)
C(2C)-C(1C)-Sn(1C)	175.4(3)	C(41C)-C(42C)-C(43C)	121.1(5)
C(3C)-C(2C)-C(1C)	120.5(4)	C(42C)-C(43C)-C(44C)	118.5(5)
C(3C)-C(2C)-P(1C)	119.3(3)	C(45C)-C(44C)-C(43C)	121.1(5)
C(1C)-C(2C)-P(1C)	120.3(3)	C(44C)-C(45C)-C(46C)	119.6(5)
C(2C)-C(3C)-C(4C)	121.4(4)	C(45C)-C(46C)-C(41C)	120.9(5)
C(2C)-C(3C)-P(2C)	120.2(3)	C(52C)-C(51C)-Sn(1C)	117.1(4)
C(4C)-C(3C)-P(2C)	118.2(3)	C(51C)-C(52C)-C(53C)	115.5(5)
O(4C)-C(4C)-O(3C)	121.3(4)	C(54C)-C(53C)-C(52C)	114.3(6)
O(4C)-C(4C)-C(3C)	123.6(4)	C(62C)-C(61C)-Sn(1C)	115.0(4)
O(3C)-C(4C)-C(3C)	115.0(4)	C(63C)-C(62C)-C(61C)	112.5(5)
C(12C)-C(11C)-C(16C)	116.4(5)	C(62C)-C(63C)-C(64C)	112.6(6)

Table**26** bond distances [Å] for Compound **6b** polymorph 2

Sn(1A)-O(1A)	2.093(3)	CC(34A)-C(35A)	1.379(8)
Sn(1A)-C(61A)	2.094(4)	C(35A)-C(36A)	1.383(7)
Sn(1A)-O(3C)	2.096(3)	C(41A)-C(42A)	1.390(7)
Sn(1A)-C(51A)	2.104(4)	C(41A)-C(46A)	1.394(7)
O(1A)-C(1A)	1.296(5)	C(42A)-C(43A)	1.396(7)
O(2A)-C(1A)	1.255(5)	C(43A)-C(44A)	1.365(8)
O(3A)-C(4A)	1.290(5)	C(44A)-C(45A)	1.369(9)
O(3A)-Sn(1B)	2.134(3)	C(45A)-C(46A)	1.383(8)
O(4A)-C(4A)	1.247(5)	C(51A)-C(52D)	1.5095(10)
O(4A)-Sn(1B)	2.536(3)	C(51A)-C(52A)	1.5097(10)
P(1A)-C(11A)	1.830(5)	C(52A)-C(53A)	1.5095(7)
P(1A)-C(21A)	1.841(5)	C(53A)-C(54A)	1.5302(10)
P(1A)-C(2A)	1.858(4)	C(52D)-C(53D)	1.5100(7)
P(2A)-C(31A)	1.830(5)	C(53D)-C(54D)	1.5300(10)
P(2A)-C(41A)	1.831(5)	C(61A)-C(62A)	1.535(6)
P(2A)-C(3A)	1.844(4)	C(62A)-C(63A)	1.5125(10)
C(1A)-C(2A)	1.477(6)	C(63A)-C(64A)	1.5285(10)
C(2A)-C(3A)	1.346(6)	C(63D)-C(64D)	1.5293(10)
C(3A)-C(4A)	1.500(5)	Sn(1B)-C(51B)	2.108(5)
C(11A)-C(16A)	1.387(7)	Sn(1B)-C(61B)	2.121(4)
C(11A)-C(12A)	1.388(7)	Sn(1B)-O(1B)	2.165(3)
C(12A)-C(13A)	1.378(7)	Sn(1B)-O(2B)	2.350(3)
C(13A)-C(14A)	1.363(8)	Sn(1B)-C(1B)	2.640(4)
C(14A)-C(15A)	1.395(9)	O(1B)-C(1B)	1.299(4)
C(15A)-C(16A)	1.394(8)	O(2B)-C(1B)	1.260(5)
C(21A)-C(22A)	1.382(7)	O(3B)-C(4B)	1.283(4)
C(21A)-C(26A)	1.398(7)	O(3B)-Sn(1C)	2.130(3)
C(22A)-C(23A)	1.400(7)	O(4B)-C(4B)	1.239(5)
C(23A)-C(24A)	1.408(9)	P(1B)-C(21B)	1.827(4)
C(24A)-C(25A)	1.360(10)	P(1B)-C(11B)	1.839(4)
C(25A)-C(26A)	1.359(8)	P(1B)-C(2B)	1.845(4)
C(31A)-C(36A)	1.380(7)	P(2B)-C(31B)	1.829(4)
C(31A)-C(32A)	1.390(7)	P(2B)-C(41B)	1.836(4)
C(32A)-C(33A)	1.378(8)	P(2B)-C(3B)	1.857(4)
C(33A)-C(34A)	1.392(9)	C(1B)-C(2B)	1.484(6)

C(2B)-C(3B)	1.351(5)	Sn(1C)-O(2C)	2.551(3)
C(3B)-C(4B)	1.507(5)	O(1C)-C(1C)	1.298(5)
C(11B)-C(12B)	1.380(6)	O(2C)-C(1C)	1.234(5)
C(11B)-C(16B)	1.395(6)	O(3C)-C(4C)	1.296(5)
C(12B)-C(13B)	1.388(7)	O(4C)-C(4C)	1.248(5)
C(13B)-C(14B)	1.376(8)	P(1C)-C(21C)	1.836(4)
C(14B)-C(15B)	1.386(8)	P(1C)-C(11C)	1.845(4)
C(15B)-C(16B)	1.386(7)	P(1C)-C(2C)	1.849(4)
C(21B)-C(26B)	1.386(6)	P(2C)-C(41C)	1.819(5)
C(21B)-C(22B)	1.395(6)	P(2C)-C(31C)	1.832(4)
C(22B)-C(23B)	1.387(7)	P(2C)-C(3C)	1.845(4)
C(23B)-C(24B)	1.379(7)	C(1C)-C(2C)	1.498(5)
C(24B)-C(25B)	1.350(8)	C(2C)-C(3C)	1.344(5)
C(25B)-C(26B)	1.388(7)	C(3C)-C(4C)	1.495(5)
C(31B)-C(36B)	1.375(6)	C(11C)-C(12C)	1.367(6)
C(31B)-C(32B)	1.395(6)	C(11C)-C(16C)	1.399(6)
C(32B)-C(33B)	1.378(6)	C(12C)-C(13C)	1.390(7)
C(33B)-C(34B)	1.385(7)	C(13C)-C(14C)	1.379(8)
C(34B)-C(35B)	1.370(7)	C(14C)-C(15C)	1.369(8)
C(35B)-C(36B)	1.392(6)	C(15C)-C(16C)	1.375(7)
C(41B)-C(42B)	1.372(6)	C(21C)-C(26C)	1.395(6)
C(41B)-C(46B)	1.404(6)	C(21C)-C(22C)	1.397(6)
C(42B)-C(43B)	1.381(7)	C(22C)-C(23C)	1.385(6)
C(43B)-C(44B)	1.373(8)	C(23C)-C(24C)	1.386(7)
C(44B)-C(45B)	1.372(8)	C(24C)-C(25C)	1.362(7)
C(45B)-C(46B)	1.388(6)	C(25C)-C(26C)	1.395(7)
C(51B)-C(52B)	1.5104(10)	C(31C)-C(32C)	1.398(6)
C(52B)-C(53B)	1.5095(10)	C(31C)-C(36C)	1.407(6)
C(53B)-C(54B)	1.5296(10)	C(32C)-C(33C)	1.379(7)
C(52E)-C(53E)	1.5101(11)	C(33C)-C(34C)	1.363(7)
C(53E)-C(54E)	1.5298(10)	C(34C)-C(35C)	1.392(6)
C(61B)-C(62B)	1.519(6)	C(35C)-C(36C)	1.378(6)
C(62B)-C(63B)	1.556(7)	C(41C)-C(42C)	1.379(7)
C(63B)-C(64B)	1.505(8)	C(41C)-C(46C)	1.402(6)
Sn(1C)-C(51C)	2.118(4)	C(42C)-C(43C)	1.386(7)
Sn(1C)-O(1C)	2.119(3)	C(43C)-C(44C)	1.377(9)
Sn(1C)-C(61C)	2.120(4)	C(44C)-C(45C)	1.370(10)

C(62C)-C(63C)	1.521(7)
C(63C)-C(64C)	1.526(7)
O(70)-C(71)	1.374(8)
O(70)-C(73)	1.423(8)
C(71)-C(72)	1.440(11)
C(73)-C(74)	1.455(10)
C(52C)-C(53C)	1.511(7)
C(53C)-C(54C)	1.519(8)
C(61C)-C(62C)	1.522(6)
C(51C)-C(52C)	1.515(6)
C(45C)-C(46C)	1.382(9)

Table **27**bond angle [°] Compound **6b** polymorph **2**

O(1A)-Sn(1A)-C(61A)	108.37(13)	C(22A)-C(21A)-C(26A)	118.9(5)
O(1A)-Sn(1A)-O(3C)	82.52(10)	C(22A)-C(21A)-P(1A)	125.5(4)
C(61A)-Sn(1A)-O(3C)	104.70(15)	C(26A)-C(21A)-P(1A)	115.6(4)
O(1A)-Sn(1A)-C(51A)	110.22(17)	C(21A)-C(22A)-C(23A)	119.7(5)
C(61A)-Sn(1A)-C(51A)	134.93(17)	C(22A)-C(23A)-C(24A)	119.6(6)
O(3C)-Sn(1A)-C(51A)	102.55(13)	C(25A)-C(24A)-C(23A)	119.8(5)
C(1A)-O(1A)-Sn(1A)	103.4(2)	C(26A)-C(25A)-C(24A)	120.6(6)
C(4A)-O(3A)-Sn(1B)	100.5(2)	C(25A)-C(26A)-C(21A)	121.4(6)
C(4A)-O(4A)-Sn(1B)	83.0(2)	C(36A)-C(31A)-C(32A)	118.0(5)
C(11A)-P(1A)-C(21A)	103.1(2)	C(36A)-C(31A)-P(2A)	125.0(3)
C(11A)-P(1A)-C(2A)	100.82(19)	C(32A)-C(31A)-P(2A)	116.9(4)
C(21A)-P(1A)-C(2A)	102.91(19)	C(33A)-C(32A)-C(31A)	121.3(6)
C(31A)-P(2A)-C(41A)	103.3(2)	C(32A)-C(33A)-C(34A)	119.9(5)
C(31A)-P(2A)-C(3A)	103.16(19)	C(35A)-C(34A)-C(33A)	119.0(5)
C(41A)-P(2A)-C(3A)	101.78(19)	C(34A)-C(35A)-C(36A)	120.4(5)
O(2A)-C(1A)-O(1A)	119.4(4)	C(31A)-C(36A)-C(35A)	121.2(5)
O(2A)-C(1A)-C(2A)	122.4(4)	C(42A)-C(41A)-C(46A)	118.4(5)
O(1A)-C(1A)-C(2A)	118.3(4)	C(42A)-C(41A)-P(2A)	124.3(4)
C(3A)-C(2A)-C(1A)	120.5(4)	C(46A)-C(41A)-P(2A)	116.9(4)
C(3A)-C(2A)-P(1A)	118.4(3)	C(41A)-C(42A)-C(43A)	119.9(5)
C(1A)-C(2A)-P(1A)	121.0(3)	C(44A)-C(43A)-C(42A)	121.0(5)
C(2A)-C(3A)-C(4A)	118.8(4)	C(43A)-C(44A)-C(45A)	119.4(5)
C(2A)-C(3A)-P(2A)	121.4(3)	C(44A)-C(45A)-C(46A)	120.9(6)
C(4A)-C(3A)-P(2A)	119.8(3)	C(45A)-C(46A)-C(41A)	120.4(5)
O(4A)-C(4A)-O(3A)	120.9(4)	C(52D)-C(51A)-Sn(1A)	126.6(8)
O(4A)-C(4A)-C(3A)	120.5(4)	C(52A)-C(51A)-Sn(1A)	118.8(7)
O(3A)-C(4A)-C(3A)	118.6(3)	C(53A)-C(52A)-C(51A)	114.60(10)
C(16A)-C(11A)-C(12A)	117.5(5)	C(52A)-C(53A)-C(54A)	113.38(10)
C(16A)-C(11A)-P(1A)	116.7(4)	C(51A)-C(52D)-C(53D)	114.51(10)
C(12A)-C(11A)-P(1A)	125.8(3)	C(52D)-C(53D)-C(54D)	113.33(10)
C(13A)-C(12A)-C(11A)	121.8(5)	C(62A)-C(61A)-Sn(1A)	115.4(3)
C(14A)-C(13A)-C(12A)	120.6(5)	C(63A)-C(62A)-C(61A)	112.7(3)
C(13A)-C(14A)-C(15A)	119.3(5)	C(62A)-C(63A)-C(64A)	113.33(11)
C(16A)-C(15A)-C(14A)	119.8(5)	C(51B)-Sn(1B)-C(61B)	142.31(18)
C(11A)-C(16A)-C(15A)	121.0(6)	C(51B)-Sn(1B)-O(3A)	102.23(16)

C(61B)-Sn(1B)-O(3A)	102.29(14)	C(2B)-C(3B)-C(4B)	124.2(3)
C(51B)-Sn(1B)-O(1B)	106.11(17)	C(2B)-C(3B)-P(2B)	119.0(3)
C(61B)-Sn(1B)-O(1B)	103.67(14)	C(4B)-C(3B)-P(2B)	116.7(3)
O(3A)-Sn(1B)-O(1B)	86.19(10)	O(4B)-C(4B)-O(3B)	122.0(3)
C(51B)-Sn(1B)-O(2B)	87.67(17)	O(4B)-C(4B)-C(3B)	120.5(3)
C(61B)-Sn(1B)-O(2B)	89.10(15)	O(3B)-C(4B)-C(3B)	117.3(3)
O(3A)-Sn(1B)-O(2B)	143.91(10)	C(12B)-C(11B)-C(16B)	118.9(4)
O(1B)-Sn(1B)-O(2B)	57.76(10)	C(12B)-C(11B)-P(1B)	117.2(3)
C(51B)-Sn(1B)-O(4A)	84.56(17)	C(16B)-C(11B)-P(1B)	123.8(3)
C(61B)-Sn(1B)-O(4A)	86.16(14)	C(11B)-C(12B)-C(13B)	120.9(5)
O(3A)-Sn(1B)-O(4A)	55.61(9)	C(14B)-C(13B)-C(12B)	119.7(5)
O(1B)-Sn(1B)-O(4A)	141.80(9)	C(13B)-C(14B)-C(15B)	120.4(5)
O(2B)-Sn(1B)-O(4A)	160.41(9)	C(16B)-C(15B)-C(14B)	119.6(5)
C(51B)-Sn(1B)-C(1B)	97.04(17)	C(15B)-C(16B)-C(11B)	120.4(5)
C(61B)-Sn(1B)-C(1B)	97.74(15)	C(26B)-C(21B)-C(22B)	117.7(4)
O(3A)-Sn(1B)-C(1B)	115.43(11)	C(26B)-C(21B)-P(1B)	116.6(3)
O(1B)-Sn(1B)-C(1B)	29.29(10)	C(22B)-C(21B)-P(1B)	125.2(3)
O(2B)-Sn(1B)-C(1B)	28.48(10)	C(23B)-C(22B)-C(21B)	121.1(4)
O(4A)-Sn(1B)-C(1B)	170.96(10)	C(24B)-C(23B)-C(22B)	119.3(5)
C(1B)-O(1B)-Sn(1B)	96.1(2)	C(25B)-C(24B)-C(23B)	120.4(5)
C(1B)-O(2B)-Sn(1B)	88.7(2)	C(24B)-C(25B)-C(26B)	120.7(5)
C(4B)-O(3B)-Sn(1C)	101.0(2)	C(21B)-C(26B)-C(25B)	120.6(5)
C(21B)-P(1B)-C(11B)	104.74(19)	C(36B)-C(31B)-C(32B)	118.2(4)
C(21B)-P(1B)-C(2B)	102.97(18)	C(36B)-C(31B)-P(2B)	118.2(3)
C(11B)-P(1B)-C(2B)	102.84(18)	C(32B)-C(31B)-P(2B)	123.7(3)
C(31B)-P(2B)-C(41B)	102.47(19)	C(33B)-C(32B)-C(31B)	121.1(4)
C(31B)-P(2B)-C(3B)	100.60(18)	C(32B)-C(33B)-C(34B)	120.1(5)
C(41B)-P(2B)-C(3B)	105.04(18)	C(35B)-C(34B)-C(33B)	119.3(4)
O(2B)-C(1B)-O(1B)	117.4(4)	C(34B)-C(35B)-C(36B)	120.6(4)
O(2B)-C(1B)-C(2B)	120.3(3)	C(31B)-C(36B)-C(35B)	120.8(4)
O(1B)-C(1B)-C(2B)	122.2(3)	C(42B)-C(41B)-C(46B)	118.3(4)
O(2B)-C(1B)-Sn(1B)	62.9(2)	C(42B)-C(41B)-P(2B)	123.1(3)
O(1B)-C(1B)-Sn(1B)	54.60(19)	C(46B)-C(41B)-P(2B)	117.7(3)
C(2B)-C(1B)-Sn(1B)	174.7(3)	C(41B)-C(42B)-C(43B)	121.5(5)
C(3B)-C(2B)-C(1B)	122.3(3)	C(44B)-C(43B)-C(42B)	119.8(5)
C(3B)-C(2B)-P(1B)	118.0(3)	C(45B)-C(44B)-C(43B)	120.2(5)
C(1B)-C(2B)-P(1B)	119.5(3)	C(44B)-C(45B)-C(46B)	120.2(5)

C(45B)-C(46B)-C(41B)	120.0(5)	O(4C)-C(4C)-O(3C)	121.7(4)
C(52B)-C(51B)-Sn(1B)	114.1(5)	O(4C)-C(4C)-C(3C)	121.5(4)
C(53B)-C(52B)-C(51B)	114.54(11)	O(3C)-C(4C)-C(3C)	116.8(3)
C(52B)-C(53B)-C(54B)	124.7(9)	C(12C)-C(11C)-C(16C)	118.9(4)
C(52E)-C(53E)-C(54E)	113.33(11)	C(12C)-C(11C)-P(1C)	125.5(3)
C(54E)-C(53E)-H(53L)	108.9	C(16C)-C(11C)-P(1C)	115.5(4)
C(62B)-C(61B)-Sn(1B)	116.0(3)	C(11C)-C(12C)-C(13C)	120.3(4)
C(61B)-C(62B)-C(63B)	111.4(4)	C(14C)-C(13C)-C(12C)	120.7(5)
C(64B)-C(63B)-C(62B)	111.1(5)	C(15C)-C(14C)-C(13C)	119.0(5)
C(51C)-Sn(1C)-O(1C)	104.34(14)	C(14C)-C(15C)-C(16C)	120.8(5)
C(51C)-Sn(1C)-C(61C)	142.35(17)	C(15C)-C(16C)-C(11C)	120.3(5)
O(1C)-Sn(1C)-C(61C)	104.03(14)	C(26C)-C(21C)-C(22C)	118.6(4)
C(51C)-Sn(1C)-O(3B)	101.84(13)	C(26C)-C(21C)-P(1C)	117.3(3)
O(1C)-Sn(1C)-O(3B)	83.97(10)	C(22C)-C(21C)-P(1C)	123.9(3)
C(61C)-Sn(1C)-O(3B)	105.29(14)	C(23C)-C(22C)-C(21C)	120.7(4)
C(51C)-Sn(1C)-O(2C)	91.67(13)	C(22C)-C(23C)-C(24C)	119.5(5)
O(1C)-Sn(1C)-O(2C)	55.43(9)	C(25C)-C(24C)-C(23C)	121.0(5)
C(61C)-Sn(1C)-O(2C)	84.49(12)	C(24C)-C(25C)-C(26C)	119.8(5)
O(3B)-Sn(1C)-O(2C)	139.32(9)	C(21C)-C(26C)-C(25C)	120.4(4)
C(1C)-O(1C)-Sn(1C)	100.9(2)	C(32C)-C(31C)-C(36C)	117.4(4)
C(1C)-O(2C)-Sn(1C)	82.5(2)	C(32C)-C(31C)-P(2C)	117.2(3)
C(4C)-O(3C)-Sn(1A)	103.8(2)	C(36C)-C(31C)-P(2C)	125.2(3)
C(21C)-P(1C)-C(11C)	102.68(19)	C(33C)-C(32C)-C(31C)	121.0(4)
C(21C)-P(1C)-C(2C)	102.41(17)	C(34C)-C(33C)-C(32C)	121.0(4)
C(11C)-P(1C)-C(2C)	102.18(18)	C(33C)-C(34C)-C(35C)	119.5(4)
C(41C)-P(2C)-C(31C)	102.40(19)	C(36C)-C(35C)-C(34C)	120.2(4)
C(41C)-P(2C)-C(3C)	102.66(19)	C(35C)-C(36C)-C(31C)	120.9(4)
C(31C)-P(2C)-C(3C)	102.59(17)	C(42C)-C(41C)-C(46C)	118.5(5)
O(2C)-C(1C)-O(1C)	121.2(3)	C(42C)-C(41C)-P(2C)	126.1(3)
O(2C)-C(1C)-C(2C)	121.1(3)	C(46C)-C(41C)-P(2C)	115.4(4)
O(1C)-C(1C)-C(2C)	117.7(3)	C(41C)-C(42C)-C(43C)	121.4(5)
C(3C)-C(2C)-C(1C)	120.7(3)	C(44C)-C(43C)-C(42C)	119.0(6)
C(3C)-C(2C)-P(1C)	118.5(3)	C(45C)-C(44C)-C(43C)	120.7(6)
C(1C)-C(2C)-P(1C)	120.8(3)	C(44C)-C(45C)-C(46C)	120.3(6)
C(2C)-C(3C)-C(4C)	120.7(3)	C(52C)-C(51C)-Sn(1C)	116.3(3)
C(2C)-C(3C)-P(2C)	119.4(3)	C(53C)-C(52C)-C(51C)	114.3(4)
C(4C)-C(3C)-P(2C)	119.7(3)	C(52C)-C(53C)-C(54C)	113.2(5)

C(62C)-C(61C)-Sn(1C)	115.2(3)
C(63C)-C(62C)-C(61C)	114.9(4)
C(62C)-C(63C)-C(64C)	113.0(4)
C(71)-O(70)-C(73)	114.4(6)
O(70)-C(71)-C(72)	113.4(7)
O(70)-C(73)-C(74)	109.0(6)

Appendix 8

Comprehensive Tables for Compound $Au(dpmaaH_2)(dpmaaH^-)$

Table **28.** Bond lengths [Å] for [$Au(dpmaaH_2)(dpmaaH)$]

Au-P(2)	2.3725(19)	C(1)-C(2)	1.532(11)
Au-P(3)	2.3753(18)	C(2)-C(3)	1.322(10)
Au-P(1)	2.3840(18)	C(3)-C(4)	1.551(14)
Au-P(4)	2.3882(19)	C(5)-C(6)	1.507(11)
P(1)-C(11)	1.806(7)	C(6)-C(7)	1.352(11)
P(1)-C(21)	1.818(8)	C(7)-C(8)	1.547(13)
P(1)-C(2)	1.849(7)	C(11)-C(16)	1.370(11)
P(2)-C(31)	1.817(8)	C(11)-C(12)	1.379(12)
P(2)-C(41B)	1.824(5)	C(12)-C(13)	1.381(12)
P(2)-C(3)	1.825(8)	C(13)-C(14)	1.383(15)
P(2)-C(41)	1.826(5)	C(14)-C(15)	1.356(15)
P(3)-C(51)	1.821(4)	C(15)-C(16)	1.390(13)
P(3)-C(61B)	1.827(6)	C(21)-C(22)	1.384(10)
P(3)-C(61)	1.827(5)	C(21)-C(26)	1.389(11)
P(3)-C(61C)	1.830(6)	C(22)-C(23)	1.381(12)
P(3)-C(6)	1.847(8)	C(23)-C(24)	1.383(13)
P(4)-C(81)	1.809(8)	C(24)-C(25)	1.360(12)
P(4)-C(7)	1.817(8)	C(25)-C(26)	1.383(11)
P(4)-C(71)	1.831(8)	C(32)-C(31)	1.389(11)
O(1)-C(4)	1.292(13)	C(32)-C(33)	1.403(13)
O(2)-C(4)	1.182(13)	C(33)-C(34)	1.352(15)
O(3)-C(1)	1.288(11)	C(34)-C(35)	1.349(14)
O(4)-C(1)	1.199(10)	C(35)-C(36)	1.388(12)
O(5)-C(5)	1.223(13)	C(36)-C(31)	1.381(11)
O(6)-C(5)	1.231(12)	C(41)-C(42)	1.3900
O(7)-C(8)	1.319(12)	C(41)-C(46)	1.3900
O(8)-C(8)	1.174(12)	C(42)-C(43)	1.3900

C(43)-C(44)	1.3900
C(44)-C(45)	1.3900
C(45)-C(46)	1.3900
C(41B)-C(42B)	1.3900
C(41B)-C(46B)	1.3900
C(42B)-C(43B)	1.3900
C(43B)-C(44B)	1.3900
C(44B)-C(45B)	1.3900
C(71)-C(72)	1.377(11)
C(71)-C(76)	1.399(11)
C(61B)-C(62B)	1.3900
C(61B)-C(66B)	1.3900
C(62B)-C(63B)	1.3900
C(63B)-C(64B)	1.3900
C(64B)-C(65B)	1.3900
C(65B)-C(66B)	1.3900
C(81)-C(82)	1.362(12)
C(81)-C(86)	1.374(13)
C(61C)-C(62C)	1.3900
C(61C)-C(66C)	1.3900
C(62C)-C(63C)	1.3900
C(63C)-C(64C)	1.3900
C(64C)-C(65C)	1.3900
C(65C)-C(66C)	1.3900
C(72)-C(73)	1.386(12)
C(73)-C(74)	1.353(15)
C(74)-C(75)	1.379(15)
C(75)-C(76)	1.392(12)
C(82)-C(83)	1.411(12)
C(83)-C(84)	1.348(14)
C(84)-C(85)	1.307(14)
C(85)-C(86)	1.407(13)
O(9)-C(91)	1.422(5)
C(91)-C(92)	1.462(5)
O(10)-C(93)	1.418(5)
C(93)-C(94)	1.456(5)

Table **29**Bond angles [°] for [Au(dpmaaH$_2$)(dpmaaH)]

P(2)-Au-P(3)	111.87(8)
P(2)-Au-P(1)	87.09(7)
P(3)-Au-P(1)	133.96(7)
P(2)-Au-P(4)	135.61(7)
P(3)-Au-P(4)	86.63(7)
P(1)-Au-P(4)	109.09(7)
C(11)-P(1)-C(21)	106.1(4)
C(11)-P(1)-C(2)	101.8(3)
C(21)-P(1)-C(2)	107.7(3)
C(11)-P(1)-Au	112.4(3)
C(21)-P(1)-Au	122.9(2)
C(2)-P(1)-Au	103.9(2)
C(31)-P(2)-C(41B)	103.6(5)
C(31)-P(2)-C(3)	106.6(4)
C(41B)-P(2)-C(3)	96.7(6)
C(31)-P(2)-C(41)	108.2(4)
C(3)-P(2)-C(41)	102.8(4)
C(31)-P(2)-Au	122.3(3)
C(41B)-P(2)-Au	119.4(7)
C(3)-P(2)-Au	104.6(3)
C(41)-P(2)-Au	110.4(4)
C(51)-P(3)-C(61B)	99.4(4)
C(51)-P(3)-C(61)	106.2(5)
C(51)-P(3)-C(61C)	110.5(4)
C(51)-P(3)-C(6)	106.6(3)
C(61B)-P(3)-C(6)	98.5(3)
C(61)-P(3)-C(6)	102.1(4)
C(61C)-P(3)-C(6)	107.2(4)
C(51)-P(3)-Au	117.4(2)
C(61B)-P(3)-Au	127.4(4)
C(61)-P(3)-Au	118.2(5)
C(61C)-P(3)-Au	109.8(3)
C(6)-P(3)-Au	104.7(3)
C(81)-P(4)-C(7)	105.5(4)
C(81)-P(4)-C(71)	106.3(4)
C(7)-P(4)-C(71)	102.1(4)
C(81)-P(4)-Au	121.3(3)
C(7)-P(4)-Au	105.4(3)
C(71)-P(4)-Au	114.4(2)
O(4)-C(1)-O(3)	127.7(9)
O(4)-C(1)-C(2)	119.3(9)
O(3)-C(1)-C(2)	113.0(8)
C(3)-C(2)-C(1)	118.6(7)
C(3)-C(2)-P(1)	121.8(6)
C(1)-C(2)-P(1)	119.5(6)
C(2)-C(3)-C(4)	120.0(8)
C(2)-C(3)-P(2)	122.5(6)
C(4)-C(3)-P(2)	117.5(7)
O(2)-C(4)-O(1)	127.0(13)
O(2)-C(4)-C(3)	118.9(11)
O(1)-C(4)-C(3)	114.1(11)
O(5)-C(5)-O(6)	125.1(10)
O(5)-C(5)-C(6)	119.2(10)
O(6)-C(5)-C(6)	115.7(9)
C(7)-C(6)-C(5)	119.3(8)
C(7)-C(6)-P(3)	121.6(6)
C(5)-C(6)-P(3)	119.1(7)
C(6)-C(7)-C(8)	117.9(8)
C(6)-C(7)-P(4)	121.4(6)
C(8)-C(7)-P(4)	120.5(7)
O(8)-C(8)-O(7)	125.9(11)
O(8)-C(8)-C(7)	122.9(11)

O(7)-C(8)-C(7)	111.2(9)	C(46B)-C(41B)-P(2)	117.1(4)
C(16)-C(11)-C(12)	118.6(8)	C(41B)-C(42B)-C(43B)	120.0
C(16)-C(11)-P(1)	122.3(7)	C(42B)-C(43B)-C(44B)	120.0
C(12)-C(11)-P(1)	118.8(6)	C(45B)-C(44B)-C(43B)	120.0
C(11)-C(12)-C(13)	120.6(10)	C(44B)-C(45B)-C(46B)	120.0
C(12)-C(13)-C(14)	119.6(11)	C(45B)-C(46B)-C(41B)	120.0
C(15)-C(14)-C(13)	120.4(9)	C(52)-C(51)-C(56)	120.0
C(14)-C(15)-C(16)	119.4(10)	C(52)-C(51)-P(3)	123.4(4)
C(11)-C(16)-C(15)	121.3(10)	C(56)-C(51)-P(3)	116.2(4)
C(22)-C(21)-C(26)	117.7(8)	C(51)-C(52)-C(53)	120.0
C(22)-C(21)-P(1)	125.2(6)	C(52)-C(53)-C(54)	120.0
C(26)-C(21)-P(1)	117.1(6)	C(55)-C(54)-C(53)	120.0
C(23)-C(22)-C(21)	121.0(8)	C(56)-C(55)-C(54)	120.0
C(22)-C(23)-C(24)	119.8(9)	C(55)-C(56)-C(51)	120.0
C(25)-C(24)-C(23)	120.4(9)	C(62)-C(61)-C(66)	120.0
C(24)-C(25)-C(26)	119.5(9)	C(62)-C(61)-P(3)	122.4(4)
C(25)-C(26)-C(21)	121.6(8)	C(66)-C(61)-P(3)	117.6(4)
C(31)-C(32)-C(33)	119.2(10)	C(61)-C(62)-C(63)	120.0
C(34)-C(33)-C(32)	120.5(10)	C(62)-C(63)-C(64)	120.0
C(35)-C(34)-C(33)	120.9(10)	C(65)-C(64)-C(63)	120.0
C(34)-C(35)-C(36)	119.9(10)	C(64)-C(65)-C(66)	120.0
C(31)-C(36)-C(35)	120.8(9)	C(65)-C(66)-C(61)	120.0
C(42)-C(41)-C(46)	120.0	C(72)-C(71)-C(76)	119.4(8)
C(42)-C(41)-P(2)	122.9(3)	C(72)-C(71)-P(4)	123.6(7)
C(46)-C(41)-P(2)	116.9(4)	C(76)-C(71)-P(4)	116.9(6)
C(41)-C(42)-C(43)	120.0	C(62B)-C(61B)-C(66B)	120.0
C(42)-C(43)-C(44)	120.0	C(62B)-C(61B)-P(3)	122.4(4)
C(45)-C(44)-C(43)	120.0	C(66B)-C(61B)-P(3)	117.6(4)
C(44)-C(45)-C(46)	120.0	C(61B)-C(62B)-C(63B)	120.0
C(45)-C(46)-C(41)	120.0	C(64B)-C(63B)-C(62B)	120.0
C(36)-C(31)-C(32)	118.6(8)	C(63B)-C(64B)-C(65B)	120.0
C(36)-C(31)-P(2)	117.4(6)	C(66B)-C(65B)-C(64B)	120.0
C(32)-C(31)-P(2)	124.0(7)	C(65B)-C(66B)-C(61B)	120.0
C(42B)-C(41B)-C(46B)	120.0	C(82)-C(81)-C(86)	117.9(9)
C(42B)-C(41B)-P(2)	122.9(4)	C(82)-C(81)-P(4)	125.4(7)

C(86)-C(81)-P(4)	116.5(7)
C(62C)-C(61C)-C(66C)	120.0
C(62C)-C(61C)-P(3)	122.5(4)
C(66C)-C(61C)-P(3)	117.5(4)
C(63C)-C(62C)-C(61C)	120.0
C(62C)-C(63C)-C(64C)	120.0
C(63C)-C(64C)-C(65C)	120.0
C(66C)-C(65C)-C(64C)	120.0
C(65C)-C(66C)-C(61C)	120.0
C(71)-C(72)-C(73)	120.2(10)
C(74)-C(73)-C(72)	120.4(10)
C(73)-C(74)-C(75)	120.9(10)
C(74)-C(75)-C(76)	119.6(10)
C(75)-C(76)-C(71)	119.5(9)
C(81)-C(82)-C(83)	120.2(10)
C(84)-C(83)-C(82)	119.8(10)
C(85)-C(84)-C(83)	121.1(11)
C(84)-C(85)-C(86)	120.4(11)
C(81)-C(86)-C(85)	120.6(10)
O(9)-C(91)-C(92)	111.7(5)
O(10)-C(93)-C(94)	112.4(6)

Symmetry transformation ns used to generate equivalent atoms: